

**Sevoflurane but not Xenon Interferes with Synaptic Remodeling via Elevation
of BACE-Derived Signaling Pathways and Reduction of Nectin-3 Expressions**

Xingxing Wang

Vollständiger Abdruck der von der Fakultät für Medizin der Technischen Universität
München zur Erlangung des akademischen Grades einer
Doktorin der Naturwissenschaften (Dr. rer. nat.)
genehmigten Dissertation.

Vorsitz: Prof. Dr. Mikael Simons

Prüfer*innen der Dissertation:

1. apl. Prof. Dr. Gerhard Rammes
2. Prof. Dr. Aphrodite Kapurniotu

Die Dissertation wurde am 03.06.2023 bei der Technischen Universität München eingereicht
und durch die Fakultät für Medizin am 11.10.2022 angenommen.

Acknowledgments

In the beginning, I am extremely grateful to Prof. Dr. Gerhard Rammes, my supervisor, who has offered me this great chance to perform my Ph.D. thesis in the group of Experimental Neuropharmacology at the Department of Anesthesiology and Intensive Care Medicine in Klinikum rechts der Isar, Munich, Germany. He has offered me great support to address scientific problems about my project and Ph.D. study.

Great thanks to my secondary supervisor Prof. Dr. Aphrodite Kapurniotu and my mentor Dr. Mathias V. Schmidt for their professional advice and kind help during my Ph.D. study and work.

Many thanks to my colleagues for their kind help during the work. I would like to thank Qinfang Shi and Arpit Pradhan Kumar for their help with the bench work and proofreading of the manuscript. Great thanks also go to colleagues including Andreas Blaschke, Nina Bayer, Claudia Kopp, Carolin Knoll, Xenia Puig, Nour Kassab El Dine, and so on.

I feel also grateful to Prof. Dr. Dieter Saur, Prof. Dr. Stefan Lichtenthaler, and other colleagues in the Transla TUM for their technical help.

Special thanks to the China Scholarship Council (CSC) for financing me during my Ph.D. study in Germany.

I could not have undertaken this journey without the support and love of my family. Thank you, my parents, my husband, and especially my children. You all give me the strength to go through the difficulties and finally achieve this work.

Abstract

Recently, anesthesia by isoflurane and sevoflurane has been suggested to accumulate amyloid beta 1-42 ($A\beta_{1-42}$), which contributes to synaptic impairment and potentially evokes the progression of Alzheimer's disease. In the $A\beta_{1-42}$ generation through amyloid precursor protein (APP), the β -site APP-cleaving enzyme (BACE) is essential. New evidence indicates that inhalational anesthesia enhances BACE activity and modulates spine morphology. However, the exact mechanism regarding inhalational anesthesia on spine dynamics as well as the BACE-dependent APP proteolysis process in the hippocampus remains to be investigated. In the present thesis, brain sections including the hippocampus from adult mice were treated with equivalent isoflurane (0.6%), sevoflurane (1.4%), or xenon (65%) for 1.5h with or without pre-incubation of the BACE inhibitor LY2886721 (3 μ M, 2h). Additionally, dendritic spine complexity, APP proteolysis-process-related molecules, nectin-3 expressions, as well as CA1-long-term potentiation (CA1-LTP) were tested. Adeno-associated virus (AAV) was injected for the knockdown of CA1-nectin-3 levels. The nectin-3 reduction effects on spine density and CA1-LTP were thereafter evaluated. Results showed that sevoflurane upregulated hippocampal mouse $A\beta_{1-42}$ (mA β_{1-42}), blocked CA1-LTP, reduced CA1-dendritic spine complexity, and decreased CA1-nectin-3 expressions. Furthermore, nectin-3 knockdown specifically in CA1 abolished potentiation and induced spine loss. Moreover, isoflurane exposure reduced spines count and impaired LTP in the CA1 region. In comparison, the attenuated CA1 potentiation by xenon was also observed, but it did not alternate spine dynamics, nectin-3 levels, or APP processing in the hippocampus. Further results showed that BACE inhibition partially reversed sevoflurane-induced abnormalities in spine density, LTP, mA β_{1-42} , and nectin-3. The colocalization of APP and nectin-3 was detailed in

CA1. In conclusion, this thesis indicates that, in CA1, sevoflurane mildly enhances BACE activity and modulates synaptic plasticity, while isoflurane modestly interferes with synaptic plastic alternations. By comparison, xenon does not change dendritic spine dynamics.

Zusammenfassung

Die Exposition gegenüber Inhalationsanästhetika kann die synaptische Plastizität beeinträchtigen. Zusätzlich wird vermutet, dass die Anwendung der Inhalationsanästhetika Isofluran und Sevofluran zu einer Akkumulation von β -Amyloid 1-42 ($A\beta_{1-42}$) führen kann. $A\beta_{1-42}$ ist zur synaptischen Dysfunktion beitragen und die Alzheimer-Krankheit auslösen kann. Bei der Bildung von $A\beta_{1-42}$ durch das Amyloid-Vorläuferprotein (APP) spielt das β -site APP-cleaving enzyme (BACE) eine zentrale Rolle. Neue Erkenntnisse deuten darauf hin, dass die Inhalationsanästhesie die BACE-Aktivität erhöht und die Dynamik der dendritischen Spines moduliert. Der Mechanismus der Inhalationsanästhesie auf die dendritische Spine-Plastizität und die BACE-abhängige APP-Verarbeitung im Hippocampus bleibt jedoch unklar. In dieser Studie wurden hippocampale Hirnschnitte von adulten Mäusen für 1,5 Stunden mit äquipotenten Konzentrationen Isofluran (0,6%), Sevofluran (1,4 %) und Xenon (65 %), mit oder ohne Vorbehandlung mit dem BACE-Inhibitor LY2886721 (3 μ M für 2 Stunden) inkubiert. Zusätzlich wurde die Dichte der dendritischen Spines in der CA1-Region, die Expression von APP-verarbeitenden Enzymen und Nectin-3 sowie die Langzeitpotenzierung (LTP) untersucht. Um die Auswirkungen einer Nectin-3 Depletion auf die LTP und die dendritischen Spines zu untersuchen, wurde ein adeno-assoziiertes Virus (AAV) eingesetzt, welches das Zelladhäsionsmolekül Nectin-3 ausschaltet. Die Ergebnisse zeigten, dass Sevofluran die Konzentrationen von murinem $A\beta_{1-42}$ ($mA\beta_{1-42}$) im Hippocampus erhöhte, CA1-LTP blockierte, die dendritische Spinedichte sowie die Expression von Nectin-3 in der CA1 Region verringerte. Gleichsam reduzierte der AAV-induzierte spezifische Nectin-3 Knockdown die LTP und die Spinedichte in der CA1-Region. In Anwesenheit von Isofluran wurden auch eine verringerte Spinedichte und eine abgeschwächte LTP im

Hippocampus beobachtet. Obwohl Xenon die LTP blockierte, konnte kein Einfluss auf die dendritische Spinedichte und auch nicht auf die Nectin-3 Konzentration oder die APP-Verarbeitung beobachtet werden. Schließlich konnte durch die Antagonisierung der BACE-Aktivität die durch Sevofluran verursachten Defizite bezüglich der Spinedichte, der LTP sowie der erhöhten $\text{mA}\beta_{1-42}$ und Nectin-3 levels teilweise wieder hergestellt werden. Ich habe außerdem ein Kolokalisationsprofil von APP und Nectin-3 im CA1 detailliert untersucht. Meine Daten deuten darauf hin, dass Sevofluran in der CA1-Region die BACE-Aktivität teilweise erhöht und den Umbau von Spines beeinträchtigt, während Isofluran die Veränderungen der synaptischen Plastizität nur leicht moduliert. Im Gegensatz dazu führt Xenon nicht zu einem Umbau der dendritischen Spines.

Table of Contents

Acknowledgments	iii
Abstract	v
Zusammenfassung	vii
List of Figures	xii
List of Tables	xv
Introduction	1
1. Inhalational anesthetics and mechanisms	1
1.1 Inhalational anesthetics	1
1.1.1 Inhalational anesthetic compounds	1
1.1.2 Minimum alveolar concentration (MAC) of inhalational anesthetics.....	2
1.2 Mechanisms of inhalational anesthesia.....	4
1.2.1 The lipid hypotheses	4
1.2.2 Anesthetics act on ion channels and neurotransmitter receptors at synapses ...	5
1.2.3 The heterotrimeric guanine nucleotide-binding proteins (G proteins) coupled mechanism	9
2. Inhalational anesthetics and dendritic spine remodeling	12
2.1 Dendritic spines structure and function	13
2.2 Modulation of dendritic spine dynamics by inhalational anesthetics	14
3. Inhalational anesthetics and neurodegeneration	16
3.1 The neurotoxicity induced by inhalational anesthetics.....	16
3.2 Alzheimer disease and amyloid cascade hypothesis.....	18

3.2.1 Alzheimer disease	18
3.2.2 Amyloid cascade hypothesis	19
3.3 Amyloid precursor protein structure and function	23
3.3.1 The structure of APP and its proteolysis process.....	23
3.3.2 APP functions.....	25
3.4 BACE1 structure and function.....	27
3.5 Regulation of APP processing by inhaled anesthetics	29
3.6 Xenon functions as a neuroprotective anesthetic.....	30
4. Nectin-3 and the regulation of synaptic plasticity.....	32
Aim of the dissertation	35
Materials and Methods	36
1. Mice	36
2. Compounds.....	36
2.1 Inhalational anesthetics	36
2.2 Mouse A β ₁₋₄₂	37
2.3 BACE inhibitor	37
3. Hippocampal slices preparation.....	37
4. field excitatory postsynaptic potentials (fEPSPs) recordings.....	37
5. Stereotaxic virus injection	39
6. Immunofluorescence	40
7. Immunohistochemistry	41
8. Western blot.....	42

9. Enzyme-linked immunosorbent assay (ELISA).....	45
10. Quantitative real-time PCR (RT-PCR).....	45
11. Dendritic spines classification	46
12. Statistical analysis.....	47
Results	48
1. The sevoflurane-induced $mA\beta_{1-42}$ increase was reversed by BACE inhibition	48
2. Abnormal potentiation and dendritic spine complexity in CA1 by $mA\beta_{1-42}$	49
3. Spine elimination by sevoflurane was partly restored by BACE inhibition.....	51
4. Reduced CA1-nectin-3 expressions were reversed by BACE inhibition	52
5. Nectin-3 knockdown in CA1 impaired potentiation and reduced spine counts	54
6. Regulation of APP processing-related molecules in hippocampus	56
7. Co-stainings of APP and nectin-3.....	59
8. Isoflurane, sevoflurane, and xenon attenuated LTP dramatically	60
9. BACE inhibition partially reversed the LTP deficits induced by sevoflurane	61
Discussion	63
Reference	71
List of abbreviations	97

List of Figures

Figure 1. Relation of concentration and actions of a general anesthetic (Campagna et al., 2003).....	2
Figure 2. Relation between anesthetic potency and hydrophobicity property (Campagna et al., 2003).....	3
Figure 3. Integration of excitation and inhibition on synapses with an anesthetic (Urban, 2002).....	6
Figure 4. Basic topology structure of the ligand-gated ion channel (Krasowski & Harrison, 1999).	6
Figure 5. Anesthetic sites on ion channels (Campagna et al., 2003).....	9
Figure 6. Typical GPCR signaling (Pierce, Premont, & Lefkowitz, 2002).....	9
Figure 7. Schematic diagram GPCR signaling (Neumann et al., 2014).	10
Figure 8. Gq-coupled receptor expressions of <i>Xenopus</i> oocytes (K. Minami & Uezono, 2013).....	12
Figure 9. A spiny neuron (Wikipedia).	13
Figure 10. Morphological classifications of dendritic spines (Hering & Sheng, 2001).	13
Figure 11. A mushroom-shaped dendritic spine structure (Hering & Sheng, 2001)..	14
Figure 12. Anesthesia-induced neurotoxicity at extreme ages (S. C. Johnson et al., 2019).....	17
Figure 13. Mechanisms of POCD and research perspectives (Casella & Bimonte, 2017).....	17
Figure 14. Pathological hallmarks of AD (O'Brien & Wong, 2011).	19
Figure 15. The amyloid cascade hypothesis (D. J. Selkoe & Hardy, 2016; Singh et al., 2016).....	21

Figure 16. APP schematic structure (O'Brien & Wong, 2011; Thinakaran & Koo, 2008).	24
Figure 17. Two pathways of APP proteolysis processing (O'Brien & Wong, 2011; Thinakaran & Koo, 2008).	25
Figure 18. APP family functions at the synapse (Schilling et al., 2017).	26
Figure 19. BACE1 structure (Dislich & Lichtenthaler, 2012).....	28
Figure 20. c-Fos expressions by treatment of xenon, N ₂ O, and ketamine (D Ma et al., 2002).....	31
Figure 21. The mechanism of xenon action (Alam et al., 2017).	32
Figure 22. Nectins structure and the binding proteins (Mori et al., 2014).	33
Figure 23. LY2886721 structure.....	37
Figure 24. Sagittal hippocampal slice (Kratzer. et al., 2012).....	38
Figure 25. Typical fEPSP curve (https://www.winltp.com/OverviewOfWinLTP.html).38	
Figure 26. Full vector sequence for Pvr13 AAV siRNA pooled virus (Serotype 9, from abm).....	40
Figure 27. Dendritic spines classes (Harris KM & Jensen FE, 1992).	47
Figure 28. BACE inhibition reversed the increased mA β ₁₋₄₂ levels induced by sevoflurane.	48
Figure 29. BACE inhibitor LY2886721 partially reduced hippocampal mA β ₁₋₄₂ levels.	49
Figure 30. Mouse A β ₁₋₄₂ blocked potentiation and reduced CA1-spine complexity... 50	
Figure 31. No alternations of dendritic spine density by xenon exposure, and inhibition of BACE partially restored only the sevoflurane-induced spine loss.....	51
Figure 32. BACE inhibition restored the reduction of nectin-3 in CA1 by sevoflurane.	53
Figure 33. Nectin-3 expressions in regions of DG, CA3, and HC.....	54

Figure 34. Attenuated LTP and reduced dendritic spines density under nectin-3 downregulation in CA1.....	55
Figure 35. Nectin-3 knockdown in the CA1 region did not alternate hippocampal APP, sAPP β , or BACE.....	56
Figure 36. APP-amyloidogenic-process related molecular changes in hippocampus.	57
Figure 37. Expression levels of APP in either DG, CA3, or HC.....	58
Figure 38. APP levels were not changed by BACE inhibition via western blot and immunohistochemistry.....	58
Figure 39. Co-stainings of APP and nectin-3 in CA1.....	59
Figure 40. BACE inhibition partially reversed the LTP deficits induced only by sevoflurane.....	60
Figure 41. Beta-secretase inhibitor LY2886721 exposure did not block LTP.....	61

List of Tables

Table 1. Inhalational anesthetics generations (Campagna, Miller, & Forman, 2003)..	1
Table 2. Properties of isoflurane, sevoflurane, and xenon.....	2
Table 3. MAC _{awake} values of anesthetics administrated alone in humans (Goto et al., 2000).....	4
Table 4. MAC values for mice and rats (%) (Mazze, Rice, & Baden, 1985).....	4
Table 5. Some anesthetic-sensitive ion channels (Campagna et al., 2003).	7
Table 6. Inhalational anesthetics act on ion channels (Campagna et al., 2003).	8
Table 7. Signaling of G protein-coupled receptors (K. Minami & Uezono, 2013).....	11
Table 8. Inhalational anesthetics actions on Gq-coupled receptor (K. Minami & Uezono, 2013).....	12
Table 9. Inhalational anesthesia effects on dendritic spine dynamics (Granak et al., 2021).....	14
Table 10. Primary antibodies used in immunofluorescence.	41
Table 11. Lysis buffer for western blot.....	42
Table 12. Separating and stacking gels cocktails.....	43
Table 13. Primary antibodies used in western blot.....	44
Table 14. Primer sets information.	46

Introduction

1. Inhalational anesthetics and mechanisms

1.1 Inhalational anesthetics

The discovery of general anesthesia revolutionized modern medicine and surgical practice. In 1800, the first case of inhalational anesthesia with synthesized nitrous oxide was reported by Humphry Davy (Davy, 1800). In 1846, inhalational anesthesia by ether finally came into clinical practice (Weinrich & Worcester, 2018). Thereafter, numerous reagents were reported with anesthetic properties (N. P. Franks, 2006; Sanders, Franks, & Maze, 2003).

1.1.1 Inhalational anesthetic compounds

General anesthetics can be roughly classified into volatile/intravenous anesthetics and anesthetic gases (Krasowski & Harrison, 1999). Of those, volatile anesthetics consist numerous compounds (Seeman, 1972; Sewell & Sear, 2004, 2006; Sonner & Cantor, 2013) (Table 1).

	Hydrocarbons	Ethers	Others
1840–1950	$\begin{array}{c} \text{Cl} \\ \\ \text{H}-\text{C}-\text{Cl} \\ \\ \text{Cl} \end{array}$ Chloroform $\begin{array}{c} \text{CH}_2 \\ / \quad \backslash \\ \text{H}_2\text{C}-\text{CH}_2 \end{array}$ Cyclopropane $\text{H}_2\text{C}=\text{CH}_2$ Ethylene	$\begin{array}{c} \text{H} \quad \text{H} \\ \quad \\ \text{H}_3\text{C}-\text{C}-\text{O}-\text{C}-\text{CH}_3 \\ \quad \\ \text{H} \quad \text{H} \end{array}$ Diethyl ether	$\text{N}=\text{N}-\text{O}$ Nitrous oxide
1951–1990	$\begin{array}{c} \text{F} \quad \text{Br} \\ \quad \\ \text{F}-\text{C}-\text{C}-\text{H} \\ \quad \\ \text{F} \quad \text{Cl} \end{array}$ Halothane	$\begin{array}{c} \text{F} \quad \text{F} \quad \text{F} \\ \quad \quad \\ \text{H}-\text{C}-\text{C}-\text{O}-\text{C}-\text{H} \\ \quad \quad \\ \text{F} \quad \text{Cl} \quad \text{F} \end{array}$ Enflurane $\begin{array}{c} \text{Cl} \quad \text{F} \quad \text{F} \\ \quad \quad \\ \text{H}-\text{C}-\text{C}-\text{O}-\text{C}-\text{H} \\ \quad \quad \\ \text{Cl} \quad \text{F} \quad \text{F} \end{array}$ Methoxyflurane $\begin{array}{c} \text{F} \quad \text{H} \quad \text{F} \\ \quad \quad \\ \text{F}-\text{C}-\text{C}-\text{O}-\text{C}-\text{H} \\ \quad \quad \\ \text{F} \quad \text{Cl} \quad \text{F} \end{array}$ Isoflurane $\begin{array}{c} \text{F} \quad \text{H} \quad \text{H} \\ \quad \quad \\ \text{F}-\text{C}-\text{C}-\text{O}-\text{C}=\text{C} \\ \quad \quad \\ \text{F} \quad \text{H} \quad \text{H} \end{array}$ Fluroxene	Xe Xenon
1991–2003		$\begin{array}{c} \text{CF}_3 \quad \text{H} \\ \quad \\ \text{H}-\text{C}-\text{O}-\text{CH}_2\text{F} \\ \quad \\ \text{CF}_3 \quad \text{H} \end{array}$ Sevoflurane $\begin{array}{c} \text{F} \quad \text{F} \quad \text{F} \\ \quad \quad \\ \text{F}-\text{C}-\text{C}-\text{O}-\text{C}-\text{H} \\ \quad \quad \\ \text{F} \quad \text{H} \quad \text{F} \end{array}$ Desflurane	

Table 1. Inhalational anesthetics generations (Campagna, Miller, & Forman, 2003).

The physicochemical properties of those compounds differ in various aspects (Jerath, Parotto, Wasowicz, & Ferguson, 2016; Ye & Zuo, 2017). Regarding the present thesis, the differences of properties of the three anesthetics are roughly listed in Table 2.

Property	Isoflurane	Sevoflurane	Xenon
Boiling point (°C)	49	59	-108
Odour	Unpleasant	Pleasant	Pleasant
Blood-gas partition coefficient in blood	1.46	0.65	0.115
Blood-gas partition coefficient in brain	2.6	1.7	-
Minimum alveolar concentration (MAC, %)	human: 1.15 rodent: 1.34	human: 2 rodent: 3.2	human: 63 rodent: 140
Metabolized in the body (%)	0.2	2-5	0
Rate of onset & recovery	Medium	Rapid	Rapid

Table 2. Properties of isoflurane, sevoflurane, and xenon.

1.1.2 Minimum alveolar concentration (MAC) of inhalational anesthetics

Potency represents the drug's capacity to achieve a standard effect. It is statistically inversely related to the required drug concentration (Figure 1, 2). That means, an inhalational anesthetic with higher potency can trigger a specific response at lower concentrations (Campagna et al., 2003).

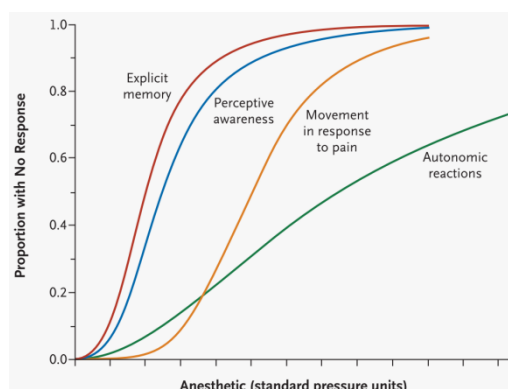


Figure 1. Relation of concentration and actions of a general anesthetic (Campagna et al., 2003).

The potency or capacity of a general inhalational anesthetic is measured by its MAC value (Campagna et al., 2003). MAC refers to the end-tidal concentration at 1 atm of a general anesthetic that can suppress motor response (eg. movement) of 50% subjects under surgical (pain) stimulation (Campagna et al., 2003).

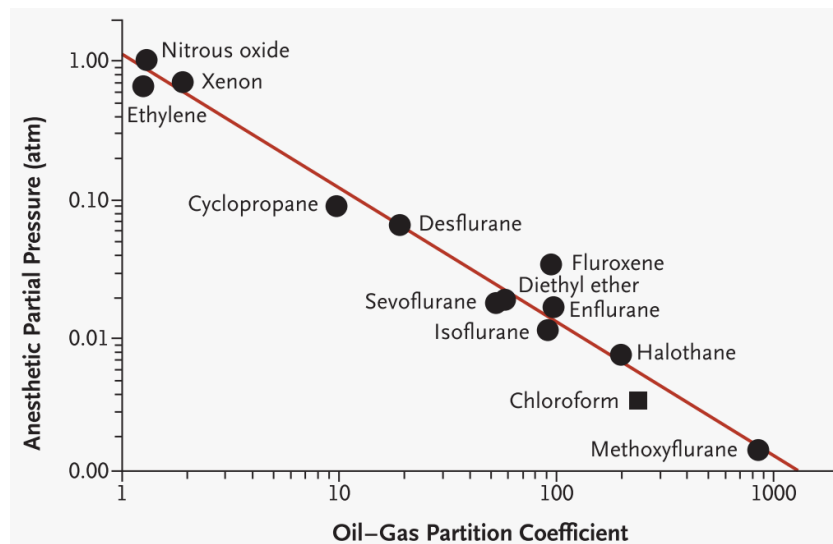


Figure 2. Relation between anesthetic potency and hydrophobicity property (Campagna et al., 2003).

MAC_{awake} is defined by the end-tidal concentration of a general inhalational anesthetic at 1 atm that appropriately suppresses response to spoken commands (such as raise your arm) of 50% subjects (Dwyer, Bennett, Eger, & Heilbron, 1992; E. I. I. Eger, 2001). Statistically, it is around 0.3-0.4 MAC (Table 3, 4) (Aranake, Mashour, & Avidan, 2013). For isoflurane and sevoflurane, MAC_{awake} is statistically around a third of MAC. While for xenon, MAC_{awake} in humans is around 33% or 0.46% of its MAC value (Goto et al., 2000). Table 4 shows the MAC value for mice and rats. Besides, regarding the present thesis, the MAC value for sevoflurane is around 3.25% (Cesarovic et al., 2010; Nishino, Jin, Nozaki-Taguchi, & Isono, 2020). It has been shown a correlation between learning and memory suppression and the MAC_{awake} concentration application of an inhalational anesthetic (Aranake et al., 2013; Dwyer et al., 1992; E. I. I. Eger, 2001).

	Xenon	N ₂ O	Isoflurane	Sevoflurane
MAC-awake (%)	32.6 ± 6.1	63.3 ± 7.1	0.40 ± 0.07	0.59 ± 0.10
(95% Confidence interval)	(30.5–34.6)	(59.8–66.9)	(0.37–0.43)	(0.54–0.64)
MAC-awake/MAC	0.46 ± 0.09	0.61 ± 0.07	0.35 ± 0.06	0.35 ± 0.06
(95% Confidence interval)	(0.43–0.49)	(0.57–0.64)	(0.32–0.38)	(0.32–0.38)

The minimum alveolar concentration (MAC)-awake/MAC ratios were significantly different between anesthetic groups ($P < 0.001$, analysis of variance and Student–Newman–Keuls tests), except between isoflurane and sevoflurane.

N₂O = nitrous oxide.

Table 3. MAC_{awake} values of anesthetics administrated alone in humans (Goto et al., 2000).

TABLE 1. MAC Values for Mice and Rats (%)*

	Pregnant Female	Nonpregnant Female	Male	Mean ± SD
Mice				
Halothane	0.98	0.96	0.89	0.95 ± 0.07 (6)†
Isoflurane	1.35	1.35	1.32	1.34 ± 0.10 (6)
Enflurane	2.08	1.97	1.85	1.95 ± 0.16 (6)
Rats				
Halothane	1.02‡	1.03	1.04‡	1.03 ± 0.04 (4)
Isoflurane	1.43‡	1.52	1.44	1.46 ± 0.06 (5)
Enflurane	2.22‡	2.17	2.25	2.21 ± 0.08 (5)

Table 4. MAC values for mice and rats (%) (Mazze, Rice, & Baden, 1985).

1.2 Mechanisms of inhalational anesthesia

Inhalational anesthetics have been used in the clinic for over 170 years. Despite many studies have reported the mechanisms of general inhalational anesthetics, the understanding of inhaled anesthesia remains obscure (Eckenhoff, 2001; E. I. Eger, 2nd, Raines, Shafer, Hemmings, & Sonner, 2008; N. P. Franks, 2006; Hemmings et al., 2005; Sonner & Cantor, 2013). These studies have proposed several hypotheses, and some of these hypotheses have been summarized below.

1.2.1 The lipid hypotheses

In the 20th century, the correlation of potency and solubility of an anesthetic in fatty tissues are noticed by Meyer and Overton. They firstly forwarded the connection of the cell membrane lipid and anesthetic actions, which was soon be validated by anesthetic

potency and oil solubility (Figure 2) (Eckenhoff, 2001; Feldman, Scurr, & Paton, 1993; Weinrich & Worcester, 2018).

However, the lipid hypothesis was later shown with shortcomings. A report has shown that the expected alternations in the membrane bilayer were too tiny (N. P. Franks, 2006). Later on, in-vivo experiments demonstrated that 100 bar pressure application reversed the anesthesia effects. Thus, researchers forwarded the hypothesis that anesthetics would partition into fluid membranes, which could further expand and thicken them (F. H. Johnson & Flagler, 1950; Lever, Miller, Paton, & Smith, 1971). However, opposite evidence showed that the fluid membranes were thickened but not thinned under hydrostatic pressure (Braganza & Worcester, 1986). On the other hand, no big alternations of the bilayer membrane structure were observed at the concentrations of anesthetics well above clinical requirements by X-ray-based studies (N. Franks & Lieb, 1979).

Until now, the lipid hypothesis is still under debate and it remains to be further studied.

1.2.2 Anesthetics act on ion channels and neurotransmitter receptors at synapses

Inhalational anesthetics are involved in complex interactions with various molecules expressed on the pre- and post-synaptic sites. Most likely, anesthetics act on the targets of neurotransmitter receptors and ion channels and further depress the nervous system in a direct and/or indirect manner (Figure 3) (Sonner et al., 2003; Urban, 2002).

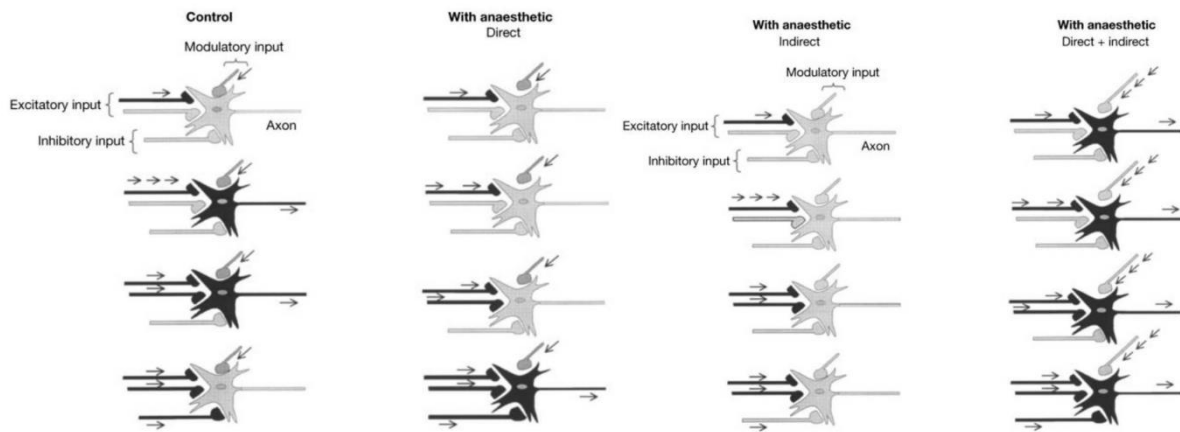


Figure 3. Integration of excitation and inhibition on synapses with an anesthetic (Urban, 2002).

Ion channels refer to proteins that can modulate ion flows through the cytoplasmic membrane (Campagna et al., 2003). Figure 4 demonstrates the basic topology structures of the ligand-gated ion channel and the $\alpha\beta$ complex of a γ -Aminobutyric acid type A (GABA_A) receptor (Krasowski & Harrison, 1999).

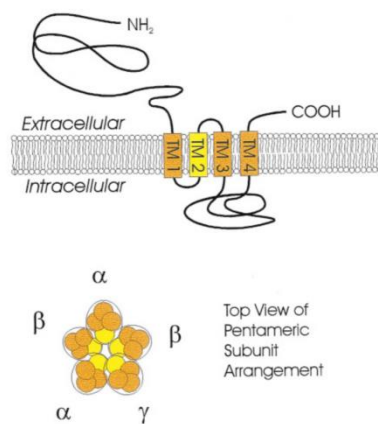


Figure 4. Basic topology structure of the ligand-gated ion channel (Krasowski & Harrison, 1999).

As shown in Table 5, some ion channels are sensitive to anesthetics. They roughly include the ligand-gated ion channels, potassium channels, sodium channels, calcium channels, etc. These channels can modulate cellular excitability, electrical activity, behavior, and physiological actions of anesthetics (Campagna et al., 2003; Krasowski & Harrison, 1999; Sonner & Cantor, 2013) (Table 6).

Ion Channel	Cellular Roles	Behavioral, Physiological, and Pharmacologic Roles
Ligand-gated		
γ -Aminobutyric acid type A receptors	Increased chloride permeability; membrane hyperpolarization; inhibition of excitability	Enhanced activity associated with anxiolysis, sedation, amnesia, myorelaxation, anticonvulsant action
Glycine receptors	Increased chloride permeability; membrane hyperpolarization; inhibition of excitability	Spinal reflexes and startle responses; major inhibitory receptor in spinal cord
Neuronal nicotinic acetylcholine receptors	High permeability to monovalent cations and calcium; release of neurotransmitters	Association with memory, nociception, mutations linked with seizure disorders; autonomic functions
Muscle nicotinic acetylcholine receptors	Neuromuscular transmission	Skeletal-muscle contraction
Serotonin type 3 receptors	Enhance excitability by inhibiting resting potassium-leak currents	Arousal; possible role in emesis
Glutamate receptors* N-methyl-D-aspartate	Fast excitatory neurotransmission Cation conductance for calcium and magnesium	Perception; learning and memory; nociception
α -Amino-3-hydroxy-5-methyl-4-isoxazole propionic acid and kainate	Cation conductance for calcium and magnesium	Perception and memory
Other types		
Potassium channels		
Non-voltage-gated background channels	Modulation of cell resting potential and excitability; role in chemical, mechanical, and pH sensitivity	Nonspecific role; most likely widespread
Voltage-activated	Recovery from action potentials	Nerve conduction; cardiac action potentials; mutations associated with cardiac arrhythmias
Non-voltage-dependent neurotransmitter or ATP-activated	Inward rectifying channels; pH-sensitive	Glucose sensor in β -cells Possible role in ischemic preconditioning
Sodium channels	Generation and propagation of action potentials	Nerve conduction; cardiac action potentials (arrhythmias)
Calcium channels		
Voltage-gated cardiac (T-, N-, L-, and P-type)	Generation of pacemaker potentials in neurons (T-type)	Cardiac inotropy and chronotropy; vascular tone
Voltage-gated neuronal	Presynaptic localization; neurotransmitter release	Nonspecific role; most likely widespread
Calcium-induced calcium release Ryanodine receptor Inositol triphosphate receptors	Intracellular channels Release of intracellular calcium stores after stimulation of surface receptors; production of calcium oscillations	Excitation-contraction coupling

Table 5. Some anesthetic-sensitive ion channels (Campagna et al., 2003).

At the synapse level, ion channels modify the neurotransmitter's release presynaptically and change the neuronal excitability postsynaptically. By influencing ion channels and receptors, inhalational anesthetics reduce excitation and neurotransmitter release presynaptically and decrease neurotransmitter

activity postsynaptically (Table 5, 6) (Campagna et al., 2003).

Ion Channel	Halogenated Alkanes and Ethers	Nonhalogenated Alkanes	Xenon and Nitrous Oxide
γ -Aminobutyric acid type A ^{59,60}	Enhancement	No effect	No effect
Glycine receptors ^{60,61}	Enhancement	No effect	No effect
Neuronal nicotinic acetylcholine receptors ⁶²⁻⁶⁵	Strong inhibition	Strong inhibition	Inhibition
Muscle nicotinic acetylcholine receptors ⁶⁶	Inhibition	Inhibition	ND
Serotonin receptors ^{64,67}	Weak inhibition	ND	No effect
Glutamate receptors N-methyl-D-aspartate ^{64,68,69} α -Amino-3-hydroxy-5-methyl-4-isoxazole propionic acid and kainate ^{64,69,70}	Inhibition Inhibition	Inhibition ND	Inhibition No effect
Background potassium channels ^{71,72}	Enhancement or no effect [†]	ND	ND
Voltage-activated potassium channels ^{72,73}	Inhibition or no effect	ND	No effect
ATP-activated potassium channels ⁷⁴	Enhancement or no effect [†]	ND	ND
Voltage-activated sodium channels ^{75,76}	Weak inhibition	Weak inhibition	ND
Voltage-activated calcium channels ^{73,77,78}	Weak inhibition	ND	No effect
Ryanodine-activated calcium channels ^{79,80}	Enhancement or inhibition	ND	ND

Table 6. Inhalational anesthetics act on ion channels (Campagna et al., 2003).

Among the mediators, GABA_A is the leading candidate (Hemmings et al., 2005). The inhalational anesthesia upregulated GABA_A receptor capacity (Hemmings et al., 2005; Krasowski & Harrison, 1999) by opening the channel at both synaptic and extrasynaptic receptors. Under inhalational anesthesia, the sensitivity of receptors to the neurotransmitter GABA was increased, which enhanced the inhibition of postsynaptic excitation (Campagna et al., 2003; Jones & Harrison, 1993) (Figure 5).

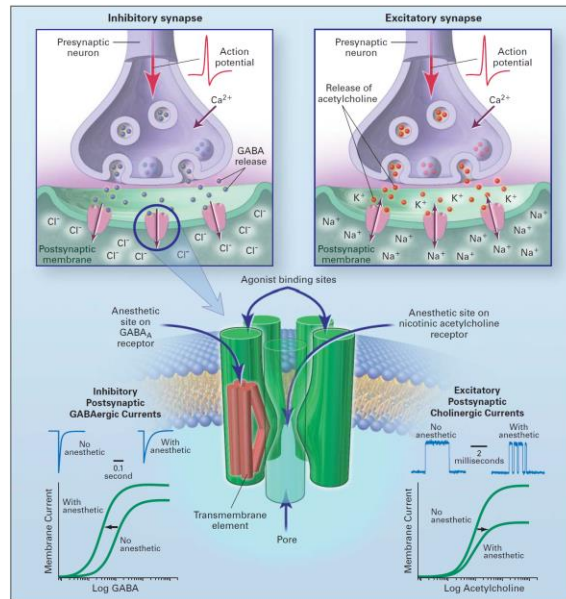


Figure 5. Anesthetic sites on ion channels (Campagna et al., 2003).

From the 1980s, the ion channels were proposed as the sole action site of general inhalational anesthesia. Although there have been tremendous studies reporting on this, the exact mechanism remains unknown.

1.2.3 The heterotrimeric guanine nucleotide-binding proteins (G proteins) coupled mechanism

Recent studies have illustrated that inhalational anesthetics could also function via G protein-coupled receptors (GPCRs) and intracellular signaling pathways (Campagna et al., 2003; Ishizawa, Pidikiti, Liebman, & Eckenhoff, 2002; Jerath et al., 2016; Kouichiro Minami & Uezono, 2005; K. Minami & Uezono, 2013).

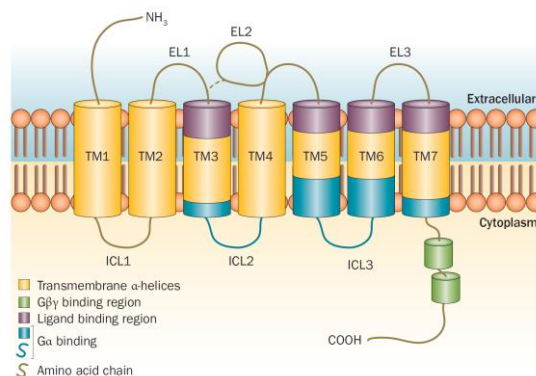


Figure 6. Typical GPCR signaling (Pierce, Premont, & Lefkowitz, 2002).

G proteins are signal transmembrane proteins (Ross & Gilman, 1980). A single G protein is heterotrimeric and comprises α -, β -, and γ - subunits (Pierce et al., 2002). G proteins can allow the transfer of signals across the cell membrane (Figure 6, 7) (Neumann, Khawaja, & Muller-Ladner, 2014).

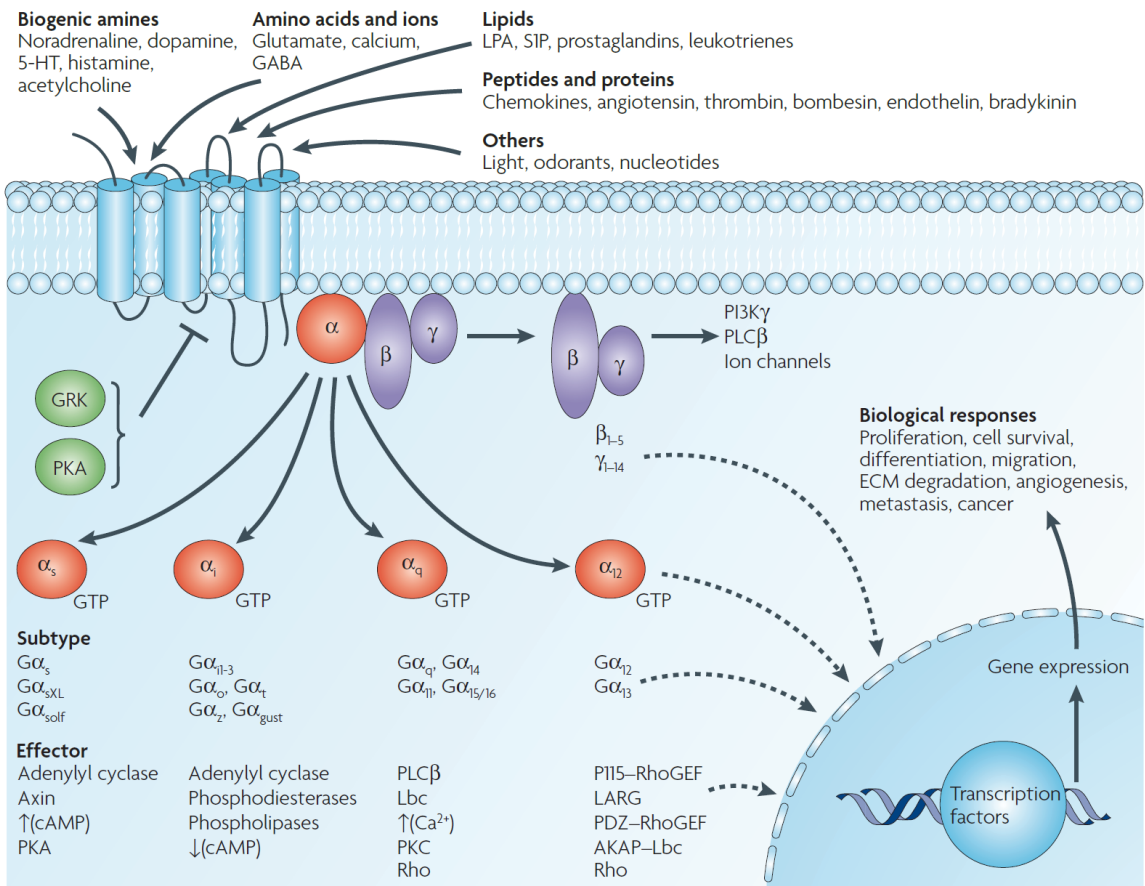


Figure 7. Schematic diagram GPCR signaling (Neumann et al., 2014).

A lot of neurotransmitter receptors, such as corticotropin-releasing hormone receptors, muscarinic acetylcholine (MR), dopamine, noradrenaline, GABA_B, etc., belong to GPCRs (Baldwin, Schertler, & Unger, 1997). The GPCRs are the single biggest target for various drugs (K. Minami & Uezono, 2013). Since a variety of ligands are capable to stimulate the targets via GPCRs. Moreover, each GPCRs can trigger a few downstream effectors (Table 7) (Dorsam & Gutkind, 2007; Neves, Ram, & Iyengar, 2002).

G protein	G _q	G _{i/o}	G _s
Effector	PLC↑	Adenylate cyclase↓	Adenylate cyclase↑
Second messenger	IP ₃ ↑ DAG↑	cAMP↓	cAMP↑
Intracellular reaction	PKC↑ Ca ²⁺ ↑	PKA↓	PKA↑
Receptor	M ₁ M ₃ Substance P Orexin 1 5HT _{2A} mGluR1 mGluR1	M ₂ μ Opioid	β-Adrenergic

Table 7. Signaling of G protein-coupled receptors (K. Minami & Uezono, 2013).

Early studies demonstrated that some agonists and/or antagonists that function via GPCRs could alter anesthetic requirements, for example, the MAC value, both in humans and animals (Glass, Gan, Scott Howell, & Brian Ginsberg, 1997; Ishizawa, Ma, Dohi, & Shimonaka, 2000; Ishizawa et al., 2002; Seitz, ter Riet, Rush, & Merrell, 1990). Furthermore, in vitro experiments showed that general inhalational anesthetics interfere with GPCR signaling directly (Durieux, 1995; Honemann, Nietgen, Podranski, Chan, & Durieux, 1998; Schotten et al., 1998). Most of these studies focused on G_q-coupled receptors.

With the *Xenopus* oocyte expression system, studies have shown that stimulation of G_q-coupled receptors can activate Cl⁻ currents by Ca²⁺ and phospholipase C (PLC) by G protein. Furthermore, the activated PLC evokes IP₃ formation, which triggers Ca²⁺ release from the endoplasmic reticulum. This will in turn open more Cl⁻ channels (Figure 8) (K. Minami & Uezono, 2013).

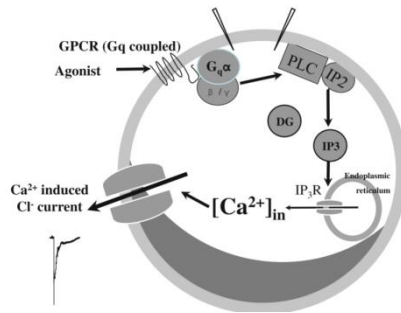


Figure 8. Gq-coupled receptor expressions of *Xenopus* oocytes (K. Minami & Uezono, 2013).

An inhibition of Gq-coupled receptors under inhaled anesthesia is observed according to previous studies (Table 8).

	Halothane	Isoflurane	Enflurane	Desflurane	Sevoflurane
M ₁	↓	→		↓↑	↓
M ₃	↓	↓		→	↓
5HT _{2A}	↓				
5HT _{2C}		↓	↓		
mGluR1	→				
mGluR5	↓				
Substance P	↓	↓	↓		↓
Orexin 1	↓	↓	↓		

Table 8. Inhalational anesthetics actions on Gq-coupled receptor (K. Minami & Uezono, 2013).

The GPCRs-mediated, especially, via Gq protein-coupled receptors, mechanism by anesthetics have become more relevant (Schotten et al., 1998). However, compared with the ion channels, additional investigations are required regarding the anesthesia effects on GPCRs-related mechanisms.

2. Inhalational anesthetics and dendritic spine remodeling

Dendritic spines refer to the tiny membranous protrusions. The biophysiological function of dendritic spines is for the transduction of synaptic signals. Therefore, aberrant dendritic spine dynamics contribute to physiological abnormalities. Studies have indicated that inhalational anesthetics contributed to the abnormal modulation of dendritic spines morphology.

2.1 Dendritic spines structure and function

Dendritic spines vary in shapes and sizes. The typical dendritic spines are 1-2 μm in length and 0.01-0.8 μm^3 in volume (Gipson & Olive, 2017) (Figure 9).

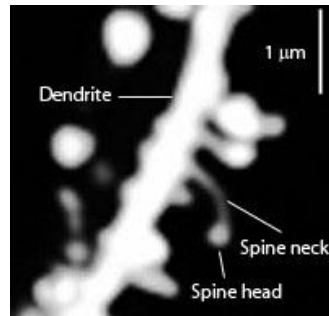


Figure 9. A spiny neuron (Wikipedia).

Three categories of dendritic spines are coarsely classified (X. D. Wang et al., 2013). As shown in Figure 10, they are thin, stubby, and mushroom spines. Besides, in some studies, dendritic filopodia and cup-shaped spines are also defined as dendritic spines (Runge, Cardoso, & de Chevigny, 2020).

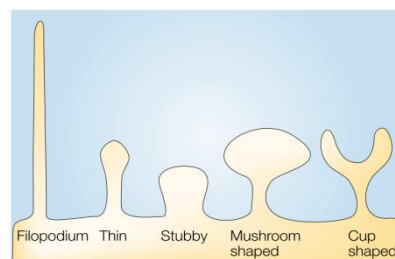


Figure 10. Morphological classifications of dendritic spines (Hering & Sheng, 2001).

Different dendritic spines contain divergent organelles and molecules. Generally speaking, the larger spines usually have bigger synapses and contain more complex organelles. Figure 11 shows a mushroom-shaped dendritic spine. The post-synaptic density (PSD), an electron-dense submembrane cytoskeleton, accounts for approximately 10% of the spine surface area. PSD is thought to be the reason why the spine head size is correlated with synaptic transmission. Apart from that, the number

of presynaptic vesicles as well as postsynaptic receptors also contribute to synaptic transmission strength (Berry & Nedivi, 2017; Hering & Sheng, 2001; Rochefort & Konnerth, 2012).

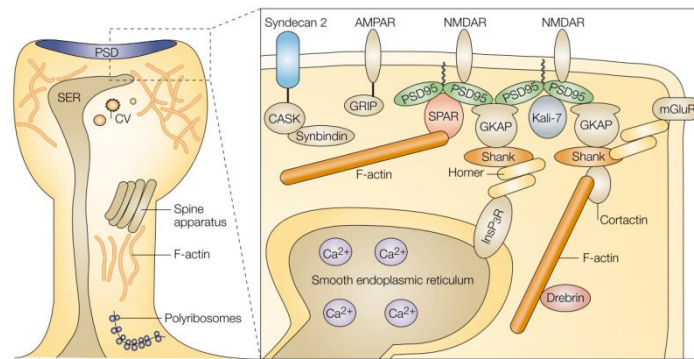


Figure 11. A mushroom-shaped dendritic spine structure (Hering & Sheng, 2001).

2.2 Modulation of dendritic spine dynamics by inhalational anesthetics

The dendritic spines are highly activity-dependent dynamic. Under certain conditions, spines can change their size and shape short-termly (seconds to minutes) and long-termly (hours to days). Isoflurane and sevoflurane were able to alternate dendritic spines, which has been reviewed by Simon Granak et. al, 2021 (Granak, Hoschl, & Ovsepiyan, 2021) (Table 9).

Anesthetics	Region of the brain	PND 0—7	PND 7—21	PND 21—35	PND > 35	References
Isoflurane	Hippocampus	↓ Long thin spines only ↓ Number of spines remained the same.	–	↑ in the CA1 region	↓ Anesthesia was supplemented with laparotomy	Schaefer et al. (2019), Kang et al. (2017), Qiu et al. (2020), Head et al. (2009), Yang et al. (2011), Briner et al. (2010), Landin et al. (2019)
	Cortex	–	↑	Filopodia pruning was reduced, ↑	–	
Sevoflurane	Hippocampus	Number of spines remained the same, ↓	↑	–	–	Briner et al. (2010), Qiu et al. (2016), Xiao et al. (2016), Jia et al. (2016), Liu et al. (2019), Zhou et al. (2019)
	Cortex	↑↓	↑	–	–	

Table 9. Inhalational anesthesia effects on dendritic spine dynamics (Granak et al., 2021).

Reports indicated that isoflurane induced age- and time-dependent alternations of dendritic spines (Table 9) (Briner et al., 2010).

In the postnatal day (PND) 7 mice, a single 1.5% isoflurane anesthesia lasting 4h reduced hippocampal thin spines without changing total spines for 2 weeks (Schaefer et al., 2019). It has been shown a decrease of excitatory synapses in the hippocampus of PND 5-7mice after 4h exposure to 1.4% isoflurane anesthesia (Head et al., 2009). In PND 30 mice, 1% isoflurane for 3-4 h reduced the filopodia elimination (Yang, Chang, Bekker, Blanck, & Gan, 2011). Another study reported that a 4h isoflurane (1.5%) exposure induced hippocampal dendritic spine loss and glutamatergic LTP deficits in PND-7 and -18 mice (Schaefer et al., 2019).

Although recent studies about the isoflurane anesthesia modulation of dendritic spine dynamics are mostly focused on the developmental stage, a few reports have shown that isoflurane can interfere with the dendritic spine remodeling during the later stages of postnatal life. In 16-month-old mice, 40min of 1.5% isoflurane anesthesia together with laparotomy reduced CA1-dendritic spine complexity eight days after the treatment (Qiu et al., 2020). Whereas, 18-month-old rats with 2h isoflurane (1.2%) treatment exhibited no effects on dendritic spine density (Lin et al., 2012).

Contrary to the above observations, some studies indicated an increase in dendritic spines under isoflurane exposure. A study reported that in PND16 rats, 1h isoflurane (1.5%) anesthesia increased the spine complexity in the cortex (Briner et al., 2010). Besides, a recent work has shown that in pubertal rats, 40min isoflurane (3%) exposure also upregulated spine counts in the prefrontal cortex as well as CA1 pyramidal neurons (Landin et al., 2019).

Compared with isoflurane, sevoflurane anesthesia tends to bidirectionally affect dendritic spine dynamics depending on the experimental animal's developmental stage, exposure duration, and brain regions under the study (Granak et al., 2021).

Repeated sevoflurane exposure (3%, 2h) during gestational days 13-15 evoked dendritic spine loss in the CA1 region (Wu et al., 2018). A 3x2h of 3% sevoflurane treatment induced a long-term decrease in spine density in CA1 of PND 6-8 rats (Jia et al., 2016). In PND7 mice, 6h of 2.3% sevoflurane anesthesia decreased hippocampal dendritic spine density (Bin Liu, Ou, Chen, & Zhang, 2019). Xiao et al. (2016) showed that 1h and 6h sevoflurane (3%) anesthesia of PND7 rats reduced apical dendritic spines density of CA1 pyramidal neurons at PND21 (Xiao, Liu, Chen, & Zhang, 2016).

Some studies demonstrated increased dendritic spine density under sevoflurane anesthesia. 4h of 2.5% sevoflurane exposure in PND7 mice induced considerable spine overaccount and spine alternation at PND21 (B. Zhou et al., 2019). In juvenile rats of PND16 old, a 30min sevoflurane (2.5%) anesthesia increased the apical and basal spines count in the cortex over 6h (Briner et al., 2010).

In summary, the inhaled anesthetics isoflurane and sevoflurane affect dendritic spine dynamics and remodeling in a dose-, time-, developmental stage- and brain region-dependent manner (Granak et al., 2021). However, the present studies about the modulation of general inhaled anesthetics on dendritic spine morphological alternations focus on the developmental stages. Even though a few studies have reported the effects of the inhalational anesthetics on the adult brain, further investigations are highly required.

3. Inhalational anesthetics and neurodegeneration

3.1 The neurotoxicity induced by inhalational anesthetics

Every year numerous cases of surgeries are done under anesthesia. At the same time, anesthesia-induced neurodegeneration is a matter of great concern. The adverse

neurotoxicity induced by anesthetics affects almost all ages, especially in pediatric and geriatric populations (Figure 12) (S. C. Johnson, Pan, Li, Sedensky, & Morgan, 2019).

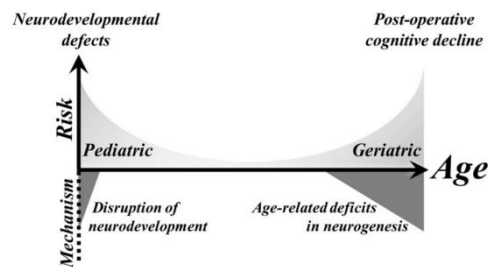


Figure 12. Anesthesia-induced neurotoxicity at extreme ages (S. C. Johnson et al., 2019).

Post-operative cognitive decline (POCD) represents syndromes with declined neuropsychological performance after anesthesia in elderly persons (Casella & Bimonte, 2017). Numerous factors, especially neuroinflammation and microglial activation, are essential to the pathophysiology of POCD (Figure 13) (Casella & Bimonte, 2017; Fodale et al., 2017; Ling, Ma, Yu, Zhang, & Liang, 2015; Vacas, Degos, Feng, & Maze, 2013; L. Wang et al., 2018).

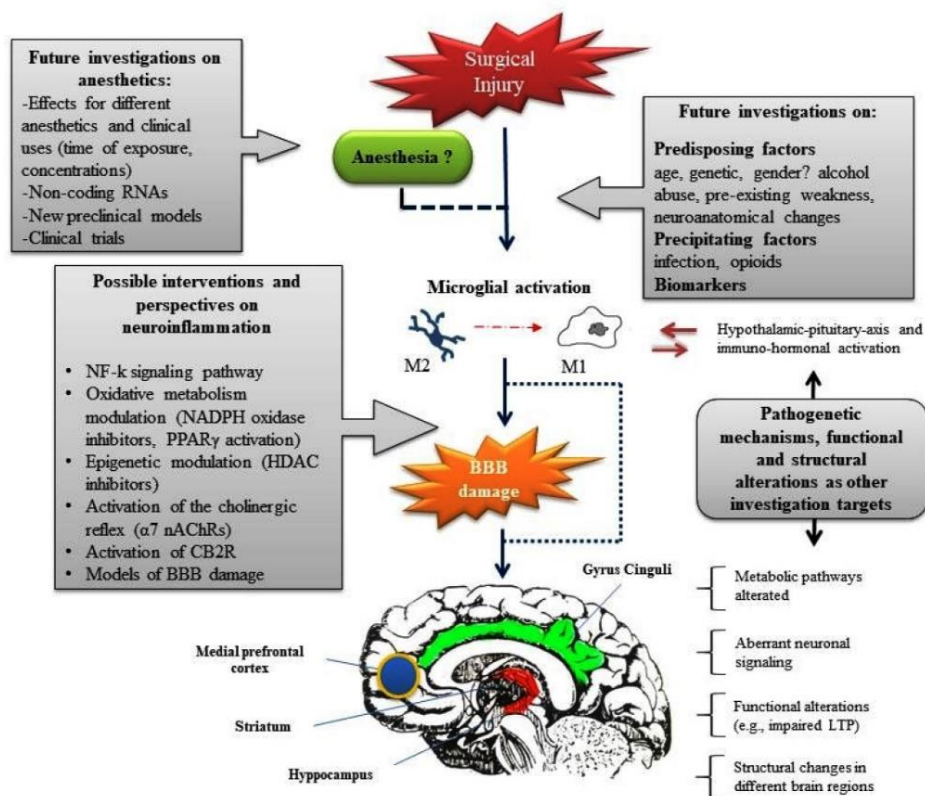


Figure 13. Mechanisms of POCD and research perspectives (Casella & Bimonte, 2017).

Annually a large number of people undergo procedures requiring anesthesia (Evered, Scott, & Silbert, 2017). New studies are still urgently required to further reveal the exact mechanism regarding the neurotoxicity and POCD induced by inhalational anesthetics, which will support the identification of novel neuroprotective strategies during anesthesia.

3.2 Alzheimer disease and amyloid cascade hypothesis

The population of the elderly increases rapidly. For example, the number of 65+ years old people globally will be from 420 million in 2000 to almost 970 million by 2030, increasing from 6.9% to 12% worldwide. The aging population will increase the largest in developing countries, and share more than half of the aged persons (to approximately 71%) worldwide (Qiu., Kivipelto., & Strauss., 2009). As the risk to develop AD is strongly associated with aging, the public health and care systems worldwide are facing extreme challenges.

3.2.1 Alzheimer disease

Senile dementia, characterized by progressive degenerative dysfunction in behavior and cognition, has been a considerable burden on individuals, caregivers, and society (Qiu. et al., 2009; Reitz & Mayeux, 2014). Around 47 million people in the world lived with this syndrome in 2016, and more than 131 million people tend to develop dementia by 2050 (*World Alzheimer Report 2016*, 2016). Of the forms of dementia, AD accounts for 50-75% proportion (*World Alzheimer Report 2009*, 2009).

In 1906, AD was first reported by Alois Alzheimer, a German psychiatrist, with a medical case report about a 51-year-old woman patient (DENNIS J. SELKOE, 2001). This was thought of as a turning timepoint for the study of AD (BERCHTOLD. & COTMAN., 1998). In 1968, AD was finally accepted as the most common form of senile

dementia (Blessed, Tomlinson, & Roth, 1968; O'Brien & Wong, 2011; DENNIS J. SELKOE, 2001).

Amyloid plaques and Neurofibrillary tangles (Figure 14) have been accepted for many years as two pathological hallmarks of AD. Amyloid plaques (Figure 14a) are a cluster of insoluble amyloid fibrils, which are accumulated extracellularly by amyloid- β ($A\beta$), a peptide with 38-43 residues (R. Vassar et al., 2014). In comparison, neurofibrillary tangles (NFTs) (Figure 14b) are aggregated by hyper-phosphorylated tau (p-tau) intracellularly (Haass & Selkoe, 2007).

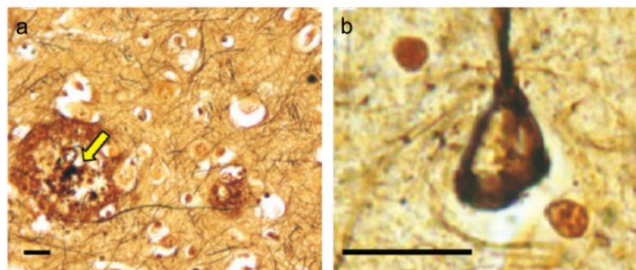


Figure 14. Pathological hallmarks of AD (O'Brien & Wong, 2011).

3.2.2 Amyloid cascade hypothesis

Even though the mechanisms of AD remain unclear, several hypotheses, such as tau hypothesis, cholinergic hypothesis, mitochondrial cascade hypothesis, and amyloid cascade hypothesis, have been proposed and studied (Barage & Sonawane, 2015; Golde, 2003; Karran, Mercken, & De Strooper, 2011; D. J. Selkoe & Hardy, 2016; Singh, Srivastav, Yadav, Srikrishna, & Perry, 2016). Thereof, only the amyloid cascade hypothesis will be discussed in this thesis. In the past decades, as new studies have been published, this hypothesis was renewed from the original amyloid cascade hypothesis to a revised new one.

Studies in the last few decades, including the early histopathological findings (Maloy., Longnecker., & Greenberg., 1981; Pepys et al., 1993; TERRY., GONATAS., & WEISS.,

1964), further biochemical (Booth et al., 1997; Castaño et al., 1986; Gustavsson, Engström, & Westermark, 1991; Westermark, Engström, Johnson, Westermark, & Betsholtz, 1990) and cell biological studies (Lopes et al., 2004), and transgenic animal models investigations (Wirak et al., 1991) had supported that amyloid fibrils were fundamental for the pathogenesis of AD (Barage & Sonawane, 2015; Ferreira, Vieira, & De Felice, 2007).

However, despite all the studies and evidence referred to in the amyloid fibrils hypothesis, it fails to explain some critical clinical and pathological issues of AD (Ferreira et al., 2007). A clinical study in 1998 showed 80%, but not 100% of demented AD patients with plaque pathology, and incipient AD patients had higher brain weights and more neurons (Katzman et al., 1988). A study in 1991 (Terry et al., 1991) presented weak relevance between psychometric indices and amyloid fibrils. Giannakopoulos et al., found the amyloid volume was of no value for the prediction of clinicopathologic correlations with NFT (Giannakopoulos et al., 2003). Intraperitoneally administration with BAM-10 to recognize the A β peptide, Linda A et al., found the memory deficits of Tg2576 animals could be fully reversed, indicating that A β is a potential target to improve memory of AD patients (Dodart et al., 2002). Similar to this report, Jean-Cosme Dodart et al., used another antibody m266, a monoclonal antibody specific for A β , to increase A β plasma concentration and reduce the deposition of A β in an AD transgenic mouse model. They showed that the application of m266 could quickly restore memory impairments with no alternations of plaque deposition (Kotilinek et al., 2002). Those controversial findings puzzled scientific researchers for a long time.

More recent studies have proposed an alternative suspect responsible for AD: soluble amyloid oligomers (A β Os) (Ferreira et al., 2007). Thus, a modified version of the

amyloid cascade hypothesis was proposed (Figure 15): once the $A\beta_{42}$ oligomers are formed and accumulated to plaques, a cascade of events is triggered thereafter and induced biological and neurological symptoms of dementia (Hardy & Selkoe, 2002; Klein, Krafft, & Finch, 2001).

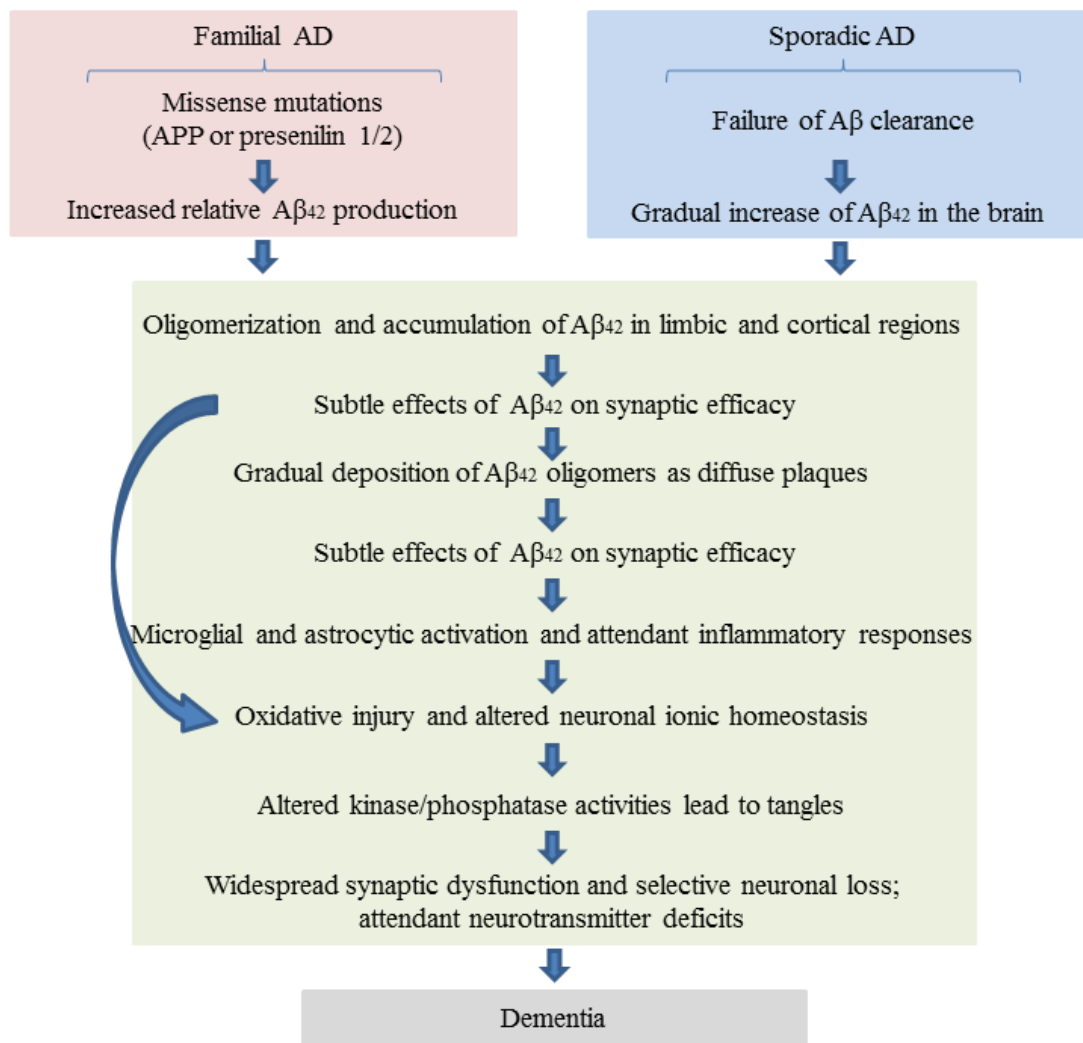


Figure 15. The amyloid cascade hypothesis (D. J. Selkoe & Hardy, 2016; Singh et al., 2016).

$A\beta$ represents peptides of 36-43 amino acids (Ferreira, Lourenco, Oliveira, & De Felice, 2015). The molecular weight of $A\beta$ is 4 kDa. It is derived from the proteolytic cleavage of APP. Full-length APP molecule is cut by β - as well as γ -secretases to generate $A\beta$ -monomers, which form oligomers and amyloid fibrils thereafter. Biologically, $A\beta$ -monomers are not neurotoxic, but can easily aggregate into toxic oligomers.

Accumulating reports indicate that soluble A β oligomers are able to induce neurotoxicity and lead to neurodegeneration (Salahuddin, Fatima, Abdelhameed, Nusrat, & Khan, 2016).

Firstly, increased levels of soluble A β oligomers were detected in Alzheimer's subjects as well as in transgenic AD mouse models (Ferreira et al., 2007). Early studies showed that soluble A β expressions were enhanced in brain tissues, cerebrospinal fluid (CSF), as well as smooth muscle cells of vessel walls of Alzheimer patients (Kuo. et al., 1996; Tabaton et al., 1994; Wisniewski, Zoltowska, & Frackowiak, 1994). Moreover, later findings showed that the A β oligomer levels in AD brains reached approximately 70x over controls (Y. Gong et al., 2003). In the CSF from the AD patients, the A β oligomer levels were consistently higher than that of non-demented age-matched controls (Georganopoulou et al., 2005). The above-mentioned elevated soluble oligomers appear to locate in the cortex, a brain region fundamental for cognition, of Alzheimer's subjects (Lacor et al., 2004). Moreover, the soluble A β oligomers in several transgenic models, including Tg2576, 3xTg-AD, and Tg6799 mice, were increased (Lesne et al., 2006; Ohno et al., 2006), which supports the hypothesis that A β oligomers are critical for AD pathogenesis.

Secondly, direct evidence has been reported to show soluble A β oligomers induce morphological and biophysiological changes. In the frontal cortex, a brain region responsible for cognition, but not in the cerebellum, Omar M. A. El-Agnaf et al., reported that fresh A β soluble oligomers solutions are harmful to SH-SY5Y cells derived from human neuroblastoma (El-Agnaf, Mahil, Patel, & Austen, 2000). Data from seven transgenic mouse lines indicated inverse correlations between soluble A β in the hippocampus and synaptophysin, a presynaptic marker, levels (Klein et al., 2001). Lambert et al., showed that A β -Derived Diffusible Ligands (ADDLs) were

diffusible and extremely potent central nervous system neurotoxins. ADDLs could evoke cell death at nanomolar doses by binding to some particular cell surface proteins. Furthermore, pre-incubation with 50nM of ADDLs disrupted LTP within an hour in hippocampal slices (Lambert et al., 1998). Our previous reports have demonstrated that A β dose-dependently blocked LTP (Rammes et al., 2015).

Moreover, despite the fact that the precise mechanisms of how soluble A β oligomers exert toxic effects on neurons are largely not clear, several possible hypotheses and mechanisms have been addressed (Ferreira et al., 2007). Those mechanisms are reviewed by Ferreira and his colleagues and listed as follows: deregulation of calcium homeostasis and oxidative stress, interactions with cell surface receptors, A β oligomers downstream target tau, and intracellular A β oligomers. They published another review thereafter and described that A β oligomers interact possibly with glutamate receptors, prion protein, frizzled receptors, neuroligin, Sigma-2/PGRMC1 receptor, and other receptors directly and/or indirectly (Ferreira et al., 2015).

3.3 Amyloid precursor protein structure and function

3.3.1 The structure of APP and its proteolysis process

APP refers to one related protein family including APP, APLP1, and APLP2 (O'Brien & Wong, 2011). In this protein family, only APP can generate amyloidogenic fragments, namely A β (Cousins, Dai, & Stephenson, 2015; Mueller, Deller, & Korte, 2017; O'Brien & Wong, 2011). The single gene encoding APP is positioned at chromosome 21 of human beings (Goate. et al., 1991). Three of eight alternative splicing isoforms (according to the differential splicing of exon 7 (Allinson., Parkin., Turner., & Hooper., 2003)) of APP transcript are well known, which are APP695, APP751, and APP770 (O'Brien & Wong, 2011; Y. W. Zhang, Thompson, Zhang, & Xu, 2011).

As is a type I single transmembrane protein (Mueller et al., 2017). Within the A β peptide domain, three sites are cleaved by secretases (Figure 16). The α -secretase is a group of zinc metalloproteinases that can cut APP between Lys¹⁶ and Leu¹⁷ (Thinakaran & Koo, 2008; Robert Vassar, 2004). The most common form of α -secretases is a disintegrin and metalloproteinase domain protein (ADAM) 10 (Mueller et al., 2017; Prox et al., 2013). The β -site APP-cleaving enzyme 1 (BACE1) consists of 501 amino acids (Robert Vassar, 2004). BACE1 can cleave the A β domain at Asp¹ and Glu¹¹ (β' -cleavage site) (R. Vassar et al., 2014). The γ -secretase consists of presenilin, nicastrin, anterior pharynx defective 1, and presenilin enhancer 2. It cleaves APP at multiple positions, through which both A β ₄₀ (90%) and A β ₄₂ (10%) are generated (D. J. Selkoe & Wolfe, 2007; Thinakaran & Koo, 2008; Y. W. Zhang et al., 2011).

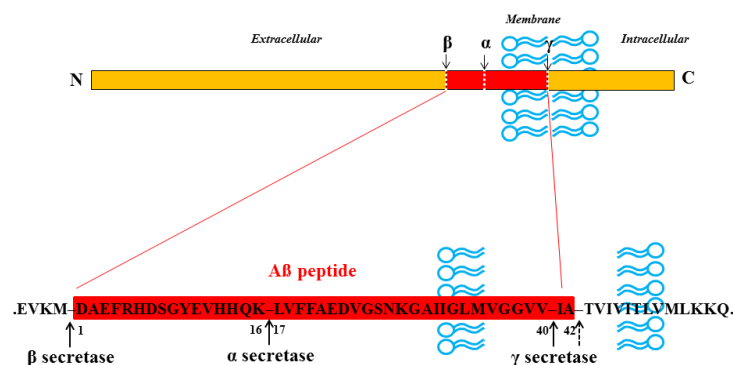


Figure 16. APP schematic structure (O'Brien & Wong, 2011; Thinakaran & Koo, 2008).

Physiologically and pathologically, APP undergoes complicated proteolytic processing and produces several biologically active fragments that have multiple functions (Mueller et al., 2017). There are two canonical APP proteolysis pathways, ie. the non-amyloidogenic pathway and the amyloidogenic pathway (Figure 17), through which different molecules are generated.

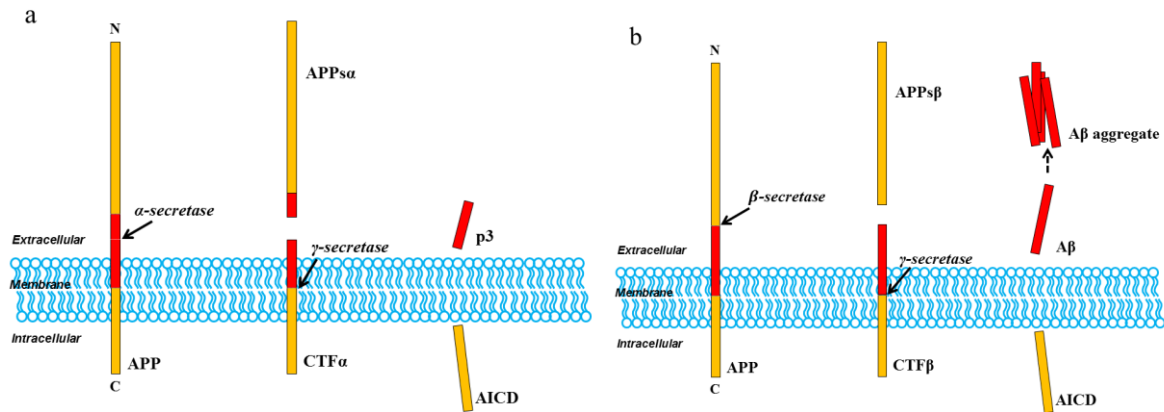


Figure 17. Two pathways of APP proteolysis processing (O'Brien & Wong, 2011; Thinakaran & Koo, 2008).

3.3.2 APP functions

Several studies have been done to investigate the biological functions of APP (Mattson, 1997; Mueller et al., 2017; Sosa et al., 2017; Thinakaran & Koo, 2008; van der Kant & Goldstein, 2015; Zheng & Koo, 2011). Generally speaking, APP functions as a cell receptor (Mattson, 1997), to be interacted with cells (Cousins et al., 2015), and as a synaptic adhesion molecule (Deyts, Thinakaran, & Parent, 2016; Mueller et al., 2017).

APP can function similarly to Notch, a membrane-bound transcription factor (Mueller et al., 2017). Besides, APP binds to the secreted molecule F-spondin and is actively involved in neuronal activity (Ho. & Südhof, 2004). Moreover, APP also binds to Netrin-1 to trigger AICD-dependent gene transcription and suppress A β production (Rama et al., 2012). Via interaction with the GluN1 subunit, APP family members co-immunoprecipitated with GluN1/GluN2A as well as GluN2B. They further regulate the homeostasis of the cell surface NMDA receptor (Cousins et al., 2015). The APP structural features, namely the extracellular and cytoplasmic domains, suggest that the APP potentially functions via cell adhesion (Mueller et al., 2017) (Figure 18). Further studies have shown that APP family indeed functions as a cell adhesion molecule and plays a role in synaptic plasticity (Schilling et al., 2017).

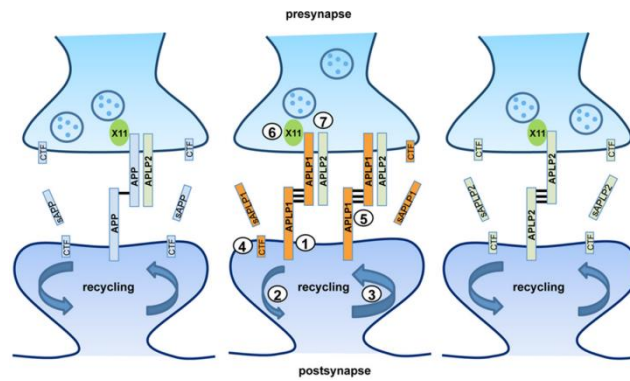


Figure 18. APP family functions at the synapse (Schilling et al., 2017).

APP is critical for morphological and functional maintenance in the central nervous system. Firstly, APP plays an important role in neuronal development (Mueller et al., 2017). By using both wildtype and APP knockout mutant mice, a study reported that during the embryonic development in the cortex, APP controlled the cell cycle progression (López-Sánchez, Müller, & Frade, 2005). Surprisingly, APP-TAG1 (a member of the F3 family, and F3 belongs to Glycophosphatidylinositol-linked recognition molecules) signaling pathway negatively modulated neurogenesis (Q. H. Ma et al., 2008). Moreover, mice lacking APP have shown decreased brain weight and forebrain commissures (Magara et al., 1999).

Besides, APP is also intensively involved in axonal growth and guidance (Mueller et al., 2017). One report revealed that APP/FE65 complex was critical to neuronal membrane stability, neuritogenesis, and synaptic modification (Sabo, Ikin, Buxbaum, & Greengard, 2003). APP is co-localized with integrins, a group of transmembrane receptors, in neural cells and axons, to enhance the viability and polarity of neurons (Perez., Zheng., Ploeg., & Koo., 1997; Yamazaki., Koo., & Selkoe., 1997). Intriguingly, a study found that neurons lacking APP or deletion of APLP1/APLP2 or exposure to sAPP α underwent neurite elongation (Young-Pearse, Chen, Chang, Marquez, & Selkoe, 2008).

Thirdly, APP is essential to dendrite complexity, spine counts, and spine dynamics (Mueller et al., 2017). Using APP^{-/-} mice, a study reported that the length of the dendrites as well as the arborization of hippocampal neurons were significantly impaired (Tyan et al., 2012). APP overexpression in cultured hippocampal neurons increased spine density. At the same time, the downregulation of APP decreased dendritic spine numbers (Lee et al., 2010). Furthermore, APP/APLP2 mutant mice exhibited synapse abnormalities. In adult APP/APLP2 double knockout mice, a prominent deficit of dendrites and synapses was found in the CA1 region (Hick et al., 2015).

Last but not least, APP is important for synaptic plasticity and cognition (Mueller et al., 2017). Studies in AD patients indicated that synapse loss was highly related to alternations in cognition (Terry et al., 1991). Moreover, a report published in Nature Medicine in 2008 showed that with the applications of soluble A β oligomers derived from AD patients, hippocampal LTP in normal rodent hippocampus was inhibited, whereas long-term depression (LTD) was enhanced, along with spines reduction (Shankar et al., 2008). Further reports have shown that only aged APP^{-/-} mice exhibited abnormal potentiation as well as behavior performance (Dawson et al., 1999; Ring et al., 2007).

3.4 BACE1 structure and function

BACE1 is a type I transmembrane molecule consisting of 501 amino acids. The D-T/S-G-T/S motifs of BACE1 are characteristic, and they are critical for its activity (Figure 19) (Dislich & Lichtenthaler, 2012; Yan et al., 1999). BACE1 accommodates up to 11 substrate residues due to its broader, more open, and less hydrophobic active cleft (Dislich & Lichtenthaler, 2012; Hong et al., 2000; Turner, Hong, Koelsch, Ghosh, &

Tang, 2005). Including APP, SEZ6, and CHL1, BACE1 has more than 35 substrates (L. Zhou et al., 2012; Zhu et al., 2018).

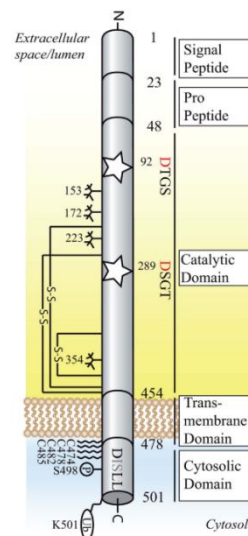


Figure 19. BACE1 structure (Dislich & Lichtenthaler, 2012).

BACE1 is enriched in the hippocampus (Yan et al., 1999). It has been shown that the mRNA expressions of BACE1 are the highest in the brain and significantly lower in other tissues (R Vassar & Cole, 2007). This is in line with the findings that BACE1 expressions in neurons are much higher than that in resting glial cells (Harada et al., 2006; Sinha et al., 1999; Yan et al., 1999). Moreover, the BACE1 expressions are developmentally regulated (Dislich & Lichtenthaler, 2012).

The cleavage by BACE initiates the amyloid cascade for neurodegeneration. An upregulation of BACE1 expression levels is reported both in human and AD mouse model brains. In AD patients, a dramatic increase in BACE1 expressions and a nearly two-fold increase of CTF β were reported (Holsinger, McLean, Beyreuther, Masters, & Evin, 2002). Of the Tg2576 and hAPP KM670–671NL (hAPPSw) transgenic mice, the BACE mRNA expression patterns are in similar anatomical localizations with A β deposition (Irizarry, Locascio, & Hyman, 2001). In AD mouse brains, the increased

BACE1 is generated in the survived neurons instead of the normal neurons in control brains (Harada et al., 2006).

BACE1 is fundamental for the amyloidogenic pathway and its activity limits the A β production rate. Studies have shown that including hypoxic and oxidative cell stress mechanisms (Tamagno et al., 2005), numerous mechanisms are regulating BACE1 activity (Dislich & Lichtenthaler, 2012; Stockley & O'Neill, 2008). Recent evidence indicates that the general inhaled anesthetics, including isoflurane and sevoflurane, can regulate BACE1 levels and will be discussed in this thesis.

3.5 Regulation of APP processing by inhaled anesthetics

Recent studies have indicated that inhalational anesthetics are involved in the abnormal modulation of APP processing (Jiang & Jiang, 2015).

Studies have demonstrated that isoflurane anesthesia increased BACE protein expressions (Xie et al., 2008) and APP mRNA levels (S. Zhang et al., 2017). Furthermore, isoflurane anesthesia enhanced A β secretion, aggregation, and oligomerization levels (Eckenhoff et al., 2004; Xie et al., 2008; S. Zhang et al., 2017). The accumulated A β levels tended to induce further cellular apoptosis (Xie et al., 2007b).

Roderic G et al. reported an increase in A β oligomerization rates by isoflurane anesthesia (Eckenhoff et al., 2004). Zhongcong et al. reported that in H4 human neuroglioma cells, a 2% isoflurane treatment for 6h dose-dependently evoked cellular apoptosis (Xie et al., 2006). They further demonstrated in another study that 6h of 2% isoflurane exposure in the H4-APP cells increased BACE levels as well as secreted A β levels (Xie et al., 2007a). Moreover, the isoflurane-induced accumulation of aggregated A β in turn promoted apoptosis (Xie et al., 2007a). The further in-vivo study

investigated, isoflurane (1.4%, 2h) evoked caspase activation and modestly elevated BACE expressions 6h after exposure. Moreover, up to 24 hours following treatment, isoflurane evoked caspase activation and upregulated BACE as well as A β expressions. They hypothesize that isoflurane might upregulate BACE expressions by reduction of BACE degradation. These above observations indicate that isoflurane anesthesia probably enhanced AD neuropathogenesis (Xie et al., 2008).

Sevoflurane anesthesia increases BACE and A β levels in a similar way compared with isoflurane (Dong et al., 2009; B. Liu, Xia, Chen, & Zhang, 2017). Yuanlin et al. found that 4.1% sevoflurane exposure for 6 hours in human H4 neuroglioma cells induced apoptosis, elevated BACE levels, and increased A β expressions (Dong et al., 2009). They further demonstrated that mice anesthetized with sevoflurane (2.5%, 2h) also increased BACE as well as A β levels. Bin et al. reported that mice at PND7 exposure with 3% sevoflurane for 6h upregulated BACE1 expression (B. Liu et al., 2019).

Of note, modulation of BACE activity partly reversed the anesthetics-mediated aberrant APP proteolysis procedure (Eckenhoff et al., 2004; S. Zhang et al., 2017). However, investigations are highly required to better demonstrate the BACE activity effects during anesthesia on physiological and morphological remodeling in the adult hippocampus. In addition, no experiments have been conducted about how xenon affects APP proteolysis processing.

3.6 Xenon functions as a neuroprotective anesthetic

The noble gas xenon was first discovered in 1898 by Ramsey and Travers in the procedure of distilling liquefied air (Joyce, 2000). It was later applied as an anesthetic in human beings in 1951 (Cullen & Gross, 1951; Joyce, 2000). In comparison with the other anesthetics, xenon has been revealed with several favorable characteristics, for example in the aspects of safety, cardiovascular stability, beneficial pharmacokinetics,

analgesia, and, especially and importantly, neuroprotection (Sanders, Ma, & Maze, 2004).

The neuroprotective properties of xenon have been reported by numerous studies (Homi et al., 2003; W. Liu, Khatibi, Sridharan, & Zhang, 2011; D Ma, Wilhelm, Maze, & Franks, 2002; Tonner, 2006). With a neuronal-glia cell coculture from mice, a study reported that xenon is neuroprotective against injury either evoked by glutamate, NMDA, or oxygen deprivation in a concentration-dependent manner (Wilhelm, Ma, Maze, & Franks, 2002). Ma et. al. found that xenon did not increase the immediate early gene-encoded protein c-Fos to accelerate neuronal injury. Meanwhile, ketamine and N₂O were shown to dose-dependently upregulated c-Fos expressions (Figure 20) (D Ma et al., 2002). In another study, 65% atm xenon application was able to attenuate the neurological and neurocognitive dysfunction in rats subjected to a neural injury (Daqing Ma et al., 2003).

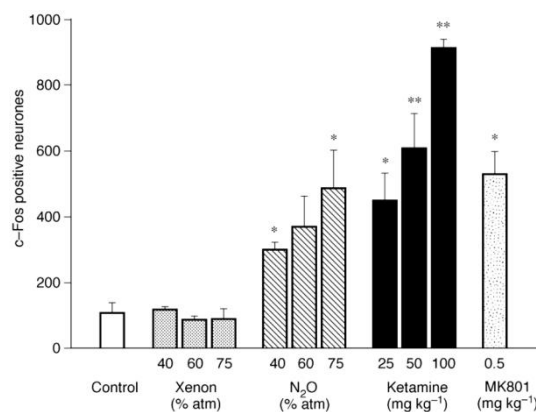


Figure 20. c-Fos expressions by treatment of xenon, N₂O, and ketamine (D Ma et al., 2002).

The reports from us illustrated that xenon affects the NMDA, AMPA, and HCN but not GABA_A receptors (Mattusch et al., 2015). Inhibiting NMDA receptor at its binding site was thought to be an essential mechanism of xenon action (Figure 21) (Alam et al., 2017; Yamakura & Shimoji, 1999). Inhibiting the NMDA receptor hinders the cation

Ca²⁺ and Na⁺ influx into the cytoplasm to trigger various anesthetic actions. Besides, the pathways of PI3K-Akt-mTOR and MARK are also enhanced by xenon exposure. Although the exact mechanisms regarding those alternations are still not clear, an increase in the efficiency of HIF-1 α , VEGF, and erythropoietin is observed in ischemic brain injury (Figure 21) (Alam et al., 2017).

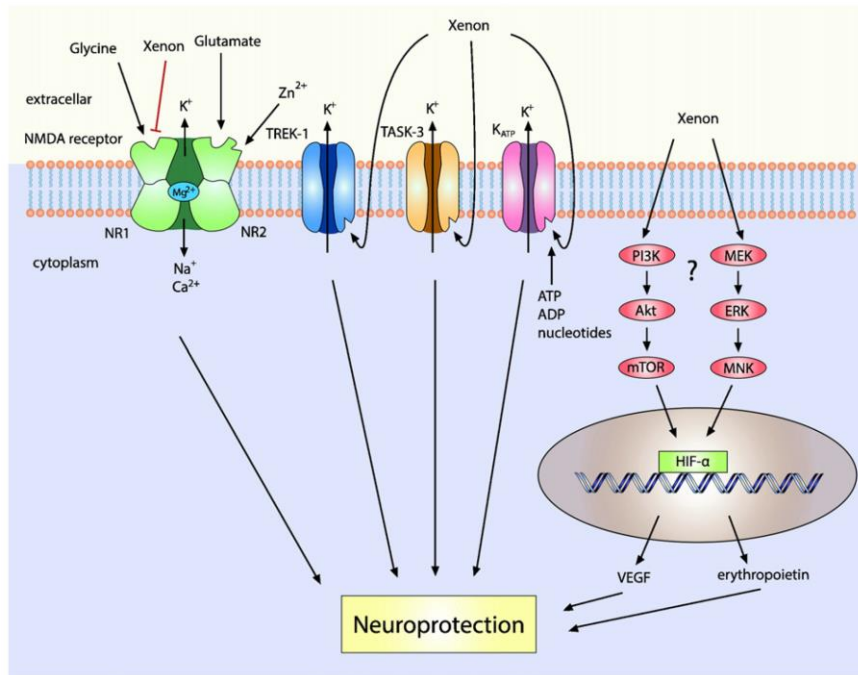


Figure 21. The mechanism of xenon action (Alam et al., 2017).

The mechanisms of the noble gas xenon have been under investigation over the years. However, the gaseous anesthetic xenon effects on dendritic spine dynamic and remodeling have yet not been reported.

4. Nectin-3 and the regulation of synaptic plasticity

Nectins represent immunoglobulin-like transmembrane cell adhesion molecules (Figure 22). The nectins family consists of nectin-1, -2, -3, and -4. They are expressed ubiquitously (Takai, 2003). The molecular structure of nectins is shown in Figure 22 (Mori, Rikitake, Mandai, & Takai, 2014).

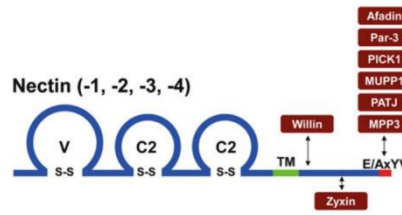


Figure 22. Nectins structure and the binding proteins (Mori et al., 2014).

Nectins exhibit a few molecular properties. First, nectins exhibit a Ca^{2+} -independent intracellular cell adhesion property. Second, they can activate several proteins. Third, nectins bind to afadin and partition defective three homologues (Par-3). Fourth, nectins interact heterophilically with necls and other Ig-like CAMs through their extracellular regions. Fifth, they interact with some growth factor receptors (Mori et al., 2014). Of those, primarily, nectins regulate cell-cell adhesions.

In the hippocampus, nectin-1 and -3 are asymmetrically positioned at either pre- or post-sites of the synapses. Nectin-1 and -3 heterophilic trans-interactions contribute to the stabilization of the axon-dendritic adhesion (van der Kooij et al., 2014), learning, and memory (X. X. Wang et al., 2017).

In the CNS, either nectin-1 or -3 expression is developmentally regulated. In C57BL/6J mice, both protein levels are gradually elevated from the embryonic period, peak at around 9th days after birth (X. X. Wang et al., 2017) to 14 (Shiotani et al., 2017), and decrease sharply afterward, especially in the animals over 1 year old (Shiotani et al., 2017).

Biologically, nectin levels are modulated partly by the stress-related system. In the developmental and adult hippocampus, both nectin-3 mRNA and protein expressions were downregulated in mice that underwent stress (X. D. Wang et al., 2013). One study showed that chronic restraint stress slightly reduced nectin-1 protein levels, and significantly reduced nectin-3 (van der Kooij et al., 2014) levels. With the chronic social

defeat stressed mice, researchers reported that the nectin-3 mRNA expressions in the cortex were reduced (Q. Gong et al., 2018).

Studies have shown the abnormal nectin-3 expressions on morphologies and functions of the hippocampus (R. Liu et al., 2019; X. X. Wang et al., 2017). Hippocampal nectin-3 downregulation by adeno-associated virus (AAV) in adult mice evoked CA3-spine loss (X. D. Wang et al., 2013), which attenuated in adult mice the behavior performance (R. Liu et al., 2019). In addition, nectin-3 overexpression in the adult hippocampus recused spine elimination, spine volume changes, and hippocampus-dependent memory deficits induced by early-life stress (X. D. Wang et al., 2013). Moreover, the downregulation of nectin-3 in adult dentate gyrus modulated differentiation and maturation of the newly generated granule neurons (X. X. Wang et al., 2017). Those morphological changes in the hippocampus induced impaired long-term spatial memory (X. D. Wang et al., 2013). They showed in one study that nectin-3 downregulation in newly-generated dentate granule cells decreased spine density, especially thin type spines. The abnormalities further evoked long-term spatial memory deficits (X. X. Wang et al., 2017). Furthermore, hippocampal nectin-3 suppression during the postnatal stage significantly impaired dendrites morphology and spine counts of pyramidal neurons (R. Liu et al., 2019). Compared with nectin-3 suppression findings, nectin-1 knockdown in postnatal mice only reduced stubby spines loss in the CA3 region (R. Liu et al., 2019). Those studies highlight that nectins, particularly nectin-3, are predominant for both developmental and adult hippocampal function and structure.

Aim of the dissertation

The present thesis aims to gain an investigation about the mechanism of inhalational anesthesia on the BACE-dependent APP proteolysis process as well as the spine plasticity of the hippocampus.

In order to fulfill the above goal, the following objectives are listed as:

- To illustrate whether and how the inhalational anesthetics affect LTP and dendritic spine morphology in the CA1 region
- To examine whether and how the inhalational anesthetics affect hippocampal mouse $A\beta_{1-42}$ levels, APP-processing related molecules, and nectin-3 expressions
- To investigate the effects of mouse $A\beta_{1-42}$ oligomers on CA1-potentiation as well as dendritic spine density
- To test nectin-3 downregulation on potentiation and spine dynamics in CA1
- To evaluate the effects of the BACE inhibitor LY2886721 at 3 μ M for 2h application on LTP and hippocampal $A\beta_{1-42}$ levels
- To study the effects of BACE inhibition during inhalational anesthesia on LTP, mouse $A\beta_{1-42}$ levels, APP-proteolysis-process related molecules, and nectin-3 expressions in the hippocampus

Materials and Methods

1. Mice

C57BL/6J and Thy1-eGFP adult male mice were used in the present thesis. The mice were of 8-12 weeks old. They were bought from Charles River company in Munich, Germany. All mice were single-housed under standardized conditions. The light/dark cycle was set at 12:12 h. The room temperature (RT) was set at 22 ± 2 °C (60% humidity). Standard food as well as tap water were supplied. All mice were assigned to each group randomly. All procedures were done in accordance to a formal document (Zhu et al., 2018).

2. Compounds

2.1 Inhalational anesthetics

Isoflurane, sevoflurane, and xenon were used in this thesis. During all procedures regarding xenon application, the oxygen supply should be sufficient and the pH value should be maintained at 7.2-7.4. This is why the maximum concentration of xenon for sections incubation is up to 65%, ie. 1.9 mM in artificial cerebrospinal fluid (aCSF) (Haseneder. et al., 2008). Thus, xenon application was performed by gassing a mixture of 65% xenon, 30% O₂, and an additional 5% CO₂ (Kratzer. et al., 2012). The control gas was therefore applied by a nitrogen mixture gas (65% N₂, 30% O₂, 5% CO₂). Both gas mixtures were applied in exchange for carbogen gas (95% O₂, 5% CO₂).

For comparability and to ensure equipotent concentrations of anesthetics according to MAC_{mouse}, the applied concentration of either isoflurane or sevoflurane was at 0.6% (0.21 mM) and 1.4% (0.29 mM). These concentrations were equal approximately to MAC_{awake} (Aranake et al., 2013). Isoflurane and sevoflurane have been supplied by a vapor together with a carbogen gas mixture.

2.2 Mouse A β ₁₋₄₂

The mA β ₁₋₄₂ (#AG542) from Sigma-Aldrich of Germany was used. The compound was suspended in hexafluoroisopropanol (37°C, 1.5h), lyophilized, and then dissolved in DMSO and aCSF to 50nM.

2.3 BACE inhibitor

The beta-secretase inhibitor (Figure 23) used in this thesis was LY2886721 (#S2156, Selleck Chemicals, Houston, TX, USA) (Satir et al., 2020). The drug was sequentially dissolved in DMSO and aCSF to 3 μ M.



Figure 23. LY2886721 structure.

3. Hippocampal slices preparation

Animals were anesthetized with an appropriate amount of isoflurane and then decapitated. Brains were quickly removed and put into aCSF containing ice (Hofmann et al., 2021). Sagittal brain sections were cut at 350 μ m thickness with a vibratome (VT1000 S, Leica, Germany). Sections were transferred to aCSF at 35°C for 0.5h, followed by recovery for at least 1h at RT (Haseneder. et al., 2008; Kratzer. et al., 2012).

4. field excitatory postsynaptic potentials (fEPSPs) recordings

The fEPSPs were recorded in the stratum radiatum region in CA1 of the brain slices (Haseneder. et al., 2008). As shown in Figure 24, two bipolar tungsten electrodes and one recording borosilicate micropipette were applied to trigger two distinct stimulations.

fEPSPs data from either fiber population were used either as an internal control (ctl) or treatment group.

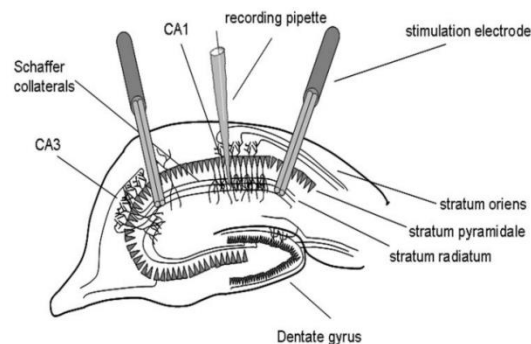


Figure 24. Sagittal hippocampal slice (Kratzer. et al., 2012).

fEPSPs were triggered via one of two electrodes. The voltage pulse was 50- μ s. A stimulus at 15-s intervals of each electrode was delivered alternatively. To minimize noise signals, the average data of two consecutive fEPSPs were calculated. For the baseline recordings, I modified the stimulation to obtain a response of around half amount of the maximal maintainable response. The fEPSPs slope data of the rising phase, ie 20%-80% of the peak amplitude (Figure 25), were used to quantify the synaptic transmission strength. After fEPSPs curve gets stabilized, recordings were kept for at least 20min.

A high-frequency stimulation (HFS, 100Hz, 1s) was applied to trigger LTP. fEPSP slopes were continuously recorded for another 1h without alternating the rate of stimulation. Slopes were normalized with data recorded within the last 20 min before the triggering of HFS.

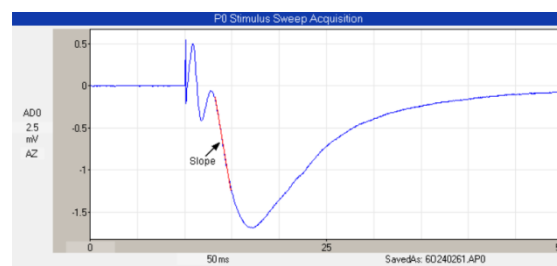


Figure 25. Typical fEPSP curve (<https://www.winltp.com/OverviewOfWinLTP.html>).

Either anesthetic or LY2886721 was added after the first HFS (HFS1) triggering. The recording of the potentiation was sustained for 1h. Either anesthetic isoflurane, sevoflurane, or xenon was thereafter added to the aCSF. 1.5h later, the secondary HFS (HFS2) was delivered followed by the recording of the fEPSP slopes for another 1h. The baseline data of the secondary potentiation was from the fEPSP slopes obtained 20min before the delivery of HFS2.

For the co-incubation of LY2886721+anesthetics groups, the BACE inhibitor was added to aCSF before the transfer of brain sections to the recording chamber. 2h later, HFS1 was delivered, and fEPSPs were recorded for 1h. Either anesthetic was applied for 1.5h. Then HFS2 was triggered with an additional recording for 1h.

Two electrodes were used for the LTP recordings with the brain sections of the AAV-infected mice, whereas, the CA1-potentiation was evoked only in one input.

5. Stereotaxic virus injection

The short hairpin RNA (shRNA) sequence which targets nectin-3 5'-TGTGTCCTGGAGGCGGCAAAGCACAACCTT-3' has been validated according to previous work (R. Liu et al., 2019; X. D. Wang & Schmidt, 2016; X. X. Wang et al., 2017). The commercial AAV-shNectin-3 (AAV9-CMV-Nectin3.shRNA-terminator-GFP-hGH-amp, $>1 \times 10^9$ viral genomes/ml) and scrambled control virus (AAV9-CMV-Scrambled.shRNA-terminator-GFP-hGH-amp, 3.5×10^{12} viral genomes/ml) were provided by Applied Biological Materials Inc. (abm; Figure 26).

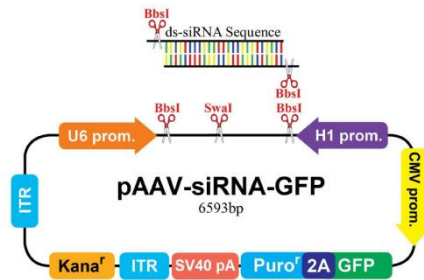


Figure 26. Full vector sequence for Pvr13 AAV siRNA pooled virus (Serotype 9, from abm).

As described previously, I performed the microinjection with AAV shown above (X. D. Wang & Schmidt, 2016; X. X. Wang et al., 2017). Shortly to say, 0.5 μ l virus was injected to both sites of the CA1 region of the mice. A Hamilton syringe (1 μ l, Hamilton, 7001) along with a 33-gauge needle (Hamilton, 65461–01) were used for the virus delivery. The syringe was connected to an injection pump and the rate of the delivery was set at 0.05 μ l/min.

The bregma was set as point 0. Thereafter, the injection site was located 1.8mm back from the bregma and 1.2mm lateral from the midline. After the injection point was set well, a bit was used to make a hole in the skull. After I have seen the brain surface under a microscope, the needle was put gently into the brain tissue till 1.4mm deep inside. During the injection, the mice were anesthetized with a sufficient amount of isoflurane. Animals were allowed recovery for 14 days to induce sufficient virus infection before CA1-potential recordings were performed.

6. Immunofluorescence

After fEPSPs recordings, the brain sections were sequentially transferred into 4% paraformaldehyde (PFA, Merck, Germany) for 24h and 30% sucrose for 36h. Thereafter, slices were cut into 40 μ m thickness with a cryostat (CryoStar NX70, Thermo Fisher Scientific, Germany).

On the first day of staining, brain slices at 40 μm were washed at RT with 0.1M PBS for 3 x 10 min, which was followed by pre-incubated with blocking buffer (0.1M PBS + 10% normal goat serum (NGS; G9023, Sigma Aldrich, Germany) + 0.3% Triton-X-100 (Sigma Aldrich, Germany)) for 1h. Thereafter, primary antibodies (Table 10) were applied and sections were put on a shaker at 4°C overnight. On the second day, after a thorough wash, the slices were treated with secondary antibodies (Alexa Fluor 488/594-conjugated goat anti-mouse/rabbit antibodies, 1:500; Invitrogen, Carlsbad, CA, USA) at RT for 3h. After 3 x 10 min washes, sections were mounted and coverslipped (Dako Mounting Medium; S2023, Dako North America, United State) (X. Wang et al., 2017).

Name of the antibody	Concentration	Information
mouse anti-APP (22C11)	1:1000	#14-9749-82, Thermo Fisher
rabbit anti-nectin-3	1:1000	sc-ab63931, abcam, UK
rabbit anti-GFP	1:500	#A-11122, Thermo Fisher Scientific, Germany

Table 10. Primary antibodies used in immunofluorescence.

Images from 4-8 sections per mouse with the Zeiss Microscope (Carl Zeiss Microscopy GmbH, Germany) were obtained. The colocalization profiles of APP and nectin-3 were quantified by Imaris software (Oxford Instruments, UK).

7. Immunohistochemistry

After LTP recordings, brain sections were put in 4% PFA for 24h and 30% sucrose for 36h. Brain sections at 40 μm thickness were prepared for immunohistochemistry.

On day one, sections were first rinsed with 0.1M PBS for 3 x 10 min. Then hydrogen peroxide block was applied for 10min. After rinsing, a blocking buffer was added at RT for 1h. Thereafter, primary antibodies of APP (mouse anti-APP (22C11), 1:2000, #14-9749-82, Thermo Fisher) and nectin-3 (mouse anti-nectin-3 (H-11), 1:1000; sc-271611, Santa Cruz) were applied. Sections were put on a shaker overnight at 4°C. On day two, after washes, biotinylated goat anti-mouse polyvalent was applied at RT for 2h on the

shaker. Following 3 x 10 min washes with 0.1M PBS, streptavidin peroxidase was applied at RT for 2h. After 3 x 10 min rinses with 0.1M PBS, 3,3'-Diaminobenzidine Horseradish Peroxidase Color Development Kit was applied for 10min. Thereafter, sections were washed with ddH₂O for 2 x 10 min and transferred onto slides. EtOH at concentrations of 70%, 95%, and 100% (5 min of each) was applied to dehydrate the brain sections. In the end, slices were treated with Xylene (3 x 5 min) and coverslipped.

Using the Zeiss Microscope, images (4-8 slices/mice) were obtained for the quantification of both nectin-3 and APP. ImageJ software (National Institute of Health, Bethesda, MD, USA) was used to quantify the relative protein expressions (protein levels = optical grey density of the region of interest - optical grey density of the corpus callosum). The corpus callosum region was lacking in staining, thus this region was used as the background (R. Liu et al., 2019). Data were shown as 100% of the control.

8. Western blot

Tissues of the hippocampus were collected after CA1-LTP recordings. Ice-cold lysis buffer (Table 11) was applied to homogenize the tissue for 15min. Thereafter, tissues were centrifuged (12000rpm, 4°C, 30min). The supernatant was stored for further usage.

Name of the product	Amount/100µl	Information
Protease Inhibitor Cocktail tables	2µl, 50x	Roche, Switzerland
Pepstatin	0.1µl	P5318, Roche, Switzerland
Phenylmethylsulfonyl fluoride	0.1µl, 100x	#7626, Sigma Aldrich, Germany
RIPA buffer	97µl	R0278, Sigma Aldrich, Germany

Table 11. Lysis buffer for western blot.

Proteins lysate was diluted into 1:5 and 1:10 with ice-cold lysis buffer, vortexed, and centrifuged for 30s. Milli-Q water, pre-diluted protein standard assay, and diluted protein samples were added and placed on a shaker for 30min at RT. Protein

concentrations were measured by absorbance microplate reader at the absorption of $\lambda=620\text{nm}$ into $1\mu\text{g}/\mu\text{l}$ or $2\mu\text{g}/\mu\text{l}$ with 4x sample buffer. Proteins were heated at 95°C for 5 min and then stored.

The glass plates were cleaned with EtOH and Mill-Q water and air-dried, after which plate sandwiches were made. Separating gels cocktails (Table 12) were prepared and applied to each gel with 1.0mm spacers for polymerization for 40 min. 1ml Milli-Q water was filled onto the gels to avoid them from drying. When the separating gels were well polymerized, the water was poured out, and stacking gels cocktails (Table 12) were made and applied to each gel, after which the combs (10 or 15 wells) were placed. Gels were allowed to polymerize for 30min and stored at 4°C for further usage.

Name of the product	Separating gels cocktails (6 ml)	Stacking gels cocktails (3 ml)
30% Acrylamide	1.98 ml	0.5ml
10% Ammonium persulfate (APS)	60 μl	30 μl
10% Sodium dodecyl sulfate (SDS)	60 μl	30 μl
Tetramethylethylenediamine (TEMED)	2.4 μl	3 μl
Tris(hydroxymethyl)aminomethane (Tris)	1.5 ml (1.5 M, pH=8.8)	0.38 ml (1.0 M, pH=6.8)

Table 12. Separating and stacking gels cocktails

Probes were placed on ice. Meanwhile, gels were put in the gel core tightly in the setup. SDS-running buffer (containing 25 mM Tris, 190 mM glycine, and 0.1% SDS) was applied to the top of the gaskets. Combs were removed carefully, and the lanes of the gels were rinsed with the buffer. After these preparations, $2\mu\text{l}$ of the sample marker was applied to the first lane and $10\mu\text{l}$ of each probe to the rest ones. Tetra Vertical Electrophoresis Cell for Mini Precast Gels setup at the constant voltage at 80V was run for the first 20min and 120V afterward until the front left the gel.

Approximately 15min before the gel running was complete, tubs, filter papers, membranes, black/white cartridges, and others were prepared. Membranes were labeled, incubated with methanol, rinsed 2 times with Milli-Q water, and placed in transferring buffer. Once the gels finished running, the setup was turned off and the

running buffer was dumped. Gels were taken out and removed from the core. Thereafter, stacking gels were removed, and separating gels were activated and imaged with ChemiDoc XRS + System and Image-lab software. Then, blot sandwiches were made and fixed in the gel tank. Afterward, the gel tank was added with sufficient transferring buffer (25 mM Tris and 192 mM glycine) with an ice block placed inside. Transfer Tetra Vertical Electrophoresis Cell with Mini Trans-Blot at the constant voltage at 80V for 1h.

Membranes were taken out of the sandwiches, washed in TBST (20 mM Tris, 150 mM NaCl, and 0.1% Tween-20, pH=7.7) for 2min, and imaged with ChemiDoc XRS + System and Image-lab software. 10% Roti-Block (Roth, Karlsruhe, Germany) was applied for 1h at RT. Membranes were incubated with primary antibodies (Table 13) and placed on the shaker at 4°C. The next day, membranes were rinsed with TBST for 3 x 5min. Horseradish peroxidase-conjugated secondary antibodies (1:10000, anti-rabbit or mouse IgG; Thermo Fisher Scientific, Germany) were applied and incubated at RT for 1h. Membranes were rinsed with TBST for 3x5min afterward.

Name of the antibody	Concentration	Information
mouse anti-APP (22C11)	1:2000	#14-9749-82, Thermo Fisher
rabbit anti-BACE	1:2000	#5606S, Cell Signaling
rabbit anti-GAPDH	1:5000	PA1-987, Thermo Fisher Scientific
rabbit anti-nectin-1	1:2000	ab-66985, abcam
mouse anti-nectin-3 (H-11)	1:1000	sc-271611, Santa Cruz
rabbit anti-sAPP β	1:2000	#813401, Biolegend

Table 13. Primary antibodies used in western blot.

Enhanced Chemiluminescence (ECL) detection imaging reagent was well mixed with 1M Tris (pH=8.5, 2 ml), 30% H₂O₂ (6.1 μ l), p-Coumaric acid stock solution (89 μ l; 44.29mg in 1ml DMSO), Luminol stock solution (200 μ l; 44.29mg in 1ml DMSO) and 18ml Milli-Q water. Membranes were placed in the ECL solution on a shaker for 1min. Images were taken with ChemiDoc XRS + System (Bio-Rad, Germany) and Image-lab software.

After labeling of the lanes of one protein, the membrane was washed with TBST for 3x5min, rinsed with Stripping Buffer (#46430, Thermo Fisher Scientific, Germany) for 30min, and 3x5min more washes with TBST.

9. Enzyme-linked immunosorbent assay (ELISA)

The hippocampal mouse A β ₁₋₄₂ levels were measured by an Elisa kit (KBM3441, Invitrogen, Germany). The tissues of the hippocampus were collected, weighed, homogenized with sufficient guanidine buffer (8x the sample weight), and incubated for 4h at RT. Thereafter, samples were diluted four times with 0.1M PBS containing 1x protease inhibitor cocktail. Finally, samples were centrifuged at 12,000x for 0.5h at 4°C. The supernatant was collected.

Standards were prepared, and 100 μ l of each standard and sample was added to bind the antigen of the appropriate wells. The plate was covered and put on the shake at RT. 4h later, the solution was thoroughly aspirated. After washing, 100 μ l of the mouse A β ₁₋₄₂ detection antibody was applied for incubation at RT for 1h. After four times wash, another 100 μ l anti-rabbit IgG horseradish peroxidase (HRP) was applied and left on the shake at RT for 0.5h. The solution was aspirated and washed thoroughly. A 100 μ l stabilized chromogen was applied to each well for incubation at RT for 0.5h in darkness. Finally, 100 μ l stop solution was applied. A microplate reader was used to read the absorbance at 450nm. Results were presented as 100% of the control.

10. Quantitative real-time PCR (RT-PCR)

The hippocampus tissue was treated with an RNA extraction assay (RNeasy kit Qiagen, Germany). Enough amount of RNA at 0.5–1 μ g was reversely transcribed. The analysis was performed on a Rotor GeneQ. APP and 18S rRNA primer sets were used (Table 14).

Primers		Information (Metabion, Bayern, Germany)
APP	sense primer	5'-GACCCGTCAGGGACCAAAAC-3'
	antisense primer	5'-AACGGTAAGGAATCACGATGTG-3'
18S rRNA	sense primer	5'-GTAACCCGTTGAACCCATT-3'
	antisense primer	5'-CCATCCAATCGGTAGTAGCG-3'

Table 14. Primer sets information.

The relative APP mRNA levels were measured by the cycle threshold (Ct) values. The Ct values of the APP gene were normalized to that of the 18S rRNA gene. Data were presented as fold change ($=2^{-\Delta\Delta Ct}$). The relative mRNA levels were quantified with the equations: $\Delta Ct = Ct (APP) - Ct (18S rRNA)$, $\Delta\Delta Ct = \Delta Ct (isoflurane/sevoflurane \text{ group}) - \Delta Ct (18S rRNA \text{ group})$.

11. Dendritic spines classification

Thy1-eGFP mice were used to quantify the spine morphology in the CA1 region. Right after the experimental process, brain sections were collected, fixed (ice-cold 4% PFA, 24h), and cryoprotected (30% sucrose, 36h). A cryostat was used to cut the slices further into 40 μ m thickness. Slices were washed with 1xPBS, transferred onto glass slides, and coverslipped.

A confocal microscope (60x oil-immersion objective, Leica SP8, Germany) was used to take images of dendritic segments from the stratum radiatum layer in CA1. The interval z-stacks were at 0.3 μ m. The length of the segments was between 20–80 μ m. 6–8 dendrites per animal were analyzed (Leica Application Suite X software, Leica, Germany).

Based on the morphology, dendritic spines were classified as thin, mushroom, and stubby (Figure 27) (Harris KM & Jensen FE, 1992). The dendritic spine density was showed as count of spines/10 μ m of dendrite.

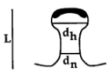
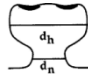
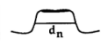

Category	Shape	Criteria
Thin		$d_n \ll L$ $d_n \leq d_h$
Mushroom		$d_n \ll d_h$
Stubby		$d_n \cong L$
Branched		> 1 head

Figure 27. Dendritic spines classes (Harris KM & Jensen FE, 1992).

12. Statistical analysis

GraphPad Prism 8 software was used to perform the statistics. The two-tailed unpaired t test (homogeneity of variance was met) or two-tailed Mann-Whitney test (homogeneity of variance was not met) was conducted for two groups analysis. One-way analysis of variance (ANOVA) followed by Tukey's post hoc multiple comparisons was used for three or four groups analysis. Data were presented as mean \pm standard error of mean (SEM). $P < 0.05$ was used to show the statistical significance.

Results

1. The sevoflurane-induced mA β ₁₋₄₂ increase was reversed by BACE inhibition

From the recent reports, it has been known that inhalational anesthetics may upregulate BACE activity and increase A β synthesis (Dong et al., 2009). Here, the mA β ₁₋₄₂ levels in the hippocampus were evaluated with or without BACE inhibition in the presence of either anesthetic by means of ELISA. In agreement with previous studies, sevoflurane at 1.4% for 1.5h treatment upregulated the mA β ₁₋₄₂ levels in the hippocampus (Figure 28b, P = 0.0134). In addition, inhibiting β -secretase activity reversed the sevoflurane-induced elevation of mA β ₁₋₄₂ in the hippocampus (Figure 28b).

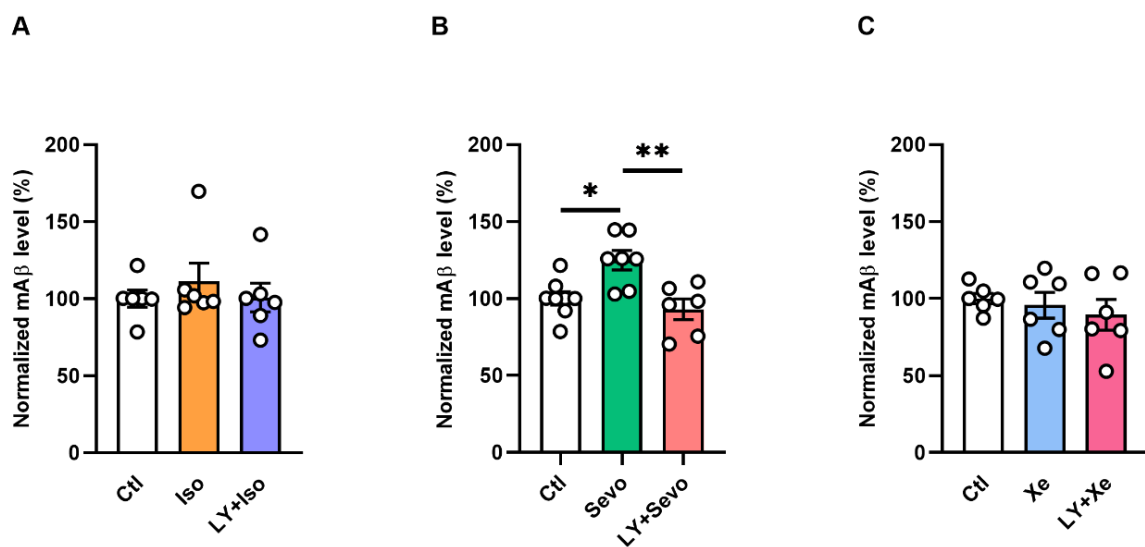


Figure 28. BACE inhibition reversed the increased mA β ₁₋₄₂ levels induced by sevoflurane. (A) No change of mA β ₁₋₄₂ levels in the hippocampus. (B) Sevoflurane upregulated hippocampal mA β ₁₋₄₂ levels significantly (ctl vs. sevo: P = 0.0134). Pre-treatment of LY2886721 reversed the upregulated mA β ₁₋₄₂ levels (sevo vs. LY+sevo: P = 0.0034). (C) Xenon and LY2886721+xenon did not alternate mA β ₁₋₄₂ levels. Tukey's test. Dots are equal to the animal number. *P < 0.05, **P < 0.01. A β : amyloid beta, ctl: control, iso isoflurane, LY: LY2886721, sevo: sevoflurane, xe: xenon.

The expression levels of hippocampal mA β ₁₋₄₂ in the other groups were measured. No alternations were observed (Figure 28 a, c).

To test LY2886721 effects alone on mA β ₁₋₄₂ levels, the hippocampal sections were incubated with LY2886721 at 3 μ M for 2h. The hippocampal mA β ₁₋₄₂ levels were decreased (Figure 29, P = 0.0286).

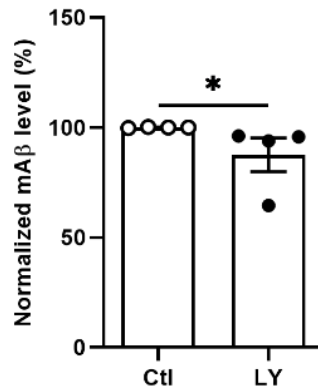


Figure 29. BACE inhibitor LY2886721 partially reduced hippocampal mA β ₁₋₄₂ levels. Mouse A β ₁₋₄₂ levels in the whole hippocampus were reduced after treatment with LY2886721 (P = 0.0286, Mann-Whitney test). *P < 0.05.

2. Abnormal potentiation and dendritic spine complexity in CA1 by mA β ₁₋₄₂

The human A β ₁₋₄₂ was shown to impair CA1-LTP in a concentration-dependent manner (Rammes, Hasenjäger, Sroka-Saidi, Deussing, & Parsons, 2011). Here, the effects of upregulated mA β ₁₋₄₂ levels in the presence of sevoflurane on synaptic transmission and spine morphology were assessed in CA1. Therefore, the extracellular recordings and the alternations of spine density were evaluated in CA1 region. The data have shown that incubation of the slices with mA β ₁₋₄₂ at a concentration of 50nM for 1.5h blocked CA1-potentiation (Figure 30 e-f, P = 0.0081).

Next, the spine density of the apical pyramidal neurons in the CA1 region was evaluated. Results have shown that mA β ₁₋₄₂ exposure decreased thin and total spines (Figure 30 g-h, thin: P = 0.0003, total: P = 0.0001).

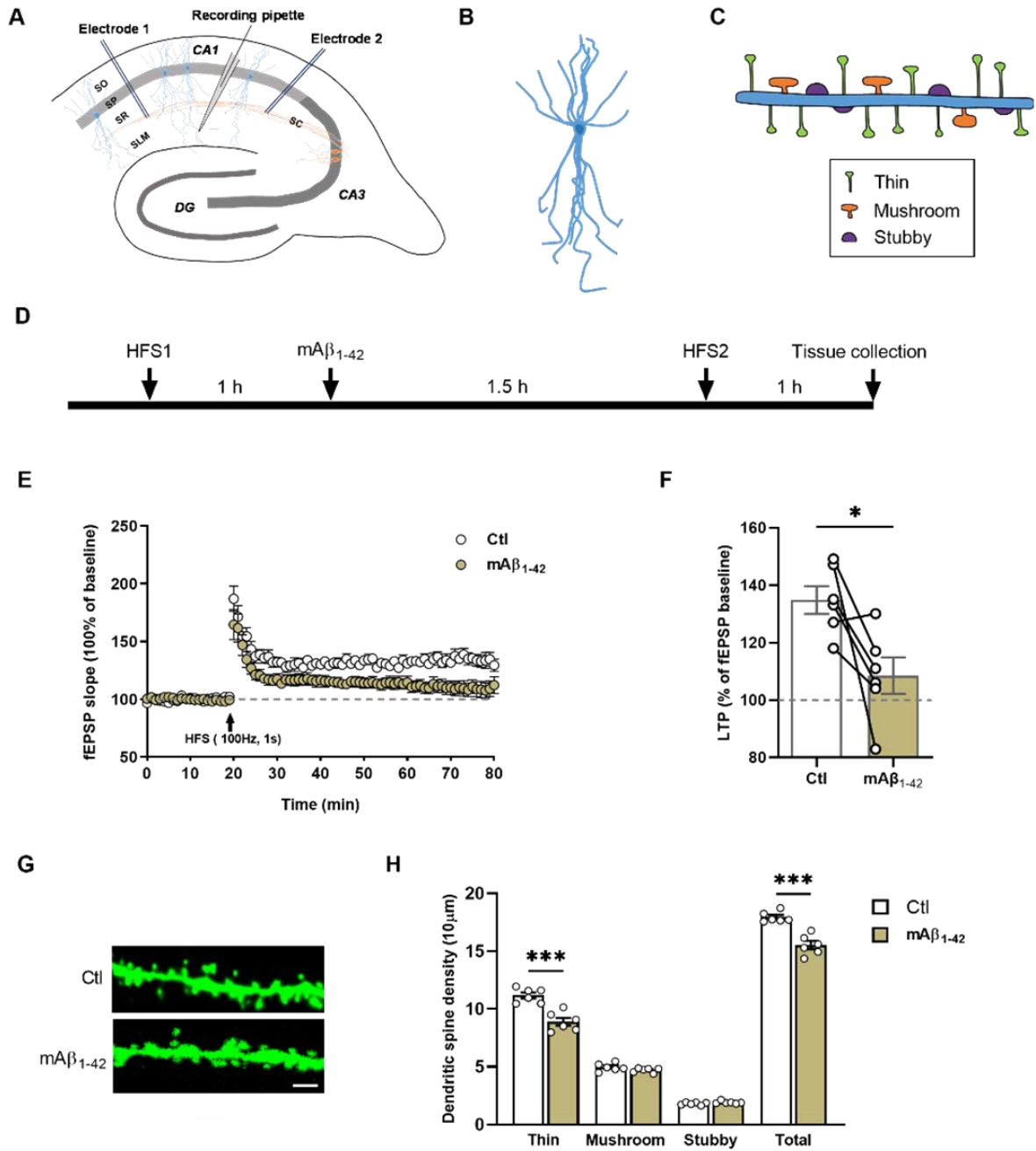


Figure 30. Mouse Aβ₁₋₄₂ blocked potentiation and reduced CA1-spine complexity.

(A) Diagram of sagittal hippocampal slices. Two bipolar stimulation electrodes were used to trigger the anterograde or retrograde high-frequency stimulation (HFS, 100Hz, 1s). Between the two electrodes, the recording pipette was placed. (B) Schematic showing a pyramidal neuron in the CA1 region. (C) In CA1 pyramidal neurons, three types of spines were categorized. (D) Design of the experiment. (E) fEPSP values were normalized as 100% of the control. (F) Mouse Aβ₁₋₄₂ attenuated potentiation ($P = 0.0081$). (G) Enhanced GFP images showing the apical dendritic segments of the CA1 neurons. Scale bar = 2 μm. (H) mAβ₁₋₄₂ decreased spine density (thin: $P = 0.0003$; total: $P = 0.0001$). t test. * $P < 0.05$, *** $P < 0.001$.

3. Spine elimination by sevoflurane was partly restored by BACE inhibition

Previous studies reported that isoflurane and sevoflurane decreased the hippocampal dendritic spine density (Tang et al., 2018). Here, I tested further the equivalent concentration of either anesthetic effects on dendritic spine dynamics in the CA1 region.

Figure 31 showed that isoflurane reduced thin (Figure 31d, $P = 0.0006$) and total (Figure 31g, $P = 0.0012$) dendritic spine density. However, The LY2886721+isoflurane did not reverse the deficits (Figure 31d, $P = 0.0036$; 31g, $P = 0.0095$) in CA1 region.

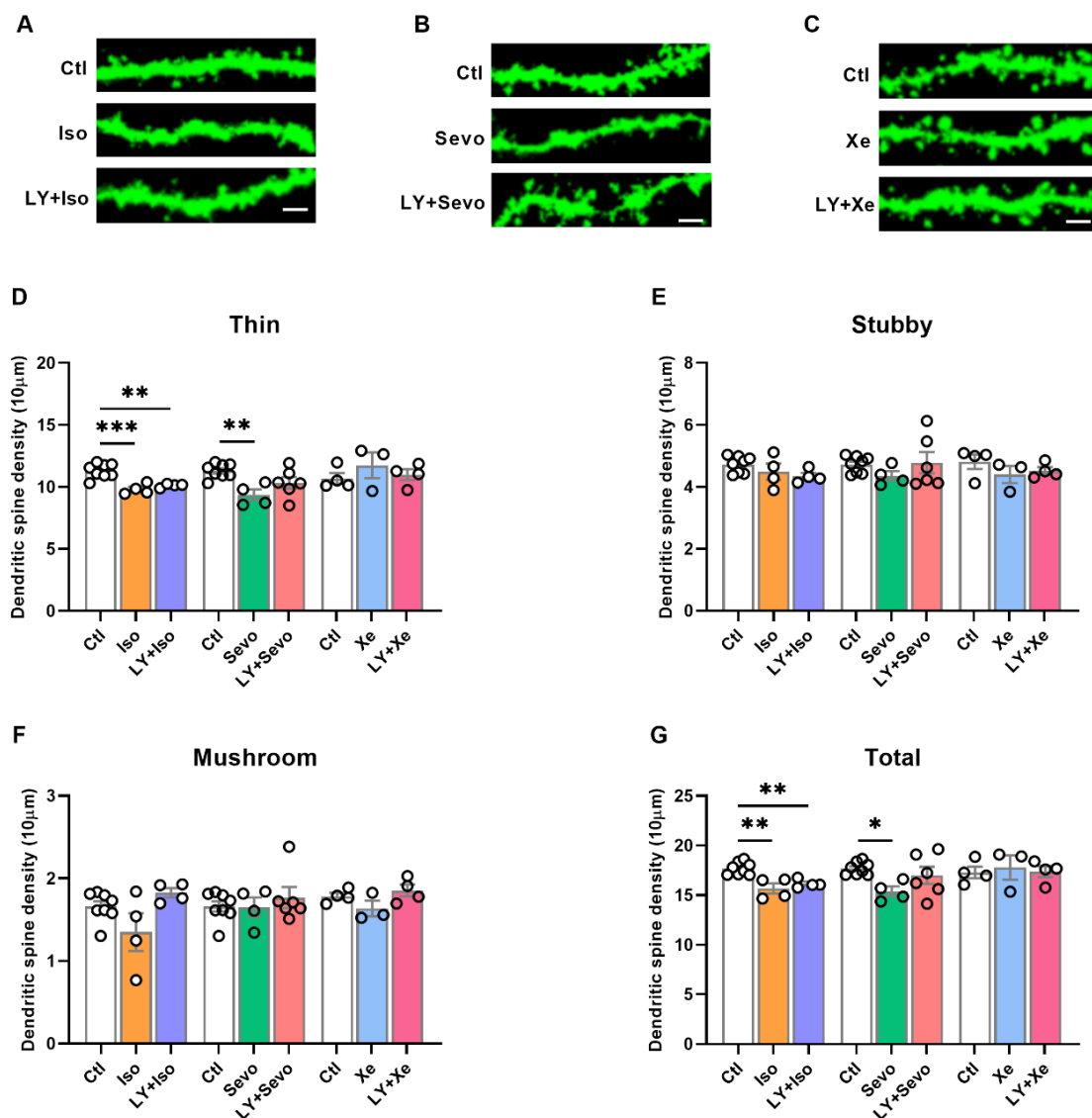


Figure 31. No alternations of dendritic spine density by xenon exposure, and inhibition of BACE partially restored only the sevoflurane-induced spine loss.

(A-C) Schematic showing the dendritic segments. Scale bars = 2 μ m. (D) A reduction of thin spines by isoflurane ($P = 0.0006$), sevoflurane ($P = 0.0066$), but not xenon. (E and F) The density of stubby and mushroom spines was not changed among groups. (G) In the presence of isoflurane ($P = 0.0012$) and sevoflurane ($P = 0.0370$), the total spines were markedly reduced. In contrast, xenon did not change the total spine density. Moreover, LY2886721 partially reversed the dysfunction only from sevoflurane (ctl vs. LY+iso: $P = 0.0095$; ctl vs. LY+sevo: $P = 0.6194$). (D-G) No change of spines under xenon or LY2886721+xenon. Tukey's test. * $P < 0.05$, ** $P < 0.01$, *** $P < 0.001$.

Sevoflurane exposure reduced thin (Figure 31d, $P = 0.0066$) and total dendritic spines (Figure 31g, $P = 0.0370$). In addition, I evaluated the effects of pre-treatment with LY2886721 during sevoflurane anesthesia on spine dynamics. Results have shown that inhibition of BACE partially restored the dysfunction of sevoflurane on dendritic spine density (Figure 31d, $P = 0.1351$; 31g, $P = 0.6194$).

Xenon was shown as a neuroprotective gas anesthetic (Breuer et al., 2015; Esencan et al., 2013). In this thesis, I applied the equipotent concentration of xenon in comparison with isoflurane and sevoflurane. Results demonstrated that xenon and LY2886721+xenon did not affect spine morphology in the CA1 region (Figure 31 d-g).

The above data indicate that isoflurane or sevoflurane reduced dendritic spines, including thin and total spines, density. Only the sevoflurane-induced spine elimination was able to be partly reversed. In comparison, xenon as well as co-treatment with the BACE inhibitor did not affect dendritic spines.

4. Reduced CA1-nectin-3 expressions were reversed by BACE inhibition

Numerous reports have shown that the cell adhesion molecules are fundamental for neuronal connectivity and communication. The disruption of the cell adhesion may induce structural and functional abnormalities, which can trigger neurodegenerative disorders, such as AD (Giagtzoglou, Ly, & Bellen, 2009; Shapiro, Love, & Colman, 2007). Nectin-3 primarily locates on the postsynaptic site. It forms heterophilic

adhesion with the presynaptic protein nectin-1. Nectin-1 and -3 complex have been implicated in hippocampus-related and -dependent cognition (X. X. Wang et al., 2017).

I first quantified the hippocampal nectin-3 expressions by western blot. No alternations were detected between groups (Figure 32 a and c). By means of immunohistochemistry, I quantified nectin-3 levels in the subregions of the hippocampus (Figure 32b), and found that sevoflurane significantly reduced nectin-3, particularly in CA1 region (P = 0.0205).

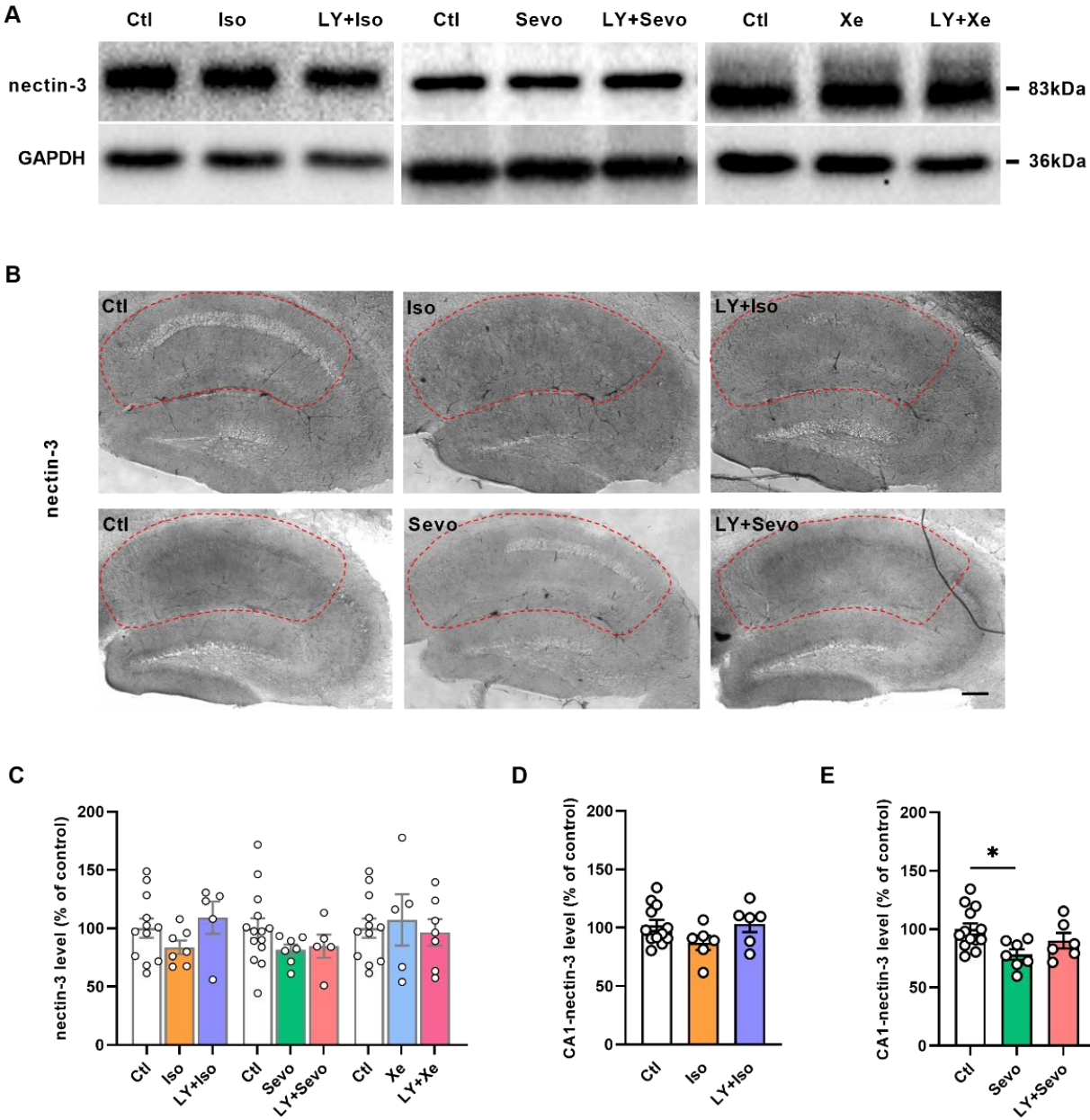


Figure 32. BACE inhibition restored the reduction of nectin-3 in CA1 by sevoflurane.

(A) Representative bands by western blot showing the nectin-3 expressions. (B) Nectin-3 immunoreactive images. (C) Nectin-3 expressions were not changed. (D) Nectin-3 levels under isoflurane and LY2886721+isoflurane. (E) Reduced CA1-nectin-3 levels ($P = 0.0205$, Tukey's test) were returned to normal by pre-treatment with LY2886721. Scale bar = 200 μm . * $P < 0.05$.

Next, I measured as well the nectin-3 expressions in the other subregions of the hippocampus. Data have shown the CA3-nectin-3 protein expressions in LY2886721+sevoflurane group were downregulated (Figure 33b, $P = 0.0153$).

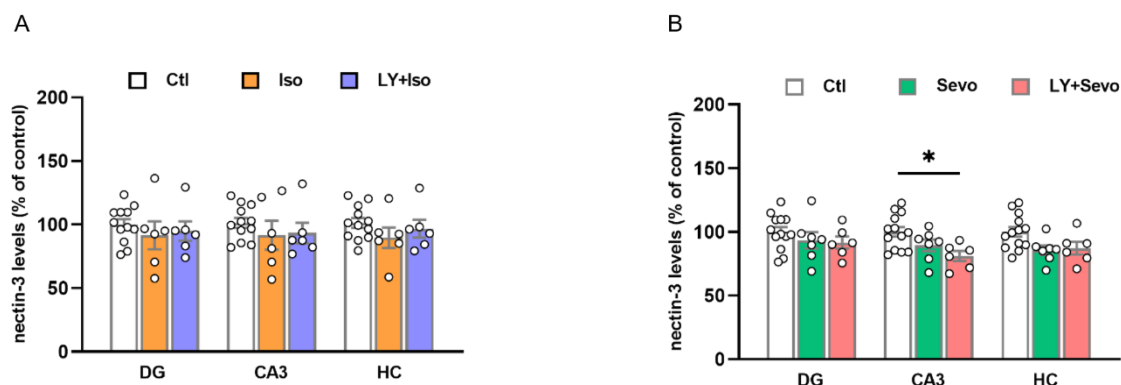


Figure 33. Nectin-3 expressions in regions of DG, CA3, and HC.

(A) No alternations of nectin-3 protein. (B) LY2886721+sevoflurane reduced nectin-3 expressions in CA3 region ($P = 0.0153$). DG, dentate gyrus. HC, hippocampus. Tukey's test. * $P < 0.05$, ** $P < 0.01$.

5. Nectin-3 knockdown in CA1 impaired potentiation and reduced spine counts

Next, a strategy of nectin-3 knockdown in CA1 by AAV was performed to mimic the downregulation effects of CA1-nectin-3 by sevoflurane. Thereafter, the CA1-nectin-3 decrease effects on LTP and spine density were investigated (Figure 34).

Fourteen days after the microinjection, I performed LTP with the virus-treated hippocampal slices. Measuring the last 10min of fEPSPs showed the impaired CA1-potentiation under nectin-3 knockdown (Figure 34 b-c, $P = 0.0089$). The transinfection of the virus was shown by immunofluorescence (Figure 34d). Besides, the downregulation efficiency of CA1-nectin-3 was validated by immunohistochemistry (Figure 34 e-f; $P = 0.0399$). Furthermore, the nectin-3 levels in other regions remain unchanged (Figure 34 f-g).

Downregulation of CA1-nectin-3 reduced total spine counts (Figure 34i, $P = 0.0253$), especially thin-type ones (Figure 34i, $P = 0.0241$).

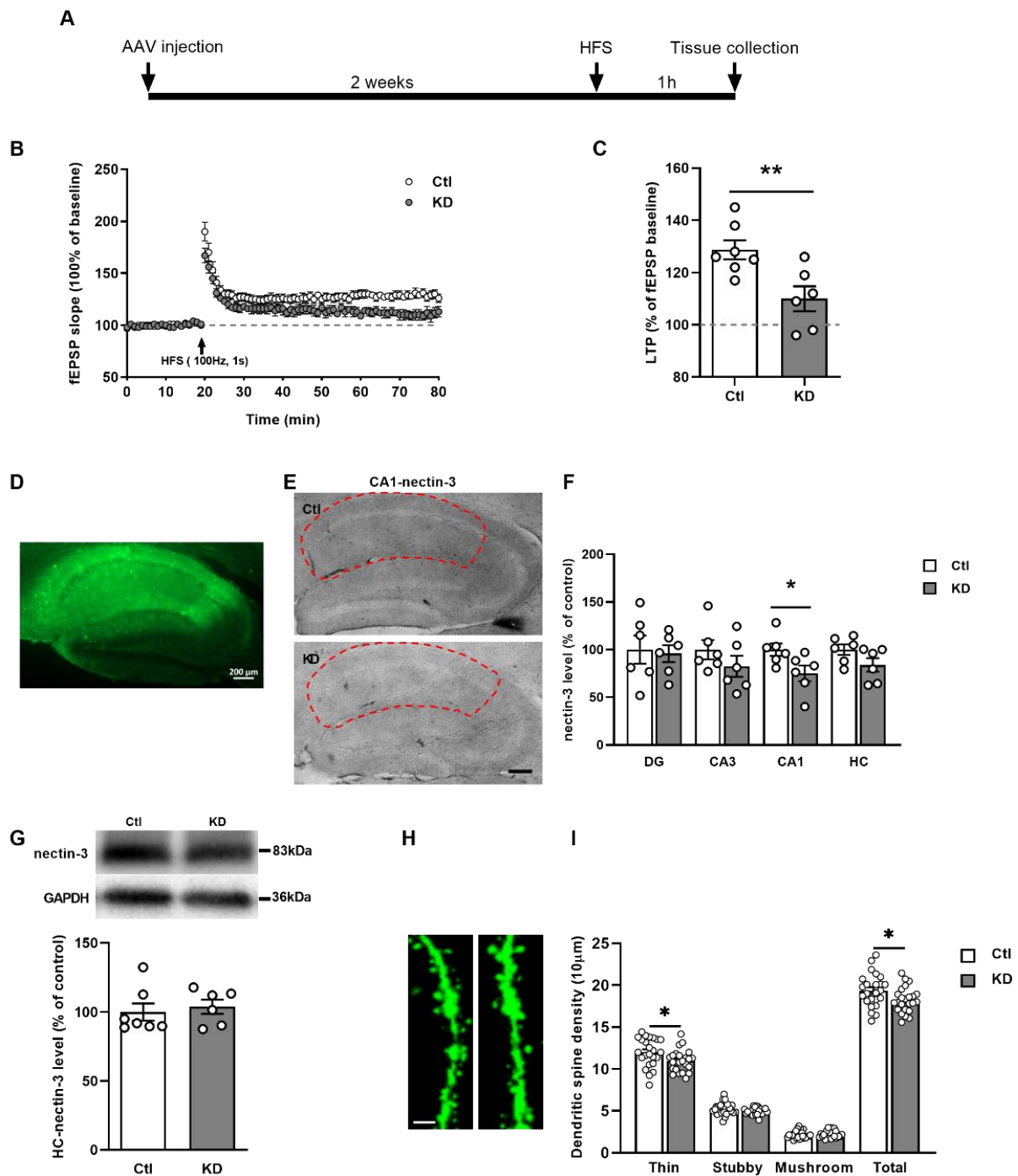


Figure 34. Attenuated LTP and reduced dendritic spines density under nectin-3 downregulation in CA1. (A) Experimental timeline. (B) LTP curves showed the normalized fEPSP of control and knockdown groups. (C) Attenuated potentiation ($P = 0.0089$) under nectin-3 reduction. (D) Validation of infection area of the AAV virus by enhanced GFP staining. Scale bar = 200 μm . (E) Immunohistochemistry images showing nectin-3 staining. (F) CA1-nectin-3 levels were downregulated in the knockdown group ($P = 0.0415$). Meanwhile, nectin-3 expressions in other regions remained unchanged. Scale bars = 200 μm .

(H) Dendritic spine segments. Scale bar = 2 μ m. (I) Reduced thin ($P = 0.0241$) and total spines ($P = 0.0253$) in the CA1 region in nectin-3 knockdown group. t test. * $P < 0.05$, ** $P < 0.01$.

Additionally, there were no significant changes in APP, sAPP β , or BACE levels in the nectin-3 knockdown group via the western blot analysis (Figure 35).

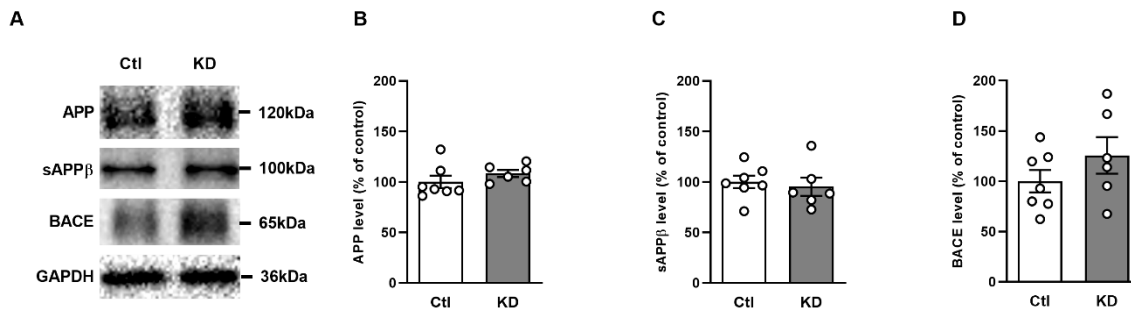


Figure 35. Nectin-3 knockdown in the CA1 region did not alternate hippocampal APP, sAPP β , or BACE. (A) Western blot bands of all groups. (B-D) Normalized molecular levels in the hippocampus. * $P < 0.05$, ** $P < 0.01$.

The above data suggest that nectin-3 plays a role in the abnormal synaptic plasticity caused by sevoflurane in CA1 region.

6. Regulation of APP processing-related molecules in hippocampus

The APP-amyloidogenic-process-related molecule expressions in the hippocampus were quantified via western blot (Figure 36). I found that the APP levels either in LY2886721+isoflurane/sevoflurane downregulated APP levels in comparison with the isoflurane/sevoflurane group (Figure 36c, iso vs. LY+iso: $P = 0.0238$; sevo vs. LY+sevo $P = 0.0225$).

In addition, I measured the hippocampal sAPP β and BACE expressions. No changes were detected (Figure 36c, d). Besides, APP expressions trended to be increased in the whole hippocampus by isoflurane/sevoflurane exposure. Further RT-PCR revealed that in the hippocampus, sevoflurane significantly elevated the APP mRNA levels (Figure 36h, $P = 0.0325$).

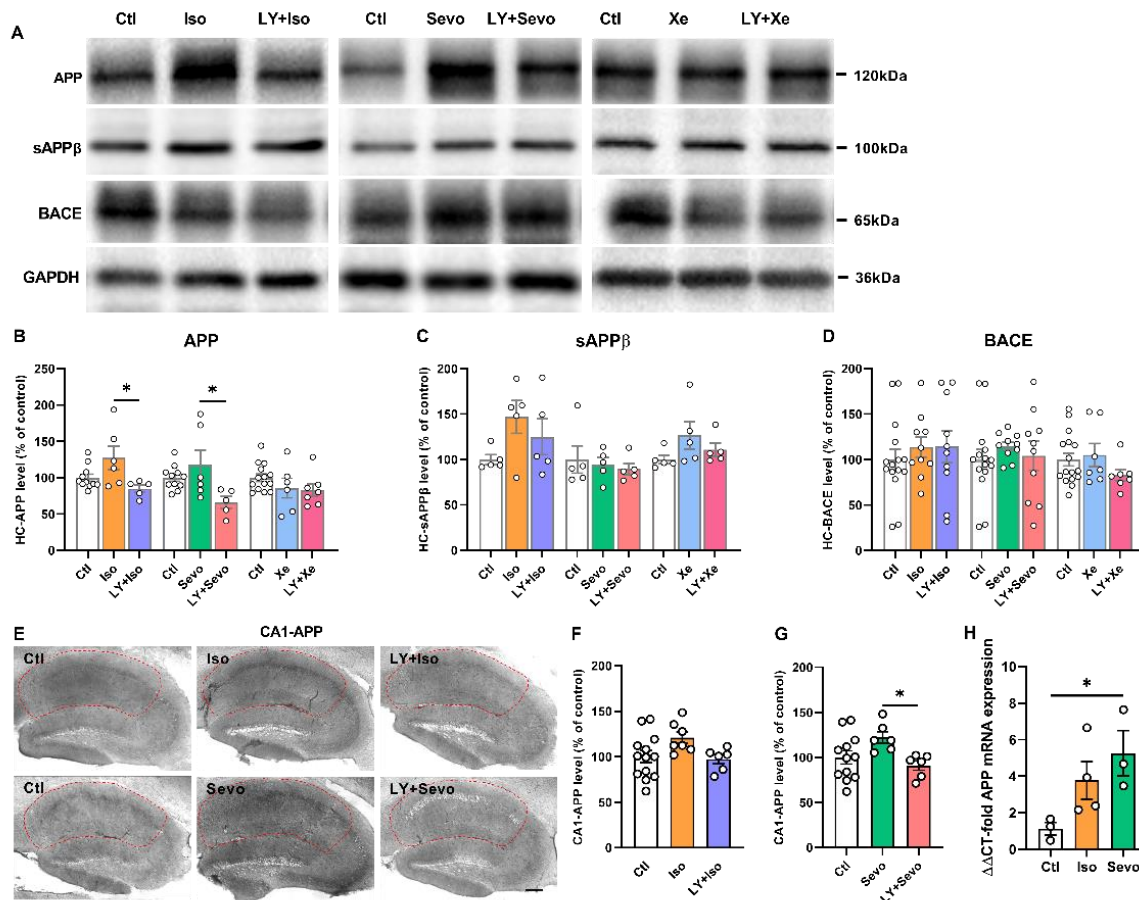


Figure 36. APP-amyloidogenic-process related molecular changes in hippocampus.

(A) Representative bands of all groups. (B-D) Hippocampal protein levels. (B) LY+iso and LY+sevo decreased APP levels compared with the isoflurane ($P = 0.0238$) or sevoflurane ($P = 0.0225$) application alone group. (C-D) No change of sAPP β and BACE expressions. (E-G) CA1-APP expressions. LY+sevo decreased APP levels in comparison with the sevoflurane application group ($P = 0.0421$, Tukey's test). (H) The hippocampal mRNA levels of APP were elevated by sevoflurane ($P = 0.0325$, t test). * $P < 0.05$.

Further immunohistochemistry methods were performed to detect APP levels either in DG, CA1, or CA3. Compared with the sevoflurane group, CA1-APP levels were decreased by treatment with LY2886721+sevoflurane (Figure 36g, $P = 0.042$). A pre-incubation with LY2886721, along with either isoflurane or sevoflurane, evoked a reduction of APP expressions in CA3 and HC dramatically compared with the

isoflurane or sevoflurane alone group (Figure 37, iso vs. LY+iso - CA3: $P = 0.006$, HC: $P = 0.038$; sevo vs. LY+sevo - CA3: $P = 0.002$, HC: $P = 0.041$).

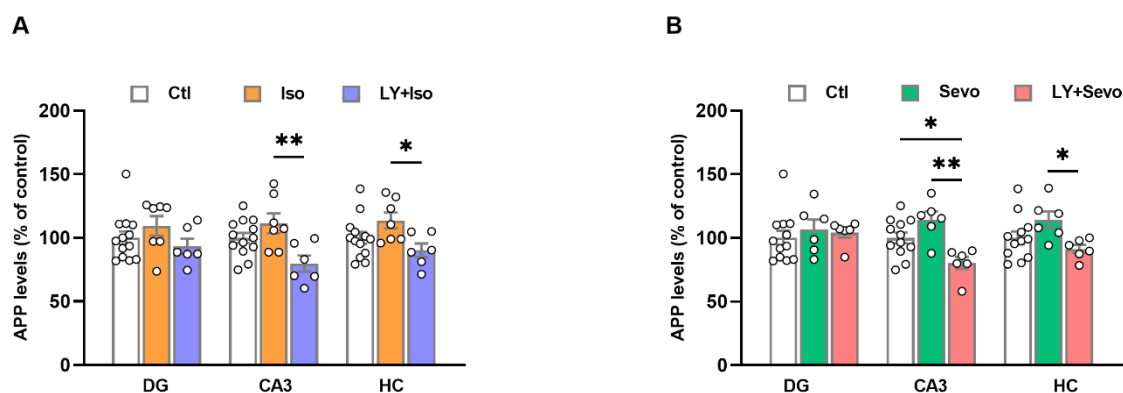


Figure 37. Expression levels of APP in either DG, CA3, or HC.

(A) Compared with isoflurane group, LY+iso decreased APP levels either in CA3 ($P = 0.006$) or the whole HC ($P = 0.038$). (B) APP levels in LY+sevoflurane were decreased in the CA3 region compared with ctl group ($P = 0.032$). Moreover, in comparison with the sevoflurane group, either in CA3 ($P = 0.002$) or the whole hippocampus ($P = 0.041$). Tukey's test. * $P < 0.05$, ** $P < 0.01$.

To make sure that LY2886721 treatment alone did not alternate APP expressions, western blot and immunohistochemistry were conducted. No alternations of APP protein levels were detected (Figure 38).

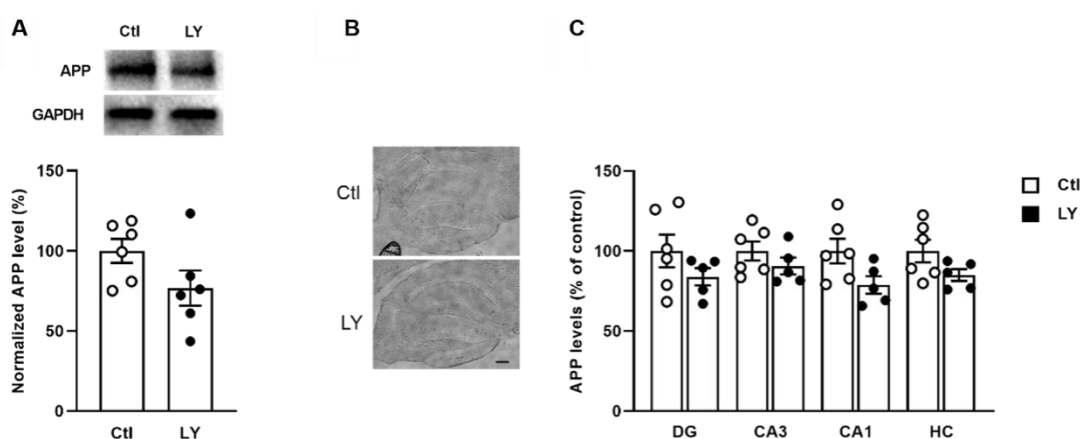


Figure 38. APP levels were not changed by BACE inhibition via western blot and immunohistochemistry. Scale bar = 200 μm . * $P < 0.05$.

7. Co-stainings of APP and nectin-3

Reports have indicated that APP adjacents cells to support dendritic spines maintenance and synaptic plasticity (Schilling et al., 2017). Surprisingly, co-localization of APP and nectin-3 were observed in the present thesis (Figure 39). Further detailed APP and nectin-3 expression patterns of the subregions in CA1 were shown in Figure 39 a-c. Compared with control conditions, LY2886721+sevoflurane reduced the percentage of APP and nectin-3 colocalizations in CA1 (Figure 39e, $P = 0.010$).

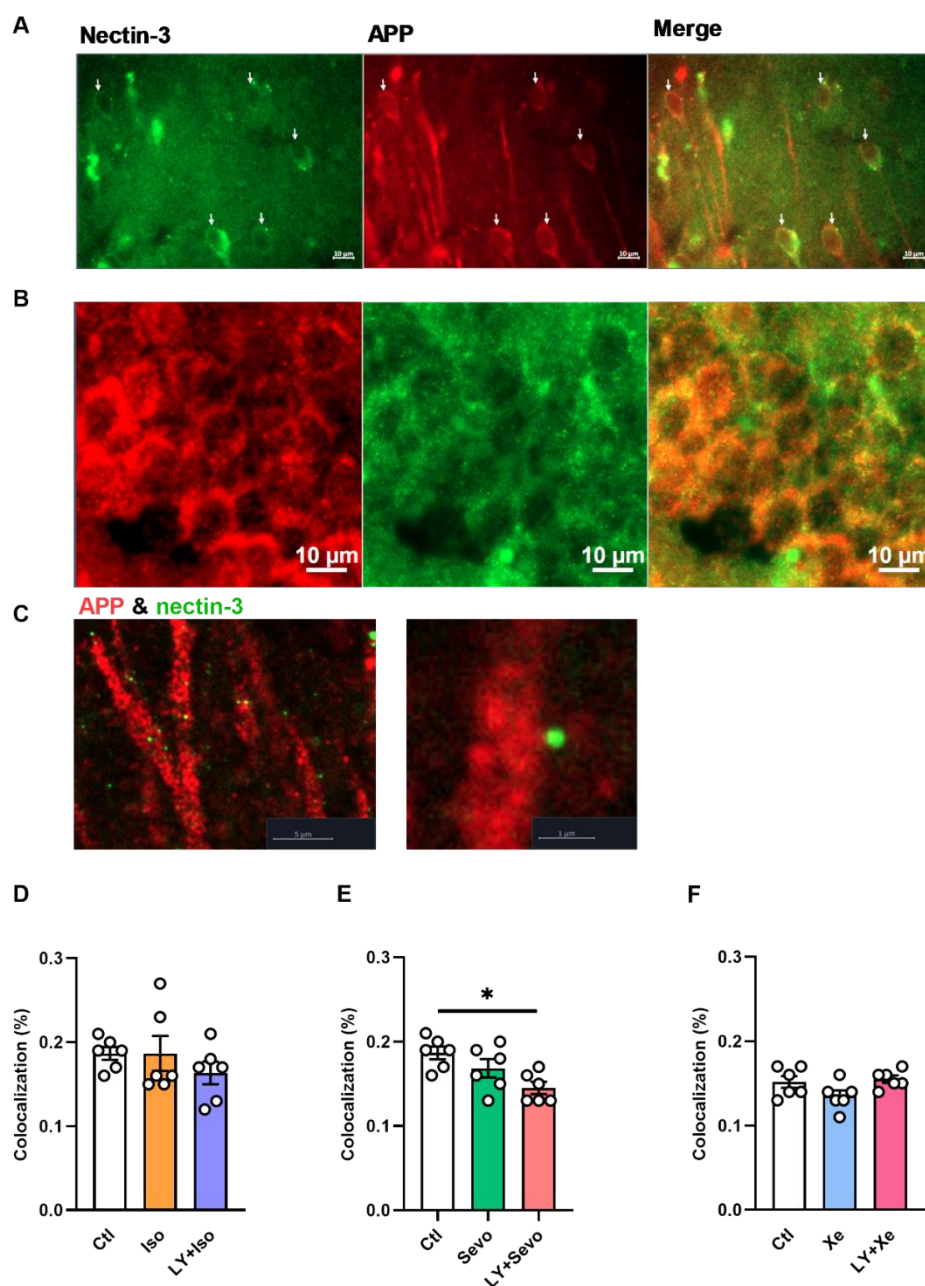


Figure 39. Co-stainings of APP and nectin-3 in CA1.

Colocalizations of the two molecules in the SO (A), SP (B), and SLM (C) regions in CA1. (D-F) Co-staining percentage of APP and nectin-3 proteins of all groups in CA1 region. Compared with the control group, LY+sevo decreased the colocalizational percentage of APP and nectin-3 (E, $P = 0.0104$). Tukey's test. Scale bars = 10 or 1 μm . * $P < 0.05$.

8. Isoflurane, sevoflurane, and xenon attenuated LTP dramatically

The above observations, including increased $\text{mA}\beta_{1-42}$ levels, abnormal spine counts, as well as aberrant cell adhesions, might alternate synaptic signal transmission. In addition, our work showed previously the anesthetic isoflurane-, sevoflurane- or xenon-induced synaptic transmission and CA1-potential deficits (Haseneder et al., 2009; Kratzer. et al., 2012). Next, I investigated whether and how the equivalent concentrations of the three inhalational anesthetics may affect CA1-potential.

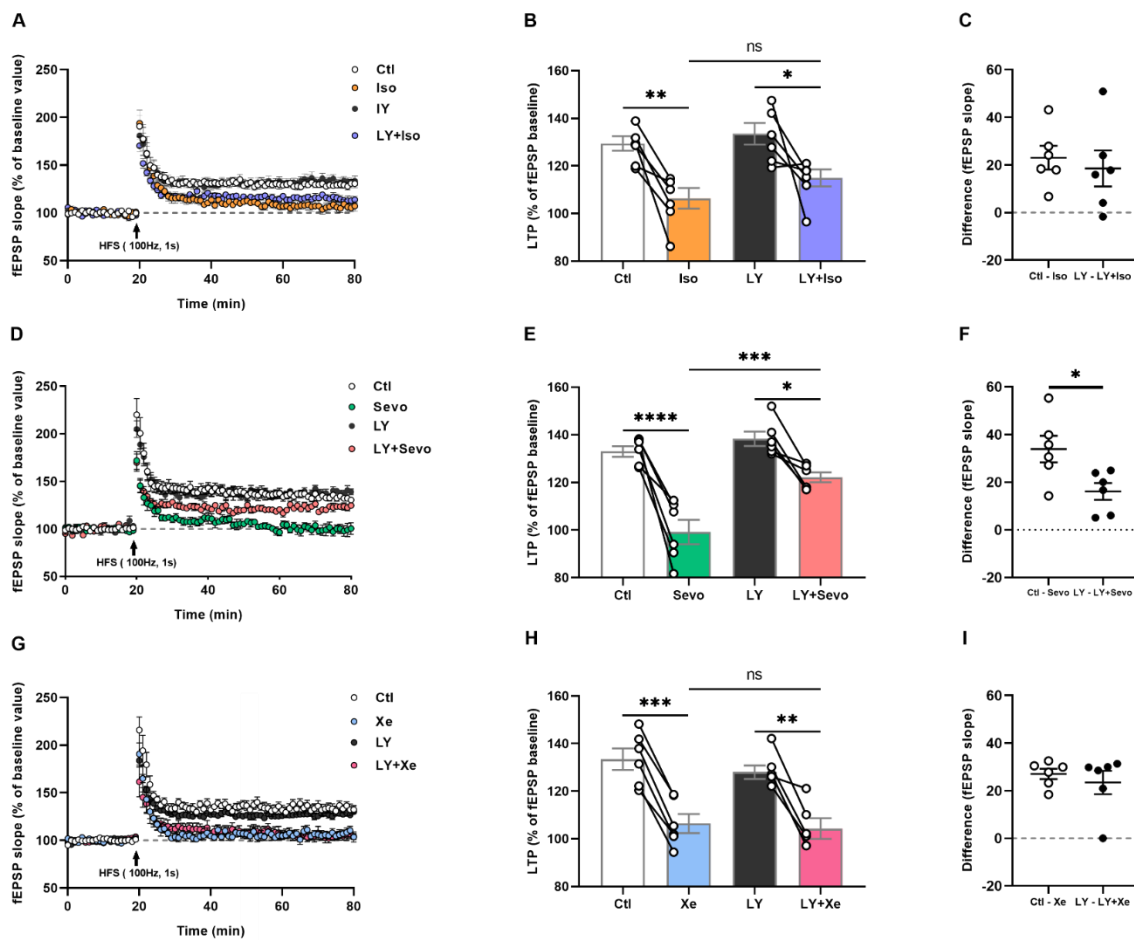


Figure 40. BACE inhibition partially reversed the LTP deficits induced only by sevoflurane.

Stable potentiation was maintained by the BACE inhibitor exposure, but not by the presence of either isoflurane, sevoflurane, or xenon (A and B, D and E, G and H). Sevoflurane abolished LTP ($P < 0.0001$),

which was partly reversed by BACE inhibition (LY vs. LY+sevo: $P = 0.0132$, sevo vs. LY+sevo: $P = 0.0005$; Tukey's test). This was further verified by the difference of the fEPSP slopes (F, $P = 0.0229$, t test). A pre-application with LY2886721 at $3\mu\text{M}$ for 2h did not reverse isoflurane or xenon-induced potentiation deficits. * $P < 0.05$, ** $P < 0.01$, *** $P < 0.001$, **** $P < 0.0001$.

Therefore, I treated the brain slices with either 0.6% isoflurane, 1.4% sevoflurane, or 65% xenon for 1.5h. fEPSP slopes were markedly reduced during 50-60min of the LTP recordings in comparison with the control conditions (Figure 40b, ctl vs. iso: $P = 0.0026$; 40e, ctl vs. sevo: $P < 0.0001$; 40h, ctl vs. Xe: $P = 0.0006$).

The above data indicate that the equipotent application of either isoflurane, sevoflurane, or xenon abolished LTP.

9. BACE inhibition partially reversed the LTP deficits induced by sevoflurane

The above findings suggested that BACE inhibition partly restored the dysfunction of both isoflurane and sevoflurane. Next, I evaluated whether and how BACE inhibition may affect the attenuated LTP induced by an either inhalational anesthetic.

In the first step, I incubated the slices with LY2886721 at $3\mu\text{M}$ for 2h and tested its effects on fEPSPs to know whether the BACE inhibitor would affect CA1-potentiation. Results have demonstrated that BACE inhibition exhibited no effects on LTP (Figure 41c, $P = 0.5234$).

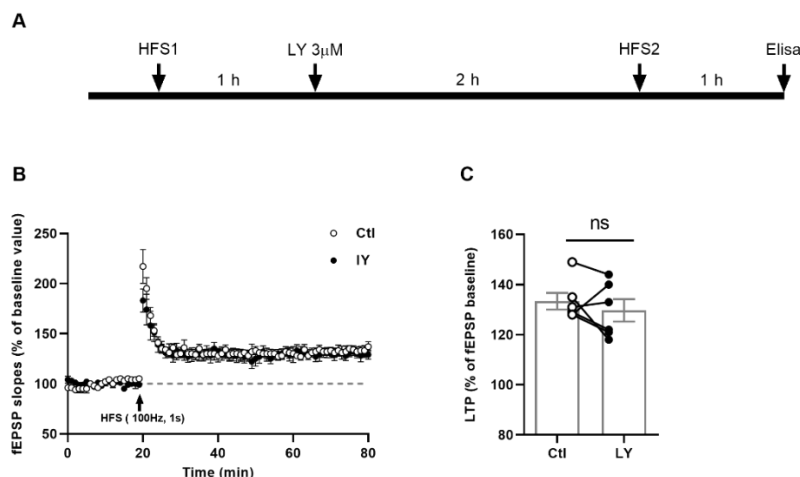


Figure 41. Beta-secretase inhibitor LY2886721 exposure did not block LTP.

(A) Experimental timeline. (B) Normalized fEPSP values of two groups. (C) Stable potentiation by LY treatment. *P < 0.05.

In the second step, I treated the hippocampal slices with LY2886721 for 2h. Afterward, either isoflurane, sevoflurane, or xenon at equivalent concentrations were applied for 1.5h. Data showed that the CA1-LTP deficits induced by sevoflurane were partly restored (Figure 40b, P = 0.4282). This was verified by the differences between the control - sevoflurane and LY2886721 - LY2886721+sevoflurane groups (Figure 40f, P = 0.0229). In contrast, the LTP deficits were not able to be reversed in other groups (Figure 40e, P = 0.0005; 40h, P = 0.9823).

The above data demonstrated that only sevoflurane anesthesia-induced potentiation deficits were partly restored by inhibition of BACE.

Discussion

This thesis has shown that sevoflurane induced an upregulation of $m\text{A}\beta_{1-42}$, a downregulation of nectin-3, abnormal APP-processing-related molecules, and a loss of dendritic spines. Moreover, isoflurane mildly decreased dendritic spine density and modulated APP processing. In comparison, xenon did not alternate dendritic spine density or synaptic connectivity, although it abolished potentiation. In addition, the deficits induced by sevoflurane were partly restored by the inhibition of BACE. These findings indicate that the inhalational anesthetics may interfere with synaptic connectivity and BACE activity.

Morphologically, the CA3 pyramidal neurons synapse via the Schaffer collaterals pathway to the CA1-pyramidal neurons. At the same time, these pyramidal neurons synapse to the subiculum region in CA1. Aberrant trisynaptic connections in the hippocampus potentially induces synaptic transmission deficits (Basu & Siegelbaum, 2015). In neuroscience, the CA1-potentiation is critical for evaluating hippocampal synaptic strength and transmission (Buerge et al., 2019).

On the dendrites of the pyramidal neurons in CA1, numerous spiny protrusions called dendritic spines are present. Spines are able to segregate and integrate electrical and chemical signals on synapses (Volfovsky, Parnas, Segal, & Korkotian, 1999), thus providing fundamental functional structures for synaptic transmission and plasticity. The functions of dendritic spines have been studied for decades. However, it remains unclear regarding the exact function of each spine type. Till now the widely accepted opinion in neuroscience is that compared with the other short-necked spines, the long-necked thin type spines exhibit a shorter latency as well as slower decay kinetics of

the cation Ca^{2+} response (Hering & Sheng, 2001; Korkotian & Segal, 2000; Majewska, Brown, Ross, & Yuste, 2000; Volfovsky et al., 1999).

The BACE inhibitor LY2886721 was used in the present thesis to suppress BACE activity, therefore decreasing the synthesis rate of mouse $\text{A}\beta_{1-42}$. As a selective inhibitor of BACE, LY2886721 does not affect other aspartyl proteases (May et al., 2015). Reports have shown that LY2886721 could reduce the deposition of $\text{A}\beta_{1-40}$ and $\text{A}\beta_{1-42}$ in rodents as well as humans (May et al., 2015). Consistently, our work has proven that LY2886721 decreased hippocampal mouse $\text{A}\beta_{1-42}$ levels.

Previous work has shown that sevoflurane anesthesia increased human $\text{A}\beta_{1-42}$ levels (Dong et al., 2009). This is in line with our finding that sevoflurane elevated m $\text{A}\beta_{1-42}$ in a murine brain slice model. Our additional experiments in this thesis showed that m $\text{A}\beta_{1-42}$ treatment induced dendritic spine loss as well as CA1-potential abolishments. The elevated m $\text{A}\beta_{1-42}$ could probably be the reason why reduced dendritic spines, particularly thin type spines, and attenuated CA1-LTP by sevoflurane anesthesia were observed.

The abnormal proteolysis process of APP may hamper synaptic connection and plasticity (O'Brien & Wong, 2011; Thinakaran & Koo, 2008). In this thesis, an elevation of APP mRNA levels as well as a tendency of elevated hippocampal APP expressions by sevoflurane exposure were observed. Moreover, in the $\text{A}\beta$ generation process, BACE is accepted as the enzyme that limits the rate of the amyloidogenic pathway. The observed elevated $\text{A}\beta$ synthesis by sevoflurane suggests that the activity of β secretase is enhanced, which may evoke synapse elimination as well as CA1-potential deficits. However, new investigations are required in the future to evaluate the alternation of BACE activity at higher concentrations (for example, at one $\text{MAC}_{\text{rodent}}$) of sevoflurane exposure (E. I. I. Eger, 2001).

The post-synaptic nectin-3 is fundamental to synaptic plasticity and memory (X. D. Wang et al., 2013). Nectin-3 expressions reduction in the hippocampus evokes spine elimination as well as cognitive dysfunction (R. Liu et al., 2019; X. D. Wang et al., 2013; X. X. Wang et al., 2017).

This thesis showed that sevoflurane induced downregulation of nectin-3 expressions, a reduction of CA1-dendritic spines, and an abolishment of CA1-potential. A downregulation strategy of nectin-3 with AAV was performed to mimic the nectin-3 reduction in CA1 neurons. Intriguingly, nectin-3 dysfunction by AAV produced deficits likewise. Since in the knockdown group, dendritic spine density was decreased and CA1-potential was abolished. These findings above indicate that the deficits in LTP and spine morphology by sevoflurane exposure might be partially attributed to nectin-3 downregulation.

From the findings above, ie. the aberrant $A\beta_{1-42}$ synthesis, nectin-3 expressions, APP proteolysis process, and spine density, at MAC-awake_{mouse}, sevoflurane is already able to modulate the potential in CA1. Additionally, inhibition of BACE partially reversed the abnormal molecular expression patterns and potential. These above results indicate that sevoflurane may modulate synapse dynamics and synaptic transmission in a BACE-dependent manner.

Consistent with the previous work, the reduction of spine density and the abolishment of CA1-potential by isoflurane were confirmed here in the present thesis (Platholi, Herold, Hemmings, & Halpain, 2014). In comparison with sevoflurane, isoflurane treatment also evoked a dramatic spine, particularly thin type, loss in CA1. Dendritic spines provide essential morphological structures for synaptic function. The reduction of dendritic spine numbers could be the reason why the impaired CA1-potential under isoflurane exposure was obtained.

The abnormal regulations of APP processing by isoflurane have been shown earlier. These include elevated APP mRNA levels, amyloid deposits as well as BACE protein levels (Dong et al., 2009; B. Liu et al., 2017; Xie et al., 2008; S. Zhang et al., 2017). In contrast, isoflurane exposure exhibited no effects on hippocampal sAPP β levels. Further immunohistochemistry results have shown that isoflurane anesthesia tended to increase APP expressions in CA3 as well as the hippocampus. These observations were reversed by inhibition of BACE activity. The above results indicate that isoflurane treatment moderately alternates the amyloidogenic process of APP molecule in the hippocampus. However, it should be taken into consideration that I only applied low concentrations of isoflurane at MAC-awake_{mouse} (30%–40% of MAC value) (Aranake et al., 2013; Dwyer et al., 1992; E. I. I. Eger, 2001) (see discussion below).

However, it is noticeable that isoflurane exposure did not enhance A β production. This is not in line with previous reports showing that isoflurane increased A β levels (Xie et al., 2007b). Considering the relatively low concentrations of isoflurane applied, I assume that a more prominent change of A β deposition would be obtained if I elevated the isoflurane concentration to one MAC_{rodent} or higher. This would also be the possible reason why nectin-3 levels were not alternated under isoflurane treatment. Even though in this thesis, isoflurane did not change A β or nectin-3 levels, it induced dendritic spine elimination and CA1-potential deficits. I hereby assume that isoflurane anesthesia affects dendritic spine dynamics by 1) alternating ion channel functions; 2) changing synapse receptors sensitivity; 3) evoking neuronal apoptosis; 4) triggering a series of neuroinflammation.

It is also noticeable that the BACE inhibitor LY2886721 did not produce a reversal of the decrease of dendritic spine density as well as CA1-potential deficits when isoflurane has been applied. In contrast, those detrimental impairments induced by

sevoflurane were able to be partially restored by co-application of LY2886721 and sevoflurane. Previous work has shown that isoflurane and sevoflurane evoked similar changes in apoptosis and neural activities (Istaphanous et al., 2013). However, in the present thesis they exhibited different effects, ie. the abnormalities caused by isoflurane were not as easily reversible as sevoflurane. Chemically, isoflurane and sevoflurane both belong to ethers. But they differ in various aspects, for example, sevoflurane has a unique polyfluorinated methyl-isopropyl structure, thus it has more rapid pharmacokinetics than isoflurane. Besides, sevoflurane exhibits fewer organo-toxic effects (Behne, Wilke, & Harder, 1999). Further studies are therefore needed to further clarify the possible mechanisms regarding the different actions of isoflurane and sevoflurane.

In comparison, even though the gaseous anesthetic xenon attenuated LTP, it did not change the CA1-dendritic spine count in the present thesis. The observed impaired potentiation was also reported by previous studies (Kratzer. et al., 2012). They showed that xenon exposure antagonized potentiation probably by modulation of NMDA receptors. Furthermore, xenon treatment alone and LY2886721+xenon obtained unchanged APP processing, nectin-3 levels, and spine density in the hippocampus. All these above indicate that xenon is neuroprotective to the hippocampus.

Importantly, in the present thesis, I adjusted the concentrations of anesthetics isoflurane, sevoflurane, and xenon to be equipotent. The MAC_{rodent} value for xenon is at 161 atm, which is hyperbaric (Koblin et al., 1998). Previous work has demonstrated that the maximum feasible concentration for xenon in the brain section incubation experiments is up to 65% (Mattusch et al., 2015). This is why I applied here the equipotent concentration of both isoflurane (0.6%) and sevoflurane(1.4%) as xenon for a better comparison. The above-mentioned concentrations are near to MAC_{awake}

(Aranake et al., 2013; E. I. I. Eger, 2001). Statistically, the MAC_{awake} is around 33% of the MAC value for the anesthetic isoflurane and sevoflurane (Aranake et al., 2013; Dwyer et al., 1992; E. I. I. Eger, 2001).

It should be paying attention that I applied in the present thesis very low concentrations of both anesthetics isoflurane and sevoflurane. Moreover, the application of the two anesthetics was relatively short. This is different from previous reports with higher anesthesia concentrations and longer exposure time (Dong et al., 2011; Jiang & Jiang, 2015; B. Liu et al., 2017; Xie et al., 2008; S. Zhang et al., 2017). This might be the reason why I obtained moderate alternations induced by both isoflurane and sevoflurane.

It is noticeable that subclinical concentrations of both anesthetics negatively affected hippocampal synaptic plasticity by enhanced $A\beta_{1-42}$ -related procedures in the present thesis. As in agreement with previous reports, the equipotent application of either anesthetic at MAC value hampered CA1-potential in brain sections in a similar way (Kratzer. et al., 2012). I applied here very low concentrations of anesthetics. Therefore, I propose a more pronounced potentiation blockage if I elevated the anesthetic concentrations to 1 MAC for the rodent. It is therefore reasonable that if I applied MAC_{rodent} concentrations of either anesthetic, a more prominent alternation in molecular expressions as well as synaptic morphologies involved in those procedures would be obtained. Interestingly, previous studies have shown that both isoflurane- and xenon-induced CA1-LTP deficits were able to be reversed after the remove of the anesthetic itself (Haseneder et al., 2009; Simon, Hapfelmeier, Kochs, Zieglgaensberger, & Rammes, 2001).

In addition, exposure of both anesthesia by isoflurane and sevoflurane might change other pathophysiological processes, for example, autophagy (Ye & Zuo, 2017). This

may be the reason why the negative effects under sevoflurane treatment, including the abnormal molecular levels, dendritic spines, and CA1-potentiation, were partially reversible by BACE inhibition. Besides, I observed in the present thesis a wider modification by inhibiting BACE. For instance, co-application of sevoflurane and LY2886721 decreased 1) expressions of APP and nectin-3 in CA3; 2) co-stainings of APP and nectin-3 in CA1. These observations might attribute to the pleiotropic functions of BACE (Parsons & Rammes, 2017).

The essential role of the post-synaptic molecule nectin-3 in the maintenance of neuronal morphologies and functions has been reported by previous studies. A downregulation strategy of nectin-3 expressions hampers learning and memory. These detrimental effects are due to spine elimination by nectin-3 reduction (X. D. Wang et al., 2013). The present thesis showed further that nectin-3 downregulation specifically in CA1 abolished potentiation as well as reduced spine density. It is therefore reasonable that nectin-3 is also essential for the maintenance of the CA1-neuronal morphologies and functions. The above observations suggest that nectin-3 is fundamental to the dendritic spine dynamics as well as synaptic connection in the hippocampus.

Surprisingly, in CA1, a co-expression pattern of APP and nectin-3 was observed. It still needs additional investigations to better understand the mechanisms regarding the co-expressions and their regulatory factors.

Taken together, the present thesis have shown that sevoflurane anesthesia elevated $A\beta_{1-42}$ production, decreased nectin-3 expressions, and therefore reduced spine count and abolished CA1-potentiation. Moreover, isoflurane anesthesia decreased dendritic spines and blocked CA1-potentiation. Even though xenon exposure attenuated CA1-

potentiation, it did not alternate the APP proteolysis process nor spine dynamics in the hippocampus.

In conclusion, this thesis suggests that the inhalational anesthetic sevoflurane is fundamental for maintaining the molecule expressions, synapse morphologies, and synaptic functions in the CA1 region. In addition, inhibition of BACE partially reversed the synaptic impairments evoked by sevoflurane anesthesia. These suggest that the detrimental effects of sevoflurane on the pathophysiology of AD is therefore predictable. In comparison, isoflurane produces pronounced dysfunction of potentiation, however, it only mildly affects the mentioned molecule levels and synaptic morphology. In contrast, xenon exhibits a neuroprotective mechanism in the hippocampus.

The present thesis unraveled how the three widely applied inhalational anesthetics on modifying the CA1-synaptic plasticity as well as spine density, and further indicates BACE might be a new target for modulating the cognition impairments produced by inhalational anesthesia.

Reference

1. Alam, A., Suen, K. C., Hana, Z., Sanders, R. D., Maze, M., & Ma, D. (2017). Neuroprotection and neurotoxicity in the developing brain: an update on the effects of dexmedetomidine and xenon. *Neurotoxicology and teratology*, *60*, 102-116.
2. Allinson., T. M. J., Parkin., E. T., Turner., A. J., & Hooper., N. M. (2003). ADAMs family members as amyloid precursor protein alpha-secretases. *J Neurosci Res*, *74*, 342–352
3. Aranake, A., Mashour, G. A., & Avidan, M. S. (2013). Minimum alveolar concentration: ongoing relevance and clinical utility. *Anaesthesia*, *68*(5), 512-522.
4. Baldwin, J. M., Schertler, G. F., & Unger, V. M. (1997). An alpha-carbon template for the transmembrane helices in the rhodopsin family of G-protein-coupled receptors. *Journal of molecular biology*, *272*(1), 144-164.
5. Barage, S. H., & Sonawane, K. D. (2015). Amyloid cascade hypothesis: Pathogenesis and therapeutic strategies in Alzheimer's disease. *Neuropeptides*, *52*, 1-18.
6. Basu, J., & Siegelbaum, S. A. (2015). The Corticohippocampal Circuit, Synaptic Plasticity, and Memory. *Cold Spring Harb Perspect Biol*, *7*(11).
7. Behne, M., Wilke, H. J., & Harder, S. (1999). Clinical pharmacokinetics of sevoflurane. *Clin Pharmacokinet*, *36*(1), 13-26.
8. BERCHTOLD., N. C., & COTMAN., C. W. (1998). Evolution in the Conceptualization of Dementia and Alzheimer's Disease: Greco-Roman Period to the 1960s. *Neurobiology of Aging*, *19*, 173-189.
9. Berry, K. P., & Nedivi, E. (2017). Spine Dynamics: Are They All the Same? *Neuron*, *96*(1), 43-55.

10. Blessed, G., Tomlinson, B. E., & Roth, M. (1968). The Association Between Quantitative Measures of Dementia and of Senile Change in the Cerebral Grey Matter of Elderly Subjects. *British Journal of Psychiatry*, *114*(512), 797-811.
11. Booth, D. R., Sunde, M., Bellotti, V., Robinson, C. V., Hutchinson, W. L., Fraser, P. E., Hawkins, P. N., Dobson, C. M., Radford, S. E., Blake, C. C. F., & Pepys, M. B. (1997). Instability, unfolding and aggregation of human lysozyme variants underlying amyloid fibrillogenesis. *Nature*, *385*(6619), 787-793.
12. Braganza, L. F., & Worcester, D. L. (1986). Structural changes in lipid bilayers and biological membranes caused by hydrostatic pressure. *Biochemistry*, *25*(23), 7484-7488.
13. Breuer, T., Emontzpohl, C., Coburn, M., Benstoem, C., Rossaint, R., Marx, G., Schaelte, G., Bernhagen, J., Bruells, C. S., Goetzenich, A., & Stoppe, C. (2015). Xenon triggers pro-inflammatory effects and suppresses the anti-inflammatory response compared to sevoflurane in patients undergoing cardiac surgery. *Crit Care*, *19*, 365.
14. Briner, A., De Roo, M., Dayer, A., Muller, D., Habre, W., & Vutskits, L. (2010). Volatile Anesthetics Rapidly Increase Dendritic Spine Density in the Rat Medial Prefrontal Cortex during Synaptogenesis. *Anesthesiology*, *112*(3), 546-556.
15. Buerge, M., Kratzer, S., Mattusch, C., Hofmann, C., Kreuzer, M., Parsons, C. G., & Rammes, G. (2019). The anaesthetic xenon partially restores an amyloid beta-induced impairment in murine hippocampal synaptic plasticity. *Neuropharmacology*, *151*, 21-32.
16. Campagna, J. A., Miller, K. W., & Forman, S. A. (2003). Mechanisms of Actions of Inhaled Anesthetics. *New England Journal of Medicine*, *348*(21), 2110-2124.
17. Cascella, M., & Bimonte, S. (2017). The role of general anesthetics and the mechanisms of hippocampal and extra-hippocampal dysfunctions in the genesis of postoperative cognitive dysfunction. *Neural regeneration research*, *12*(11), 1780.

18. Castaño, E. M., Ghiso, J., Prelli, F., Gorevic, P. D., Migheli, A., & Frangione, B. (1986). In vitro formation of amyloid fibrils from two synthetic peptides of different lengths homologous to alzheimer's disease β -protein. *Biochemical and Biophysical Research Communications*, *141*(2), 782-789.
19. Cesarovic, N., Nicholls, F., Rettich, A., Kronen, P., Hässig, M., Jirkof, P., & Arras, M. (2010). Isoflurane and sevoflurane provide equally effective anaesthesia in laboratory mice. *Laboratory Animals*, *44*(4), 329-336.
20. Cousins, S. L., Dai, W., & Stephenson, F. A. (2015). APLP1 and APLP2, members of the APP family of proteins, behave similarly to APP in that they associate with NMDA receptors and enhance NMDA receptor surface expression. *J Neurochem*, *133*(6), 879-885.
21. Cullen, S. C., & Gross, E. G. (1951). The anesthetic properties of xenon in animals and human beings, with additional observations on krypton. *Science*, *113*(2942), 580-582.
22. Davy, H. (1800). *Researches, Chemical and Philosophical; Chiefly Concerning Nitrous Oxide: Or Dephlogisticated Nitrous Air, and its Respiration*: J. Johnson.
23. Dawson, G. R., Seabrook, G. R., Zheng, H., Smith, D. W., Graham, S., O'Dowd, G., Bowery, B. J., Boyce, S., Trumbauer, M. E., Chen, H. Y., Van der Ploeg, L. H. T., & Sirinathsinghji, D. J. S. (1999). Age-related cognitive deficits, impaired long-term potentiation and reduction in synaptic marker density in mice lacking the β -amyloid precursor protein. *Neuroscience*, *90*(1), 1-13.
24. Deyts, C., Thinakaran, G., & Parent, A. T. (2016). APP Receptor? To Be or Not To Be. *Trends Pharmacol Sci*, *37*(5), 390-411.
25. Dislich, B., & Lichtenthaler, S. F. (2012). The Membrane-Bound Aspartyl Protease BACE1: Molecular and Functional Properties in Alzheimer's Disease and Beyond. *Front Physiol*, *3*, 8.

26. Dodart, J.-C., Bales, K. R., Gannon, K. S., Greene, S. J., DeMattos, R. B., Mathis, C., DeLong, C. A., Wu, S., Wu, X., Holtzman, D. M., & Paul, S. M. (2002). Immunization reverses memory deficits without reducing brain A β burden in Alzheimer's disease model. *Nature Neuroscience*, *5*(5), 452-457.
27. Dong, Y., Xu, Z., Zhang, Y., McAuliffe, S., Wang, H., Shen, X., Yue, Y., & Xie, Z. (2011). RNA interference-mediated silencing of BACE and APP attenuates the isoflurane-induced caspase activation. *Medical gas research*, *1*(1), 5-5.
28. Dong, Y., Zhang, G., Zhang, B., Moir, R. D., Xia, W., Marcantonio, E. R., Culley, D. J., Crosby, G., Tanzi, R. E., & Xie, Z. (2009). The common inhalational anesthetic sevoflurane induces apoptosis and increases beta-amyloid protein levels. *Archives of Neurology*, *66*(5), 620-631.
29. Dorsam, R. T., & Gutkind, J. S. (2007). G-protein-coupled receptors and cancer. *Nat Rev Cancer*, *7*(2), 79-94.
30. Durieux, M. E. (1995). Halothane inhibits signaling through m1 muscarinic receptors expressed in *Xenopus* oocytes. *The Journal of the American Society of Anesthesiologists*, *82*(1), 174-182.
31. Dwyer, R., Bennett, H. L., Eger, E. I., & Heilbron, D. (1992). Effects of Isoflurane and Nitrous Oxide in Subanesthetic Concentrations on Memory and Responsiveness in Volunteers. *Anesthesiology*, *77*(5), 888-898. doi:10.1097/00000542-199211000-00009
32. Eckenhoff, R. G. (2001). Promiscuous ligands and attractive cavities. *Molecular interventions*, *1*(5), 258.
33. Eckenhoff, R. G., Johansson, J. S., Wei, H., Carnini, A., Kang, B., Wei, W., Pidikiti, R., Keller, J. M., & Eckenhoff, M. F. (2004). Inhaled anesthetic enhancement of amyloid- β oligomerization and cytotoxicity. *The Journal of the American Society of Anesthesiologists*, *101*(3), 703-709.

34. Eger, E. I., 2nd, Raines, D. E., Shafer, S. L., Hemmings, H. C., Jr., & Sonner, J. M. (2008). Is a new paradigm needed to explain how inhaled anesthetics produce immobility? *Anesth Analg*, *107*(3), 832-848.
35. Eger, E. I. I. (2001). Age, Minimum Alveolar Anesthetic Concentration, and Minimum Alveolar Anesthetic Concentration-Awake. *Anesthesia & Analgesia*, *93*(4), 947-953.
36. El-Agnaf, O. M., Mahil, D. S., Patel, B. P., & Austen, B. M. (2000). Oligomerization and toxicity of beta-amyloid-42 implicated in Alzheimer's disease. *Biochem Biophys Res Commun*, *273*(3), 1003-1007.
37. Esencan, E., Yuksel, S., Tosun, Y. B., Robinot, A., Solaroglu, I., & Zhang, J. H. (2013). XENON in medical area: emphasis on neuroprotection in hypoxia and anesthesia. *Med Gas Res*, *3*(1), 4.
38. Evered, L., Scott, D. A., & Silbert, B. (2017). Cognitive decline associated with anesthesia and surgery in the elderly: does this contribute to dementia prevalence? *Current Opinion in Psychiatry*, *30*(3).
39. Feldman, S. A., Scurr, C. F., & Paton, W. (1993). *Mechanisms of drugs in anaesthesia*: Edward Arnold.
40. Ferreira, S. T., Lourenco, M. V., Oliveira, M. M., & De Felice, F. G. (2015). Soluble amyloid-beta oligomers as synaptotoxins leading to cognitive impairment in Alzheimer's disease. *Front Cell Neurosci*, *9*, 191.
41. Ferreira, S. T., Vieira, M. N., & De Felice, F. G. (2007). Soluble protein oligomers as emerging toxins in Alzheimer's and other amyloid diseases. *IUBMB Life*, *59*(4-5), 332-345.
42. Fodale, V., Tripodi, V. F., Penna, O., Famà, F., Squadrito, F., Mondello, E., & David, A. (2017). An update on anesthetics and impact on the brain. *Expert opinion on drug safety*, *16*(9), 997-1008.

43. Franks, N., & Lieb, W. (1979). The structure of lipid bilayers and the effects of general anaesthetics: an x-ray and neutron diffraction study. *Journal of molecular biology*, *133*(4), 469-500.
44. Franks, N. P. (2006). Molecular targets underlying general anaesthesia. *Br J Pharmacol*, *147 Suppl 1*, S72-81.
45. Georganopoulou, D. G., Chang, L., Nam, J.-M., Thaxton, C. S., Mufson, E. J., Klein, W. L., & Mirkin, C. A. (2005). Nanoparticle-based detection in cerebral spinal fluid of a soluble pathogenic biomarker for Alzheimer's disease. *Proceedings of the National Academy of Sciences of the United States of America*, *102*(7), 2273.
46. Giagtzoglou, N., Ly, C. V., & Bellen, H. J. (2009). Cell adhesion, the backbone of the synapse: "vertebrate" and "invertebrate" perspectives. *Cold Spring Harb Perspect Biol*, *1*(4), a003079.
47. Giannakopoulos, P., Herrmann, F. R., Bussi re, T., Bouras, C., K vari, E., Perl, D. P., Morrison, J. H., Gold, G., & Hof, P. R. (2003). Tangle and neuron numbers, but not amyloid load, predict cognitive status in Alzheimer's disease. *Neurology*, *60*(9), 1495.
48. Gipson, C. D., & Olive, M. F. (2017). Structural and functional plasticity of dendritic spines - root or result of behavior? *Genes Brain Behav*, *16*(1), 101-117.
49. Glass, P. S., Gan, T. J., Scott Howell, M., & Brian Ginsberg, M. (1997). Drug interactions: volatile anesthetics and opioids. *Journal of clinical anesthesia*, *9*(6), 18S-22S.
50. Goate, A., Chartier-Harlin, M.-C., Mullan, M., Brown, J., Crawford, F., Fidani, L., Giuffra, L., Haynes, A., Irving, N., James, L., Mant, R., Newton, P., Rooke, K., Roques, P., Talbot, C., Pericak-Vance, M., Roses, A., Williamson, R., Rossor, M., Owen, M., & Hardy, J. (1991). Segregation of a missense mutation in the amyloid precursor protein gene with familial Alzheimer's disease. *Nature*, *349*, 704-706.

51. Golde, T. E. (2003). Alzheimer disease therapy: can the amyloid cascade be halted? *J Clin Invest*, *111*(1), 11-18.
52. Gong, Q., Su, Y. A., Wu, C., Si, T. M., Deussing, J. M., Schmidt, M. V., & Wang, X. D. (2018). Chronic Stress Reduces Nectin-1 mRNA Levels and Disrupts Dendritic Spine Plasticity in the Adult Mouse Perirhinal Cortex. *Front Cell Neurosci*, *12*, 67.
53. Gong, Y., Chang, L., Viola, K. L., Lacor, P. N., Lambert, M. P., Finch, C. E., Krafft, G. A., & Klein, W. L. (2003). Alzheimer's disease-affected brain: Presence of oligomeric A β ligands (ADDLs) suggests a molecular basis for reversible memory loss. *Proceedings of the National Academy of Sciences*, *100*(18), 10417.
54. Goto, T., Nakata, Y., Ishiguro, Y., Niimi, Y., Suwa, K., & Morita, S. (2000). Minimum Alveolar Concentration–Awake of Xenon Alone and in Combination with Isoflurane or Sevoflurane. *Anesthesiology*, *93*(5), 1188-1193.
55. Granak, S., Hoschl, C., & Ovsepian, S. V. (2021). Dendritic spine remodeling and plasticity under general anesthesia. *Brain Struct Funct*, *226*(7), 2001-2017.
56. Gustavsson, Å., Engström, U., & Westermark, P. (1991). Normal transthyretin and synthetic transthyretin fragments from amyloid-like fibrils in vitro. *Biochemical and Biophysical Research Communications*, *175*(3), 1159-1164.
57. Haass, C., & Selkoe, D. J. (2007). Soluble protein oligomers in neurodegeneration: lessons from the Alzheimer's amyloid beta-peptide. *Nat Rev Mol Cell Biol*, *8*(2), 101-112.
58. Harada, H., Tamaoka, A., Ishii, K., Kametaka, S., Kametani, F., Saito, Y., & Murayama, S. (2006). Beta-site APP cleaving enzyme 1 (BACE1) is increased in remaining neurons in Alzheimer's disease brains. *Neuroscience research*, *54*(1), 24-29.
59. Hardy, J., & Selkoe, D. J. (2002). The Amyloid Hypothesis of Alzheimer's Disease: Progress and Problems on the Road to Therapeutics. *Science*, *297*(5580), 353.

60. Harris KM, & Jensen FE, T. B. (1992). Three-dimensional structure of dendritic spines and synapses in rat hippocampus (CA1) at postnatal day 15 and adult ages: implications for the maturation of synaptic physiology and long-term potentiation. *The Journal of Neuroscience*, *12*(7).
61. Haseneder, R., Kratzer, S., von Meyer, L., Eder, M., Kochs, E., & Rammes, G. (2009). Isoflurane and sevoflurane dose-dependently impair hippocampal long-term potentiation. *Eur J Pharmacol*, *623*(1-3), 47-51.
62. Haseneder., R., Kratzer., S., Kochs., E., Eckle., V.-S., Zieglgänsberger., W., & Rammes., G. (2008). Xenon reduces N-methyl-D-aspartate and alpha-amino-3-hydroxy-5-methyl-4-isoxazolepropionic acid receptor-mediated synaptic transmission in the amygdala. *Anesthesiology*, *109*, 998–1006.
63. Head, Brian P., Patel, Hemal H., Niesman, Ingrid R., Drummond, John C., Roth, David M., & Patel, Piyush M. (2009). Inhibition of p75 Neurotrophin Receptor Attenuates Isoflurane-mediated Neuronal Apoptosis in the Neonatal Central Nervous System. *Anesthesiology*, *110*(4), 813-825.
64. Hemmings, H. C., Jr., Akabas, M. H., Goldstein, P. A., Trudell, J. R., Orser, B. A., & Harrison, N. L. (2005). Emerging molecular mechanisms of general anesthetic action. *Trends Pharmacol Sci*, *26*(10), 503-510.
65. Hering, H., & Sheng, M. (2001). Dendritic spines : structure, dynamics and regulation. *Nature Reviews Neuroscience*, *2*(12), 880-888.
66. Hick, M., Herrmann, U., Weyer, S. W., Mallm, J. P., Tschape, J. A., Borgers, M., Mercken, M., Roth, F. C., Draguhn, A., Slomianka, L., Wolfer, D. P., Korte, M., & Muller, U. C. (2015). Acute function of secreted amyloid precursor protein fragment APP α in synaptic plasticity. *Acta Neuropathol*, *129*(1), 21-37.

67. Ho., A., & Südhof, T. C. (2004). Binding of F-spondin to amyloid-beta precursor protein: a candidate amyloid-beta precursor protein ligand that modulates amyloid-beta precursor protein cleavage. *Proc Natl Acad Sci USA*, *101*, 2548–2553.
68. Hofmann, C., Sander, A., Wang, X. X., Buerge, M., Jungwirth, B., Borgstedt, L., Kreuzer, M., Kopp, C., Schorpp, K., Hadian, K., Wotjak, C. T., Ebert, T., Ruitenber, M., Parsons, C. G., & Rammes, G. (2021). Inhalational Anesthetics Do Not Deteriorate Amyloid- β -Derived Pathophysiology in Alzheimer's Disease: Investigations on the Molecular, Neuronal, and Behavioral Level. *J Alzheimers Dis*, *84*(3), 1193-1218.
69. Holsinger, R. D., McLean, C. A., Beyreuther, K., Masters, C. L., & Evin, G. (2002). Increased expression of the amyloid precursor β - secretase in Alzheimer's disease. *Annals of neurology: Official journal of the American neurological association and the child neurology society*, *51*(6), 783-786.
70. Homi, H. M., Yokoo, N., Ma, D., Warner, D. S., Franks, N. P., Maze, M., & Grocott, H. P. (2003). The neuroprotective effect of xenon administration during transient middle cerebral artery occlusion in mice. *The Journal of the American Society of Anesthesiologists*, *99*(4), 876-881.
71. Honemann, C. W., Nietgen, G. W., Podranski, T., Chan, C. K., & Durieux, M. E. (1998). Influence of volatile anesthetics on thromboxane A₂ signaling. *The Journal of the American Society of Anesthesiologists*, *88*(2), 440-451.
72. Hong, L., Koelsch, G., Lin, X., Wu, S., Terzyan, S., Ghosh, A. K., Zhang, X. C., & Tang, J. (2000). Structure of the protease domain of memapsin 2 (β -secretase) complexed with inhibitor. *Science*, *290*(5489), 150-153.
73. Irizarry, M. C., Locascio, J. J., & Hyman, B. T. (2001). β -Site APP Cleaving Enzyme mRNA Expression in APP Transgenic Mice. *The American Journal of Pathology*, *158*(1), 173-177.

74. Ishizawa, Y., Ma, H.-C., Dohi, S., & Shimonaka, H. (2000). Effects of cholinomimetic injection into the brain stem reticular formation on halothane anesthesia and antinociception in rats. *Journal of Pharmacology and Experimental Therapeutics*, 293(3), 845-851.
75. Ishizawa, Y., Pidikiti, R., Liebman, P. A., & Eckenhoff, R. G. (2002). G protein-coupled receptors as direct targets of inhaled anesthetics. *Molecular pharmacology*, 61(5), 945-952.
76. Istaphanous, G. K., Howard, J., Nan, X., Hughes, E. A., McCann, J. C., McAuliffe, J. J., Danzer, S. C., & Loepke, A. W. (2013). Comparison of the Neuroapoptotic Properties of Equipotent Anesthetic Concentrations of Desflurane, Isoflurane, or Sevoflurane in Neonatal Mice. *Anesthesiology*, 114, 578-587.
77. Jerath, A., Parotto, M., Wasowicz, M., & Ferguson, N. D. (2016). Volatile Anesthetics. Is a New Player Emerging in Critical Care Sedation? *Am J Respir Crit Care Med*, 193(11), 1202-1212.
78. Jia, M., Liu, W.-X., Yang, J.-J., Xu, N., Xie, Z.-M., Ju, L.-S., Ji, M.-H., Martynyuk, A. E., & Yang, J.-J. (2016). Role of histone acetylation in long-term neurobehavioral effects of neonatal Exposure to sevoflurane in rats. *Neurobiology of Disease*, 91, 209-220.
79. Jiang, J., & Jiang, H. (2015). Effect of the inhaled anesthetics isoflurane, sevoflurane and desflurane on the neuropathogenesis of Alzheimer's disease. *Mol Med Rep*, 12(1), 3-12.
80. Johnson, F. H., & Flagler, E. A. (1950). Hydrostatic pressure reversal of narcosis in tadpoles. *Science*, 112(2899), 91-92.
81. Johnson, S. C., Pan, A., Li, L., Sedensky, M., & Morgan, P. (2019). Neurotoxicity of anesthetics: Mechanisms and meaning from mouse intervention studies. *Neurotoxicol Teratol*, 71, 22-31.

82. Jones, M. V., & Harrison, N. L. (1993). Effects of volatile anesthetics on the kinetics of inhibitory postsynaptic currents in cultured rat hippocampal neurons. *Journal of Neurophysiology*, 70(4), 1339-1349.
83. Joyce, J. A. (2000). Xenon: anesthesia for the 21st century. *AANA J*, 68(3), 259-264.
84. Karran, E., Mercken, M., & De Strooper, B. (2011). The amyloid cascade hypothesis for Alzheimer's disease: an appraisal for the development of therapeutics. *Nat Rev Drug Discov*, 10(9), 698-712.
85. Katzman, R., Terry, R., DeTeresa, R., Brown, T., Davies, P., Fuld, P., Renbing, X., & Peck, A. (1988). Clinical, pathological, and neurochemical changes in dementia: A subgroup with preserved mental status and numerous neocortical plaques. *Annals of Neurology*, 23(2), 138-144.
86. Klein, W. L., Krafft, G. A., & Finch, C. E. (2001). Targeting small A β oligomers: the solution to an Alzheimer's disease conundrum? *Trends in Neurosciences*, 24(4), 219-224.
87. Koblin, D. D., Fang, Z., Eger, E. I., 2nd, Laster, M. J., Gong, D., Ionescu, P., Halsey, M. J., & Trudell, J. R. (1998). Minimum alveolar concentrations of noble gases, nitrogen, and sulfur hexafluoride in rats: helium and neon as nonimmobilizers (nonanesthetics). *Anesth Analg*, 87(2), 419-424.
88. Korkotian, E., & Segal, M. (2000). Structure-function relations in dendritic spines: is size important? *Hippocampus*, 10(5), 587-595.
89. Kotilinek, L. A., Bacskai, B., Westerman, M., Kawarabayashi, T., Younkin, L., Hyman, B. T., Younkin, S., & Ashe, K. H. (2002). Reversible Memory Loss in a Mouse Transgenic Model of Alzheimer's Disease. *The Journal of Neuroscience*, 22(15), 6331.
90. Krasowski, M., & Harrison, N. (1999). General anaesthetic actions on ligand-gated ion channels. *Cellular and Molecular Life Sciences CMLS*, 55(10), 1278-1303.

91. Kratzer., S., Mattusch., C., Kochs., E., Eder., M., Haseneder., R., & Rammes., G. (2012). Xenon Attenuates Hippocampal Long-term Potentiation by Diminishing Synaptic and Extrasynaptic N-methyl-D-aspartate Receptor Currents. *Anesthesiology*, *116*, 673–682.
92. Kuo., Y.-M., Emmerling., M. R., Vigo-Pelfrey., C., Kasunic., T. C., Kirkpatrick., J. B., Murdoch†., G. H., Ball., M. J., & Roher., A. E. (1996). Water-soluble Abeta (N-40, N-42) Oligomers in Normal and Alzheimer Disease Brains. *J. Biol. Chem.*, *271*, 4077 – 4081.
93. Lacor, P. N., Buniel, M. C., Chang, L., Fernandez, S. J., Gong, Y., Viola, K. L., Lambert, M. P., Velasco, P. T., Bigio, E. H., Finch, C. E., Krafft, G. A., & Klein, W. L. (2004). Synaptic targeting by Alzheimer's-related amyloid beta oligomers. *J Neurosci*, *24*(45), 10191-10200.
94. Lambert, M. P., Barlow, A. K., Chromy, B. A., Edwards, C., Freed, R., Liosatos, M., Morgan, T. E., Rozovsky, I., Trommer, B., Viola, K. L., Wals, P., Zhang, C., Finch, C. E., Krafft, G. A., & Klein, W. L. (1998). Diffusible, nonfibrillar ligands derived from A β ₁₋₄₂ are potent central nervous system neurotoxins. *Proceedings of the National Academy of Sciences*, *95*(11), 6448.
95. Landin, J. D., Palac, M., Carter, J. M., Dzumaga, Y., Santerre-Anderson, J. L., Fernandez, G. M., Savage, L. M., Varlinskaya, E. I., Spear, L. P., Moore, S. D., Swartzwelder, H. S., Fleming, R. L., & Werner, D. F. (2019). General anesthetic exposure in adolescent rats causes persistent maladaptations in cognitive and affective behaviors and neuroplasticity. *Neuropharmacology*, *150*, 153-163.
96. Lee, K. J., Moussa, C. E., Lee, Y., Sung, Y., Howell, B. W., Turner, R. S., Pak, D. T., & Hoe, H. S. (2010). Beta amyloid-independent role of amyloid precursor protein in generation and maintenance of dendritic spines. *Neuroscience*, *169*(1), 344-356.

97. Lesne, S., Koh, M. T., Kotilinek, L., Kaye, R., Glabe, C. G., Yang, A., Gallagher, M., & Ashe, K. H. (2006). A specific amyloid-beta protein assembly in the brain impairs memory. *Nature*, *440*(7082), 352-357.
98. Lever, M., Miller, K., Paton, W., & Smith, E. (1971). Pressure reversal of anaesthesia. *Nature*, *231*(5302), 368-371.
99. Lin, D., Cao, L., Wang, Z., Li, J., Washington, J. M., & Zuo, Z. (2012). Lidocaine attenuates cognitive impairment after isoflurane anesthesia in old rats. *Behavioural Brain Research*, *228*(2), 319-327.
100. Ling, Y. Z., Ma, W., Yu, L., Zhang, Y., & Liang, Q. S. (2015). Decreased PSD95 expression in medial prefrontal cortex (mPFC) was associated with cognitive impairment induced by sevoflurane anesthesia. *J Zhejiang Univ Sci B*, *16*(9), 763-771.
101. Liu, B., Ou, G., Chen, Y., & Zhang, J. (2019). Inhibition of protein tyrosine phosphatase 1B protects against sevoflurane-induced neurotoxicity mediated by ER stress in developing brain. *Brain Research Bulletin*, *146*, 28-39.
102. Liu, B., Xia, J., Chen, Y., & Zhang, J. (2017). Sevoflurane-Induced Endoplasmic Reticulum Stress Contributes to Neuroapoptosis and BACE-1 Expression in the Developing Brain: The Role of eIF2alpha. *Neurotox Res*, *31*(2), 218-229.
103. Liu, R., Wang, H., Wang, H. L., Sun, Y. X., Su, Y. A., Wang, X. D., Li, J. T., & Si, T. M. (2019). Postnatal nectin-3 knockdown induces structural abnormalities of hippocampal principal neurons and memory deficits in adult mice. *Hippocampus*.
104. Liu, W., Khatibi, N., Sridharan, A., & Zhang, J. H. (2011). Application of medical gases in the field of neurobiology. *Medical gas research*, *1*(1), 1-18.
105. Lopes, D. H., Colin, C., Degaki, T. L., de Sousa, A. C., Vieira, M. N., Sebollela, A., Martinez, A. M., Bloch, C., Jr., Ferreira, S. T., & Sogayar, M. C. (2004). Amyloidogenicity and cytotoxicity of recombinant mature human islet amyloid polypeptide (rhIAPP). *J Biol Chem*, *279*(41), 42803-42810.

106. López-Sánchez, N., Müller, U., & Frade, J. M. (2005). Lengthening of G2/mitosis in cortical precursors from mice lacking β -amyloid precursor protein. *Neuroscience*, *130*(1), 51-60.
107. Ma, D., Wilhelm, S., Maze, M., & Franks, N. (2002). Neuroprotective and neurotoxic properties of the 'inert' gas, xenon. *British Journal of Anaesthesia*, *89*(5), 739-746.
108. Ma, D., Yang, H., Lynch, J., Franks, Nicholas P., Maze, M., & Grocott, Hilary P. (2003). Xenon Attenuates Cardiopulmonary Bypass-induced Neurologic and Neurocognitive Dysfunction in the Rat. *Anesthesiology*, *98*(3), 690-698.
109. Ma, Q. H., Futagawa, T., Yang, W. L., Jiang, X. D., Zeng, L., Takeda, Y., Xu, R. X., Bagnard, D., Schachner, M., Furley, A. J., Karagogeos, D., Watanabe, K., Dawe, G. S., & Xiao, Z. C. (2008). A TAG1-APP signalling pathway through Fe65 negatively modulates neurogenesis. *Nat Cell Biol*, *10*(3), 283-294.
110. Magara, F., Müller, U., Li, Z. W., Lipp, H. P., Weissmann, C., Stagljar, M., & Wolfer, D. P. (1999). Genetic background changes the pattern of forebrain commissure defects in transgenic mice underexpressing the beta-amyloid-precursor protein. *Proceedings of the National Academy of Sciences of the United States of America*, *96*(8), 4656-4661.
111. Majewska, A., Brown, E., Ross, J., & Yuste, R. (2000). Mechanisms of Calcium Decay Kinetics in Hippocampal Spines: Role of Spine Calcium Pumps and Calcium Diffusion through the Spine Neck in Biochemical Compartmentalization. *The Journal of Neuroscience*, *20*(5), 1722-1734.
112. Maloy, A. L., Longnecker, D. S., & Greenberg, E. R. (1981). The relation of islet amyloid to the clinical type of diabetes. *Human Pathology*, *12*, 917-922.
113. Mattson, M. P. (1997). Cellular actions of beta-amyloid precursor protein and its soluble and fibrillogenic derivatives. *PHYSIOLOGICAL REVIEWS*, *77*(4), 1081-1132.
114. Mattusch, C., Kratzer, S., Buerge, M., Kreuzer, M., Engel, T., Kopp, C., Biel, M., Hammelmann, V., Ying, S. W., Goldstein, P. A., Kochs, E., Haseneder, R., & Rammes,

- G. (2015). Impact of Hyperpolarization-activated, Cyclic Nucleotide-gated Cation Channel Type 2 for the Xenon-mediated Anesthetic Effect: Evidence from In Vitro and In Vivo Experiments. *Anesthesiology*, 122(5), 1047-1059.
115. May, P. C., Willis, B. A., Lowe, S. L., Dean, R. A., Monk, S. A., Cocke, P. J., Audia, J. E., Boggs, L. N., Borders, A. R., Brier, R. A., Calligaro, D. O., Day, T. A., Ereshefsky, L., Erickson, J. A., Gevorkyan, H., Gonzales, C. R., James, D. E., Jhee, S. S., Komjathy, S. F., Li, L., Lindstrom, T. D., Mathes, B. M., Martényi, F., Sheehan, S. M., Stout, S. L., Timm, D. E., Vaught, G. M., Watson, B. M., Winneroski, L. L., Yang, Z., & Mergott, D. J. (2015). The potent BACE1 inhibitor LY2886721 elicits robust central A β pharmacodynamic responses in mice, dogs, and humans. *J Neurosci*, 35(3), 1199-1210.
116. Mazze, Richard I., Rice, Susan A., & Baden, Jeffrey M. (1985). Halothane, Isoflurane, and Enflurane MAC in Pregnant and Nonpregnant Female and Male Mice and Rats. *Anesthesiology*, 62(3), 339-341.
117. Minami, K., & Uezono, Y. (2005). G-protein-coupled receptors as targets for anesthetics. *International Congress Series*, 1283, 108-112.
118. Minami, K., & Uezono, Y. (2013). The recent progress in research on effects of anesthetics and analgesics on G protein-coupled receptors. *J Anesth*, 27(2), 284-292.
119. Mori, M., Rikitake, Y., Mandai, K., & Takai, Y. (2014). Roles of Nectins and Nectin-Like Molecules in the Nervous System. In *Cell Adhesion Molecules* (pp. 91-116).
120. Mueller, U. C., Deller, T., & Korte, M. (2017). Not just amyloid: physiological functions of the amyloid precursor protein family. *Nat Rev Neurosci*, 18(5), 281-298.
121. Neumann, E., Khawaja, K., & Muller-Ladner, U. (2014). G protein-coupled receptors in rheumatology. *Nat Rev Rheumatol*, 10(7), 429-436.
122. Neves, S. R., Ram, P. T., & Iyengar, R. (2002). G protein pathways. *Science*, 296(5573), 1636-1639.

123. Nishino, T., Jin, H., Nozaki-Taguchi, N., & Isono, S. (2020). A high concentration of sevoflurane induces gasping breaths in mice. *Respiratory Physiology & Neurobiology*, 279, 103445.
124. O'Brien, R. J., & Wong, P. C. (2011). Amyloid precursor protein processing and Alzheimer's disease. *Annu Rev Neurosci*, 34, 185-204.
125. Ohno, M., Chang, L., Tseng, W., Oakley, H., Citron, M., Klein, W. L., Vassar, R., & Disterhoft, J. F. (2006). Temporal memory deficits in Alzheimer's mouse models: rescue by genetic deletion of BACE1. *Eur J Neurosci*, 23(1), 251-260.
126. Parsons, C. G., & Rammes, G. (2017). Preclinical to phase II amyloid beta (A β) peptide modulators under investigation for Alzheimer's disease. *Expert Opin Investig Drugs*, 26(5), 579-592.
127. Pepys, M. B., Hawkins, P. N., Booth, D. R., Vigushin, D. M., Tennent, G. A., Soutar, A. K., Totty, N., Nguyen, O., Blake, C. C. F., Terry, C. J., Feast, T. G., Zalin, A. M., & Hsuan, J. J. (1993). Human lysozyme gene mutations cause hereditary systemic amyloidosis. *Nature*, 362(6420), 553-557.
128. Perez., R. G., Zheng., H., Ploeg., L. H. T. V. d., & Koo., E. H. (1997). The β -Amyloid Precursor Protein of Alzheimer's Disease Enhances Neuron Viability and Modulates Neuronal Polarity. *J Neurosci*, 17, 9407-9414.
129. Pierce, K. L., Premont, R. T., & Lefkowitz, R. J. (2002). Seven-transmembrane receptors. *Nat Rev Mol Cell Biol*, 3(9), 639-650.
130. Platholi, J., Herold, K. F., Hemmings, H. C., Jr., & Halpain, S. (2014). Isoflurane reversibly destabilizes hippocampal dendritic spines by an actin-dependent mechanism. *PLoS One*, 9(7), e102978.
131. Prox, J., Bernreuther, C., Altmepfen, H., Grendel, J., Glatzel, M., D'Hooge, R., Stroobants, S., Ahmed, T., Balschun, D., Willem, M., Lammich, S., Isbrandt, D., Schweizer, M., Horr , K., De Strooper, B., & Saftig, P. (2013). Postnatal Disruption of

- the Disintegrin/Metalloproteinase ADAM10 in Brain Causes Epileptic Seizures, Learning Deficits, Altered Spine Morphology, and Defective Synaptic Functions. *The Journal of Neuroscience*, 33(32), 12915-12928.
132. Qiu, L. L., Pan, W., Luo, D., Zhang, G. F., Zhou, Z. Q., Sun, X. Y., Yang, J. J., & Ji, M. H. (2020). Dysregulation of BDNF/TrkB signaling mediated by NMDAR/Ca(2+)/calpain might contribute to postoperative cognitive dysfunction in aging mice. *J Neuroinflammation*, 17(1), 23.
133. Qiu., C., Kivipelto., M., & Strauss., E. v. (2009). Epidemiology of Alzheimer's disease occurrence, determinants, and strategies toward intervention. *Dialogues Clin Neurosci*, 11, 111-128.
134. Rama, N., Goldschneider, D., Corset, V., Lambert, J., Pays, L., & Mehlen, P. (2012). Amyloid precursor protein regulates netrin-1-mediated commissural axon outgrowth. *J Biol Chem*, 287(35), 30014-30023.
135. Rammes, G., Gravius, A., Ruitenber, M., Wegener, N., Chambon, C., Sroka-Saidi, K., Jeggo, R., Staniaszek, L., Spanswick, D., O'Hare, E., Palmer, P., Kim, E. M., Bywalez, W., Egger, V., & Parsons, C. G. (2015). MRZ-99030 - A novel modulator of A β aggregation: II - Reversal of A β oligomer-induced deficits in long-term potentiation (LTP) and cognitive performance in rats and mice. *Neuropharmacology*, 92, 170-182.
136. Rammes, G., Hasenjäger, A., Sroka-Saidi, K., Deussing, J. M., & Parsons, C. G. (2011). Therapeutic significance of NR2B-containing NMDA receptors and mGluR5 metabotropic glutamate receptors in mediating the synaptotoxic effects of β -amyloid oligomers on long-term potentiation (LTP) in murine hippocampal slices. *Neuropharmacology*, 60(6), 982-990.
137. Reitz, C., & Mayeux, R. (2014). Alzheimer disease: epidemiology, diagnostic criteria, risk factors and biomarkers. *Biochem Pharmacol*, 88(4), 640-651.

138. Ring, S., Weyer, S. W., Kilian, S. B., Waldron, E., Pietrzik, C. U., Filippov, M. A., Herms, J., Buchholz, C., Eckman, C. B., Korte, M., Wolfer, D. P., & Muller, U. C. (2007). The secreted beta-amyloid precursor protein ectodomain APPs alpha is sufficient to rescue the anatomical, behavioral, and electrophysiological abnormalities of APP-deficient mice. *J Neurosci*, *27*(29), 7817-7826.
139. Rochefort, N. L., & Konnerth, A. (2012). Dendritic spines: from structure to in vivo function. *EMBO Rep*, *13*(8), 699-708.
140. Ross, E. M., & Gilman, A. G. (1980). Biochemical properties of hormone-sensitive adenylate cyclase. *Annual review of biochemistry*, *49*(1), 533-564.
141. Runge, K., Cardoso, C., & de Chevigny, A. (2020). Dendritic Spine Plasticity: Function and Mechanisms. *Front Synaptic Neurosci*, *12*, 36.
142. Sabo, S. L., Ikin, A. F., Buxbaum, J. D., & Greengard, P. (2003). The Amyloid Precursor Protein and Its Regulatory Protein, FE65, in Growth Cones and Synapses In Vitro&/em> and In Vivo&/em>. *The Journal of Neuroscience*, *23*(13), 5407.
143. Salahuddin, P., Fatima, M. T., Abdelhameed, A. S., Nusrat, S., & Khan, R. H. (2016). Structure of amyloid oligomers and their mechanisms of toxicities: Targeting amyloid oligomers using novel therapeutic approaches. *Eur J Med Chem*, *114*, 41-58.
144. Sanders, R. D., Franks, N. P., & Maze, M. (2003). Xenon: no stranger to anaesthesia. *Br J Anaesth*, *91*(5), 709-717.
145. Sanders, R. D., Ma, D., & Maze, M. (2004). Xenon: elemental anaesthesia in clinical practice. *Br Med Bull*, *71*, 115-135.
146. Satir, T. M., Agholme, L., Karlsson, A., Karlsson, M., Karila, P., Illes, S., Bergstrom, P., & Zetterberg, H. (2020). Partial reduction of amyloid beta production by beta-secretase inhibitors does not decrease synaptic transmission. *Alzheimers Res Ther*, *12*(1), 63.

147. Schaefer, M. L., Wang, M., Perez, P. J., Coca Peralta, W., Xu, J., & Johns, R. A. (2019). Nitric Oxide Donor Prevents Neonatal Isoflurane-induced Impairments in Synaptic Plasticity and Memory. *Anesthesiology*, *130*(2), 247-262.
148. Schilling, S., Mehr, A., Ludewig, S., Stephan, J., Zimmermann, M., August, A., Strecker, P., Korte, M., Koo, E. H., Muller, U. C., Kins, S., & Eggert, S. (2017). APLP1 Is a Synaptic Cell Adhesion Molecule, Supporting Maintenance of Dendritic Spines and Basal Synaptic Transmission. *J Neurosci*, *37*(21), 5345-5365.
149. Schotten, U., Schumacher, C., Sigmund, M., Karlein, C., Rose, H., Kammermeier, H., Sivarajan, M., & Hanrath, P. (1998). Halothane, but not isoflurane, impairs the β -adrenergic responsiveness in rat myocardium. *The Journal of the American Society of Anesthesiologists*, *88*(5), 1330-1339.
150. Seeman, P. (1972). The Membrane Actions of Anesthetics and Tranquilizers. *Pharmacological Reviews*, *24*(4), 583-655.
151. Seitz, P. A., ter Riet, M., Rush, W., & Merrell, W. J. (1990). Adenosine decreases the minimum alveolar concentration of halothane in dogs. *The Journal of the American Society of Anesthesiologists*, *73*(5), 990-994.
152. SELKOE, D. J. (2001). Alzheimer's Disease Genes, Proteins, and Therapy. *PHYSIOLOGICAL REVIEWS*, *81*, 26.
153. Selkoe, D. J., & Hardy, J. (2016). The amyloid hypothesis of Alzheimer's disease at 25 years. *EMBO Mol Med*, *8*(6), 595-608.
154. Selkoe, D. J., & Wolfe, M. S. (2007). Presenilin: running with scissors in the membrane. *Cell*, *131*(2), 215-221.
155. Sewell, J. C., & Sear, J. W. (2004). Derivation of preliminary three-dimensional pharmacophores for nonhalogenated volatile anesthetics. *Anesth Analg*, *99*(3), 744-751, table of contents.

156. Sewell, J. C., & Sear, J. W. (2006). Determinants of volatile general anesthetic potency: a preliminary three-dimensional pharmacophore for halogenated anesthetics. *Anesth Analg*, *102*(3), 764-771.
157. Shankar, G. M., Li, S., Mehta, T. H., Garcia-Munoz, A., Shepardson, N. E., Smith, I., Brett, F. M., Farrell, M. A., Rowan, M. J., Lemere, C. A., Regan, C. M., Walsh, D. M., Sabatini, B. L., & Selkoe, D. J. (2008). Amyloid-beta protein dimers isolated directly from Alzheimer's brains impair synaptic plasticity and memory. *Nat Med*, *14*(8), 837-842.
158. Shapiro, L., Love, J., & Colman, D. R. (2007). Adhesion molecules in the nervous system: structural insights into function and diversity. *Annu. Rev. Neurosci.*, *30*, 451-474.
159. Shiotani, H., Maruo, T., Sakakibara, S., Miyata, M., Mandai, K., Mochizuki, H., & Takai, Y. (2017). Aging-dependent expression of synapse-related proteins in the mouse brain. *Genes to Cells*, *22*(5), 472-484.
160. Simon, W., Hapfelmeier, G., Kochs, E., Zieglgaensberger, W., & Rammes, G. (2001). Isoflurane Blocks Synaptic Plasticity in the Mouse Hippocampus. *Anesthesiology*, *94*(6), 1058-1065.
161. Singh, S. K., Srivastav, S., Yadav, A. K., Srikrishna, S., & Perry, G. (2016). Overview of Alzheimer's Disease and Some Therapeutic Approaches Targeting Abeta by Using Several Synthetic and Herbal Compounds. *Oxid Med Cell Longev*, *2016*, 7361613.
162. Sinha, S., Anderson, J. P., Barbour, R., Basi, G. S., Caccavello, R., Davis, D., Doan, M., Dovey, H. F., Frigon, N., & Hong, J. (1999). Purification and cloning of amyloid precursor protein β -secretase from human brain. *Nature*, *402*(6761), 537-540.
163. Sonner, J. M., Antognini, J. F., Dutton, R. C., Flood, P., Gray, A. T., Harris, R. A., Homanics, G. E., Kendig, J., Orser, B., Raines, D. E., Rampil, I. J., Trudell, J., Vissel, B., & Eger, E. I., 2nd. (2003). Inhaled anesthetics and immobility: mechanisms,

- mysteries, and minimum alveolar anesthetic concentration. *Anesth Analg*, 97(3), 718-740.
164. Sonner, J. M., & Cantor, R. S. (2013). Molecular mechanisms of drug action: an emerging view. *Annu Rev Biophys*, 42, 143-167.
165. Sosa, L. J., Caceres, A., Dupraz, S., Oksdath, M., Quiroga, S., & Lorenzo, A. (2017). The physiological role of the amyloid precursor protein as an adhesion molecule in the developing nervous system. *J Neurochem*, 143(1), 11-29.
166. Stockley, J. H., & O'Neill, C. (2008). Understanding BACE1: essential protease for amyloid-beta production in Alzheimer's disease. *Cell Mol Life Sci*, 65(20), 3265-3289.
167. Tabaton, M., Nunzi, M. G., Xue, R., Usiak, M., Autiliogambetti, L., & Gambetti, P. (1994). Soluble Amyloid β -Protein Is a Marker of Alzheimer Amyloid in Brain But Not in Cerebrospinal Fluid. *Biochemical and Biophysical Research Communications*, 200(3), 1598-1603.
168. Takai, Y. (2003). Nectin and afadin: novel organizers of intercellular junctions. *Journal of Cell Science*, 116(1), 17-27.
169. Tamagno, E., Parola, M., Bardini, P., Piccini, A., Borghi, R., Guglielmotto, M., Santoro, G., Davit, A., Danni, O., Smith, M. A., Perry, G., & Tabaton, M. (2005). Beta-site APP cleaving enzyme up-regulation induced by 4-hydroxynonenal is mediated by stress-activated protein kinases pathways. *J Neurochem*, 92(3), 628-636.
170. Tang, X., Li, Y., Ao, J., Ding, L., Liu, Y., Yuan, Y., Wang, Z., & Wang, G. (2018). Role of $\alpha 7$ nAChR-NMDAR in sevoflurane-induced memory deficits in the developing rat hippocampus. *PLoS One*, 13(2), e0192498.
171. Terry, R. D., Masliah, E., Salmon, D. P., Butters, N., DeTeresa, R., Hill, R., Hansen, L. A., & Katzman, R. (1991). Physical basis of cognitive alterations in alzheimer's disease: Synapse loss is the major correlate of cognitive impairment. *Annals of Neurology*, 30(4), 572-580.

172. TERRY., R. D., GONATAS., N. K., & WEISS., M. (1964). Ultrastructural studies in Alzheimer's presenile dementia. *Am J Pathol*, 44, 269-297.
173. Thinakaran, G., & Koo, E. H. (2008). Amyloid precursor protein trafficking, processing, and function. *J Biol Chem*, 283(44), 29615-29619.
174. Tonner, P. H. (2006). Xenon: one small step for anaesthesia... ? *Current Opinion in Anesthesiology*, 19(4), 382-384.
175. Turner, R. T., Hong, L., Koelsch, G., Ghosh, A. K., & Tang, J. (2005). Structural locations and functional roles of new subsites S5, S6, and S7 in memapsin 2 (β -secretase). *Biochemistry*, 44(1), 105-112.
176. Tyan, S. H., Shih, A. Y., Walsh, J. J., Maruyama, H., Sarsoza, F., Ku, L., Eggert, S., Hof, P. R., Koo, E. H., & Dickstein, D. L. (2012). Amyloid precursor protein (APP) regulates synaptic structure and function. *Mol Cell Neurosci*, 51(1-2), 43-52.
177. Urban, B. W. (2002). Current assessment of targets and theories of anaesthesia. *Br J Anaesth*, 89(1), 167-183.
178. Vacas, S., Degos, V., Feng, X., & Maze, M. (2013). The neuroinflammatory response of postoperative cognitive decline. *Br Med Bull*, 106, 161-178. doi:10.1093/bmb/ldt006
179. van der Kant, R., & Goldstein, L. S. (2015). Cellular functions of the amyloid precursor protein from development to dementia. *Dev Cell*, 32(4), 502-515.
180. van der Kooij, M. A., Fantin, M., Rejmak, E., Grosse, J., Zanoletti, O., Fournier, C., Ganguly, K., Kalita, K., Kaczmarek, L., & Sandi, C. (2014). Role for MMP-9 in stress-induced downregulation of nectin-3 in hippocampal CA1 and associated behavioural alterations. *Nat Commun*, 5, 4995.
181. Vassar, R. (2004). Bace 1. *Journal of Molecular Neuroscience*, 23(1), 105-113.
182. Vassar, R., & Cole, S. (2007). The basic biology of BACE1: A key therapeutic target for Alzheimer's disease. *Current genomics*, 8(8), 509-530.

183. Vassar, R., Kuhn, P. H., Haass, C., Kennedy, M. E., Rajendran, L., Wong, P. C., & Lichtenthaler, S. F. (2014). Function, therapeutic potential and cell biology of BACE proteases: current status and future prospects. *J Neurochem*, *130*(1), 4-28.
184. Volfovsky, N., Parnas, H., Segal, M., & Korkotian, E. (1999). Geometry of Dendritic Spines Affects Calcium Dynamics in Hippocampal Neurons: Theory and Experiments. *Journal of Neurophysiology*, *82*(1), 450-462.
185. Wang, L., Liu, B. J., Cao, Y., Xu, W. Q., Sun, D. S., Li, M. Z., Shi, F. X., Li, M., Tian, Q., Wang, J. Z., & Zhou, X. W. (2018). Deletion of Type-2 Cannabinoid Receptor Induces Alzheimer's Disease-Like Tau Pathology and Memory Impairment Through AMPK/GSK3beta Pathway. *Mol Neurobiol*, *55*(6), 4731-4744.
186. Wang, X. D., & Schmidt, M. V. (2016). Editorial: Molecular Mechanisms for Reprogramming Hippocampal Development and Function by Early-Life Stress. *Front Mol Neurosci*, *9*, 6.
187. Wang, X. D., Su, Y. A., Wagner, K. V., Avrabos, C., Scharf, S. H., Hartmann, J., Wolf, M., Liebl, C., Kuhne, C., Wurst, W., Holsboer, F., Eder, M., Deussing, J. M., Muller, M. B., & Schmidt, M. V. (2013). Nectin-3 links CRHR1 signaling to stress-induced memory deficits and spine loss. *Nat Neurosci*, *16*(6), 706-713.
188. Wang, X. X., Li, J. T., Xie, X. M., Gu, Y., Si, T. M., Schmidt, M. V., & Wang, X. D. (2017). Nectin-3 modulates the structural plasticity of dentate granule cells and long-term memory. *Transl Psychiatry*, *7*(9), e1228.
189. Weinrich, M., & Worcester, D. L. (2018). The actions of volatile anesthetics: a new perspective. *Acta Crystallogr D Struct Biol*, *74*(Pt 12), 1169-1177.
190. Westermark, P., Engström, U., Johnson, K. H., Westermark, G. T., & Betsholtz, C. (1990). Islet amyloid polypeptide: pinpointing amino acid residues linked to amyloid fibril formation. *Proceedings of the National Academy of Sciences*, *87*(13), 5036.

191. Wilhelm, S., Ma, D., Maze, M., & Franks, Nicholas P. (2002). Effects of Xenon on In Vitro and In Vivo Models of Neuronal Injury. *Anesthesiology*, 96(6), 1485-1491.
192. Wirak, D. O., Bayney, R., Ramabhadran, T. V., Fracasso, R. P., Hart, J. T., Hauer, P. E., Hsiau, P., Pekar, S. K., Scangos, G. A., Trapp, B. D., & et, a. (1991). Deposits of amyloid beta protein in the central nervous system of transgenic mice. *Science*, 253(5017), 323.
193. Wisniewski, H. M., Zoltowska, A., & Frackowiak, J. (1994). Non-Fibrillar β -Amyloid Protein is Associated with Smooth Muscle Cells of Vessel Walls in Alzheimer Disease. *Journal of Neuropathology & Experimental Neurology*, 53(6), 637-645.
194. *World Alzheimer Report 2009*. (2009).
195. *World Alzheimer Report 2016*. (2016).
196. Wu, Z., Li, X., Zhang, Y., Tong, D., Wang, L., & Zhao, P. (2018). Effects of Sevoflurane Exposure During Mid-Pregnancy on Learning and Memory in Offspring Rats: Beneficial Effects of Maternal Exercise. *Frontiers in Cellular Neuroscience*, 12.
197. Xiao, H., Liu, B., Chen, Y., & Zhang, J. (2016). Learning, memory and synaptic plasticity in hippocampus in rats exposed to sevoflurane. *International Journal of Developmental Neuroscience*, 48(1), 38-49.
198. Xie, Z., Culley, D. J., Dong, Y., Zhang, G., Zhang, B., Moir, R. D., Frosch, M. P., Crosby, G., & Tanzi, R. E. (2008). The common inhalation anesthetic isoflurane induces caspase activation and increases amyloid β - protein level in vivo. *Annals of neurology: Official journal of the American neurological association and the child neurology society*, 64(6), 618-627.
199. Xie, Z., Dong, Y., Maeda, U., Moir, R., Inouye, S. K., Culley, D. J., Crosby, G., & Tanzi, R. E. (2006). Isoflurane-induced apoptosis: a potential pathogenic link between delirium and dementia. *The Journals of Gerontology Series A: Biological Sciences and Medical Sciences*, 61(12), 1300-1306.

200. Xie, Z., Dong, Y., Maeda, U., Moir, R. D., Xia, W., Culley, D. J., Crosby, G., & Tanzi, R. E. (2007a). The Inhalation Anesthetic Isoflurane Induces a Vicious Cycle of Apoptosis and Amyloid-Protein Accumulation. *Journal of Neuroscience*, 27(6), 1247-1254.
201. Xie, Z., Dong, Y., Maeda, U., Moir, R. D., Xia, W., Culley, D. J., Crosby, G., & Tanzi, R. E. (2007b). The inhalation anesthetic isoflurane induces a vicious cycle of apoptosis and amyloid beta-protein accumulation. *J Neurosci*, 27(6), 1247-1254.
202. Yamakura, T., & Shimoji, K. (1999). Subunit-and site-specific pharmacology of the NMDA receptor channel. *Progress in neurobiology*, 59(3), 279-298.
203. Yamazaki, T., Koo, E. H., & Selkoe, D. J. (1997). Cell surface amyloid beta-protein precursor colocalizes with beta 1 integrins at substrate contact sites in neural cells. *J Neurosci*, 17, 1004–1010.
204. Yan, R., Bienkowski, M. J., Shuck, M. E., Miao, H., Tory, M. C., Pauley, A. M., Brashler, J. R., Stratman, N. C., Mathews, W. R., & Buhl, A. E. (1999). Membrane-anchored aspartyl protease with Alzheimer's disease β -secretase activity. *Nature*, 402(6761), 533-537.
205. Yang, G., Chang, Paul C., Bekker, A., Blanck, Thomas J. J., & Gan, W.-B. (2011). Transient Effects of Anesthetics on Dendritic Spines and Filopodia in the Living Mouse Cortex. *Anesthesiology*, 115(4), 718-726.
206. Ye, F., & Zuo, Z. Y. (2017). Anesthetic effects on autophagy. *Med Gas Res*, 7(3), 204-211.
207. Young-Pearse, T. L., Chen, A. C., Chang, R., Marquez, C., & Selkoe, D. J. (2008). Secreted APP regulates the function of full-length APP in neurite outgrowth through interaction with integrin beta1. *Neural Dev*, 3, 15.

208. Zhang, S., Hu, X., Guan, W., Luan, L., Li, B., Tang, Q., & Fan, H. (2017). Isoflurane anesthesia promotes cognitive impairment by inducing expression of β -amyloid protein-related factors in the hippocampus of aged rats. *PLoS One*, *12*(4), e0175654.
209. Zhang, Y. W., Thompson, R., Zhang, H., & Xu, H. (2011). APP processing in Alzheimer's disease. *Mol Brain*, *4*, 3.
210. Zheng, H., & Koo, E. H. (2011). Biology and pathophysiology of the amyloid precursor protein. *Molecular Neurodegeneration*, *6*, 16.
211. Zhou, B., Chen, L., Liao, P., Huang, L., Chen, Z., Liao, D., Yang, L., Wang, J., Yu, G., Wang, L., Zhang, J., Zuo, Y., Liu, J., & Jiang, R. (2019). Astroglial dysfunctions drive aberrant synaptogenesis and social behavioral deficits in mice with neonatal exposure to lengthy general anesthesia. *PLoS Biol*, *17*(8), e3000086.
212. Zhou, L., Barao, S., Laga, M., Bockstael, K., Borgers, M., Gijzen, H., Annaert, W., Moechars, D., Mercken, M., Gevaert, K., & De Strooper, B. (2012). The neural cell adhesion molecules L1 and CHL1 are cleaved by BACE1 protease in vivo. *J Biol Chem*, *287*(31), 25927-25940.
213. Zhu, K., Xiang, X., Filser, S., Marinkovic, P., Dorostkar, M. M., Crux, S., Neumann, U., Shimshek, D. R., Rammes, G., Haass, C., Lichtenthaler, S. F., Gunnensen, J. M., & Herms, J. (2018). Beta-Site Amyloid Precursor Protein Cleaving Enzyme 1 Inhibition Impairs Synaptic Plasticity via Seizure Protein 6. *Biol Psychiatry*, *83*(5), 428-437.

List of abbreviations

AAV	adeno-associated virus
A β ₁₋₄₂	amyloid-beta peptide 1-42
AD	Alzheimer's disease
ADAM	a disintegrin and metalloprotease domain protein
AICD	amyloid precursor protein intracellular domain
APP	amyloid precursor protein
APS	ammonium persulfate
aCSF	artificial cerebrospinal fluid
BACE	β -site amyloid precursor protein-cleaving enzyme
BBB	blood brain barrier
CAMs	cell adhesion molecules
Carbogen	gas-mixture of 95% O ₂ and 5% CO ₂
Ctl	control
DMSO	dimethylsulfoxide
CNS	central nervous system
CSF	cerebrospinal fluid
DG	dentate gyrus
(E)GFP	(enhanced) Green Fluorescent Protein
ECL	entry-level peroxidase substrate for enhanced chemiluminescence
ELISA	enzyme-linked immunosorbent assay
EtOH	Ethanol
fEPSPs	field excitatory post synaptic potential slopes

GABA	γ -aminobutyric acid
G proteins	guanine nucleotide-binding proteins
HC	hippocampus
HFS	high-frequency stimulation
HRP	horseradish peroxidase
Iso	isoflurane
GAPDH	Glyceraldehyd-3-phosphate dehydrogenase
KD	knockdown
LDH	lactate dehydrogenase
LTP	long-term potentiation
LY	LY2886721
N ₂	Nitrogen
NGS	normal goat serum
NMDA	N-Methyl-d-aspartic acid
PBS	phosphate buffered saline
PFA	paraformaldehyde
PMSF	phenylmethylsulfonylfluoride
PVDF	polyvinylidenedifluoride
RIPA	radioimmunoprecipitation assay
RT	room temperature
sAPP α	soluble ectodomain APP α
sAPP β	soluble ectodomain APP β
shRNA	short hairpin RNA
Sevo	sevoflurane
SDS	sodium dodecylsulfate

Sp	supplementary
TBST	Tris-buffered saline with Tween20
TEMED	tetramethylethyldiamin
Thy1-EGFP	(Thy1-EGFP)MJrs/J mice
Tris	Tris-(hydroxymethyl-) aminomethan
Xe	Xenon